From Department of Cardiac Surgery
Rostock Medical University
Director: Prof. Dr. med. habil. Gustav Steinhoff

Antiarrhythmic Effect of Human Bone Marrow-Derived CD271+ Mesenchymal Stem Cells tested *in vivo* using a new Infarction-Re-Infarction Mouse Model

Inaugural Dissertation
Submitted in Fulfillment of the Requirements for the Degree of
Doctor of Medicine
of the
Rostock Medical University

Submitted by
Haval Lutfalla Sadraddin | born on 19th June, 1985 in Erbil

https://doi.org/10.18453/rosdok_id00002970

Doktorarbeit
Universitätsmedizin Rostock

Dieses Werk ist lizenziert unter einer
Creative Commons Namensnennung-Nicht kommerziell 4.0
International Lizenz.

First Reviewer: Prof. Dr. med. habil. Gustav Steinhoff
Specialty: Cardiac Surgery / Stem Cell Therapy, Rostock University of Medicine

Second Reviewer: Univ.-Prof. Dr. med. Brigitte Vollmar
Specialty: Experimental Surgery, Rostock University of Medicine

Third Reviewer: Univ.-Prof. Dr. med. Christof Stamm
Specialty: Cardiac Surgery / Regenerative Therapies, Charité University of Medicine

Submitted on 15th August, 2019 | Defended on 13th, January 2021

TO MY DOCTORAL SUPERVISOR, PROF. DR. MED. HABIL. GUSTAV STEINHOFF, WHO OPENED ALL THE DOORS TO ME IN MY CAREER

TO MY PARENTS, SABEEHA AND LUTFALLA, WHO NEVER STOP IN SUPPORTING ME

TO MY LOVELY WIFE, NYAN, WHO IS BESIDE ME IN EVERY STEP IN MY LIFE

TO MY DAUGHTER, HALIN, WHO MOTIVATES ME EVERY TIME WITH HER BEAUTIFUL EYES

PARTS OF THIS RESEARCH HAVE BEEN PUBLISHED:

ORIGINAL WORK PUBLISHED ON 20TH NOVEMBER 2019:

SADRADDIN, H.; GAEBEL, R.; SKORSKA, A.; LUX, C.A.; SASSE, S.; AHMAD, B.; VASUDEVAN, P.; STEINHOFF, G.; DAVID, R. CD271+ HUMAN MESENCHYMAL STEM CELLS SHOW ANTIARRHYTHMIC EFFECTS IN A NOVEL MURINE INFARCTION MODEL. *CELLS* 2019, *8*, 1474. HTTPS://DOI.ORG/10.3390/CELLS8121474

Contents **Page no.**

1. Introduction 1

1.1. Myocardial infarction 1

1.2. Risk factors of myocardial infarction in human 1

1.3. Complications of myocardial infarction in human 2

1.4. Myocardial infarction induced in mice 2

1.5. Cardiac arrhythmias 3

1.5.1. History of electrocardiogram (ECG) 3

1.5.2. The basics of ECG 3

1.5.3. Comparison of human and murine ECGs 5

1.5.4. Morphology of murine electrocardiogram 6

1.5.5. Murine ECG changes in myocardial infarction 7

1.5.6. Implanted ECG telemetry system 8

1.5.7. Human cardiac conduction system 9

1.5.8. Murine cardiac conduction system 9

1.5.9. Mechanisms and pathogenesis of cardiac arrhythmias in human 11

1.5.10. Mechanism of ischemic arrhythmias in animal models and the role of gap junctions 15

1.5.11. Definitions of cardiac arrhythmias in experimental animal models 18

1.5.11.1. Ventricular arrhythmias 18

1.5.11.2. Atrial arrhythmias 22

1.6. Mesenchymal stem cells (MSCs) 23

1.7. Regenerative medicine and its role in cardiac arrhythmias 24

1.7.1. Gene therapies to treat arrhythmias 24

1.7.2. Role of cell therapies on cardiac electrical integrity 25

1.7.2.1. Mesenchymal stem/stromal cells (MSC) and cardiac arrhythmias 25

1.7.2.2. Skeletal myoblasts and cardiac arrhythmias 26

1.7.2.3. Embryonic stem cells and induced pleuripotent stem cells and cardiac arrhythmias 27

2. Materials and methods 28

2.1. Bone marrow aspiration 28

2.2. CD271+ cel isolation 28

2.2.1. Materials 28

2.2.2. The procedure of CD271+ cells isolation from human bone marrow 29

2.3. Flow cytometric analys 31

2.3.1. Materials 32

2.4. Animals 32

2.5. Experimental procedure 33

2.5.1. Experiment design 33

2.5.2. Materials 33

2.5.3. Ambulatory ECG monitoring and ligation of left anterior descending artery 34

2.6. Organ harvesting 35

2.7. Human cells detection 36

2.7.1. Materials 36

2.7.2. Staining procedure 37

2.8. Infarction size area analysis and leukocytes infiltration 38

2.8.1. First infarction size area analysis 38

2.8.1.1. Materials 38

2.8.1.2. Staining procedure 38

2.8.2. Analysis of leukocytes infiltration area after second infarction 39

2.8.2.1. Materials 39

2.8.2.2. Staining procedure 39

2.9. Definition of various ventricular arrhythmias 40

2.9.1. Ventricular premature beat (VPB) 41

2.9.2. Ventricular bigeminy and trigeminy 42

2.9.3. Salvos 42

2.9.4. Ventricular tachycardia (VT) 42

2.10. Statistical analysis 42

3. Results 43

3.1. Induced ventricular arrhythmias 43

3.2. Antiarrhythmic effects of CD271+ MSC engraftment 46

3.3. Retention of human cells 47

3.4. Alterations of the infarct scar 47

4. Discussion 50

4.1. Development of a new mouse model for in vivo rhythmological study of stem cells 50

4.2. The clinical relevance of the mouse model 51

4.3. Human CD271+ MSC reduce the occurrence of ventricular arrhythmias after myocardial infarction 51

4.4. Intra-myocardial implantation of human CD271+ MSC after myocardial infarction does not reduce infarct size 52

5. Conclusion 53

6. References 54

Affidavit 68

Appendix (Abbreviations) 69

Figure index **Page no.**

Figure 1: The basic pattern of electrical activity across the heart. 4

Figure 2: Comparison of the human and murine ECG. 5

Figure 3: Unprocessed six-lead electrocardiogram (ECG) traces in the mouse recorded by needle. 6

Figure 4: QT-intervals measured in vivo in genetically engineered mice. Bipolar surface electrocardiogram (lead II) obtained from a CD2F1 mouse heart in vivo. 7

Figure 5: Unprocessed (left) and averaged electrocardiogram traces from lead II recorded during ischaemia. 7

Figure 6: Radiograph/sketch showing location of the implanted telemetry transmitter. 8

Figure 7: Schematic illustration of the human cardiac conduction system 9

Figure 8: *LacZ* expression in the cardiac conduction system (CCS) of neonatal hearts. 10

Figure 9: Phases of SA nodal action potential. 11

Figure 10: Classification of active cardiac arrhythmias. 12

Figure 11: Enhanced pacemaker (a mechanism of cardiac arrhythmia). 13

Figure 12: Protected pacemaker (a mechanism of cardiac arrhythmia). 13

Figure 13: Afterdepolarization phenomena ((a mechanism of cardiac arrhythmia)) 14

Figure 14: (A) Circus-type reentry (B) Reflection. (mechanisms of cardiac arrhythmia) 15

Figure 15: A diagram showing the multiple levels of gap junction structure. 16

Figure 16: A ventricular premature beat (VPB) recorded by unipolar electrocardiogram from a rat heart perfused in the Langendorff mode. 19

Figure 17: (A) A bigeminy recorded by unipolar electrogram from a rat heart perfused in the Langendorff mode.. (B) A salvo recorded by unipolar electrogram from a rat heart perfused in the Langendorff mode. 19

Figure 18: (A) A single episode of VT recorded by unipolar electrocardiogram from a rat heart perfused in the Langendorff mode. (B) Single episode of VT recorded by unipolar electrocardiogram from a rat heart perfused in the Langendorff mode. 20

Figure 19: An archetypal example of Torsade de pointes (TDP) recorded in an anaesthetized rabbit. 21

Figure 20: A single episode of VF recorded by unipolar electrocardiogram from a marmoset (Callithrix jaccus) heart perfused in the Langendorff mode. 21

Figure 21: A single Atrial Premature Beat (APB) recorded on a continuous volume conducted ECG in a Langendorff perfused rabbit heart. 22

Figure 22: (A) A single episode of atrial flutter (AFL) recorded using body surface ECG lead II in a conscious mixed breed mongrel dog. (B) A single episode of atrial fibrillation (AF) recorded using body surface ECG lead II in a conscious mixed breed mongrel dog. 23

Figure 23: The principle of magnetic cell separation. 31

Figure 24: (A) Radiograph/sketch showing location of the implanted telemetry transmitter. (B) DSI PhysioTel® ETA-F10 for mice. 34

Figure 25: Schematic drawing of the loose LAD ligature positioning. 35

Figure 26: Illustration of the section levels of the frozen mouse heart. 36

Figure 27: Various ventricular arrhythmias detected after induced myocardial infarction via LAD ligation. 41

Figure 28: Mouse ECG changes in relation to the time of the 1st LAD ligation during ischemia-reperfusion infarction. 43

Figure 29: Mouse ECG changes in relation to the time of the permanent 2nd LAD ligation (re-infarction; URI group). 44

Figure 30: Comparison of developed ventricular arrhythmias until 12 hours post 1st LAD ligation. 45

Figure 31: Comparison of developed ventricular arrhythmias at different time periods post 2nd LAD ligation. 46

Figure 32: DAPI staining with 400x magnification of mouse heart section detecting human nuclei (arrows) 9 days after their intramyocardial delivery. 47

Figure 33: Cross section of mouse heart stained with sirius red and fast green. 48

Figure 34: Cross section of mouse heart stained with eosin and hematoxylin for leukocyte infiltration. 48

Figure 35: Alterations in myocardial infarction size. 49

1 INTRODUCTION

1.1 MYOCARDIAL INFARCTION

Over the last decade, cardiovascular disease (CVD) has become the single largest cause of death worldwide. In 2004, CVD caused an estimated 17 million deaths and led to 151 million disability-adjusted life years (DALYs) lost—about 30% of all deaths and 14% of all DALYs lost that year. (**Lopez** 2006)

Like many high-income countries during the last century, low- and middle-income countries are seeing an alarming increase in the rates of CVD, and this change is accelerating. In 2001, 75% of global deaths and 82% of total DALYs lost caused by coronary heart disease (CHD) occurred in low- and middle-income countries. (**Mathers** et al. 2008)

Myocardial ischemia occurs when the oxygen supply to the heart is not sufficient to meet metabolic needs. This mismatch can result from a decrease in oxygen supply, a rise in demand, or both. The most common underlying cause of myocardial ischemia is obstruction of coronary arteries by atherosclerosis. (**Fauci and Harrison** 2008)

The term ‘myocardial infarction’ should be used when there is evidence of myocardial necrosis in a clinical setting consistent with myocardial ischemia, in which case the detection of rise and/or fall of cardiac biomarkers (preferably troponin), with at least one value above the 99th percentile of the upper reference limit meets the diagnosis of MI. This together with at least one of the following: (1) Detection of Symptoms of ischemia, (2) ECG changes indicative of new ischemia (new ST-T changes or new left bundle branch block), (3) Development of pathological Q waves or (4) Imaging evidence of new loss of viable myocardium or new regional wall motion abnormality. A myocardial infarction could be evidenced by a sudden unexpected cardiac death, involving cardiac arrest, often with symptoms suggestive of myocardial ischemia, and accompanied by presumably new ST elevation or new left bundle branch block, and/or evidence of fresh thrombus by coronary angiography and/or at autopsy, but death occurring before blood samples could be obtained or before the appearance of cardiac biomarkers in the blood. (**Colledge** et al. 2010)

1.2 RISK FACTORS OF MYOCARDIAL INFARCTION IN HUMAN

The risk factors of developing a myocardial infarction could be divided into (1) first order risk factors (smoking, hypertension, familial disposition, disorders of lipid metabolism; increased level of total and LDL-cholesterol and diabetes mellitus), (2) second order risk factors (physical inactivity, obesity, elevated lipoprotein A, elevated homocystein and psychosocial factors;

stress, low social status) and (3) constitutional factors or non-modifiable risk factors (genetic predisposition, age and gender). The risk factor increases in men between fourth and seventh decade of life by six times, while in women it increases rapidly only after menopause. (**Sagmeister** 2013)

1.3 COMPLICATIONS OF MYOCARDIAL INFARCTION IN HUMAN

A myocardial infarction could be complicated by development of various brady- or tachyarrhythmias. Other complications include acute circulatory failure, pericarditis, whether early or late (Dressler's syndrome) and mechanical complications like rupture of the papillary muscle with severe mitral regurgitation, rupture of the interventricular septum or rupture of the ventricle. A myocardial infarction might be followed by an embolism or impaired ventricular function, remodeling and ventricular aneurysm (**Colledge** et al. 2010)

1.4 MYOCARDIAL INFARCTION INDUCED IN MICE

Mice are widely employed animals in studies of experimental MI, in part because of the ease of genetic manipulation in this species. (**Ahn** et al. 2004) Most of the currently available surgical techniques to simulate MI in experimental animals involve surgical dissection into the chest cavity to expose the left anterior descending artery (LAD) that is then occluded by a ligature for defined period in time to produce the ischemic event. (**Xu** et al. 2014) Complete occlusion of LAD induces an acute MI. (**Degabriele** et al. 2004) Coronary artery ligation to induce myocardial infarction for the purpose of investigation of heart failure (HF) was first described and performed in dogs by *Hood et al* in 1967. (**Hood** et al 1967) The induction of MI by coronary ligation in mice was initially described in 1978 by Zolotareva *et al.* (**Zolotareva** and **Kogan** 1978) More recently, in 1995, an open chest *in vivo* mouse model has been developed by Michael *et al.* (**Michael** et al. 1995) Different models of myocardial ischemia and reperfusion have been described. These include ischemia without reperfusion, open chest ischemia/reperfusion model, minimal invasive ischemia/reperfusion model, ischemia/reperfusion with ischemic preconditioning and Langendorf model (*ex vivo*). (**Conci E** et al. 2006)

It is worth to mention that the mouse coronary arterial tree is substantially different from that of human and other common large animal models, with a distinct septal coronary artery coursing along the right interventricular septum and a left coronary artery which courses over the LV free wall giving off variable branches. Thus, surgical ligation of the left coronary artery in mice produces myocardial infarction that involves the LV free wall and apex while sparing the septum. (**Kumar** et al. 2005)

Recently, another method has been utilized frequently to induce MI through cryoinjury. (**Brede** et al. 2003; **Roell** et al. 2002a; **Roell** et al. 2002b) Cryocoagulation was performed by placement of a copper probe (3 mm diameter, cooled in liquid nitrogen for 2 min) to the free left ventricular wall (3 times for 20 seconds) in order to achieve reproducible, large transmural myocardial lesion. (**Duerr** et al. 2011) Cryoinfarction is a technique with high periprocedural survival resulting in reproducible infarcts leading to significant LV dysfunction and a modest degree of ventricular remodeling over a period of 8 weeks. (**van den Bos** et al. 2005)

1.5 CARDIAC ARRHYTHMIAS

1.5.1 HISTORY OF ELECTROCARDIOGRAM (ECG)

Köllicker and Müller discovered in 1856 that the heart muscle could produce electric activity. Muirhead in London recorded the first electrocardiogram (ECG) in human in 1869 or 1870 with a siphon instrument, and Waller in 1887 with a capillary electrometer. Einthoven's string galvanometer was a breakthrough. After the initial focus on arrhythmias, ECG became more and more used in the diagnosis of myocardial ischemia and coronary heart disease. Long-term ECG registration with a portable tape recorder is important both for the diagnosis of arrhythmias and myocardial ischemia. (**Johansson** 2001)

1.5.2 THE BASICS OF ECG

The contraction of any muscle is associated with electrical changes called ´depolarization´, and these changes can be detected by electrodes attached to the surface of the body. Since all muscular contraction will be detected, the electrical changes associated with contraction of the heart muscle will only be clear if the patient is fully relaxed and no skeletal muscles are contracting. Although the heart has four chambers, from the electrical point of view it can be thought of as having only two, because the atria contract together and then the two ventricles contract together. The electrical discharge for each cardiac cycle normally starts in a special area of the right atrium called sinoatrial (SA) node. Depolarization then spreads through the atrial muscle fibers. There is a delay while the depolarization spreads through another special area in the atrium, the Atrioventricular (AV) node. Thereafter the electrical discharge travels very rapidly, down specialized conduction tissue: first a single pathway, the ´bundle of His´, which then divides in the septum between the ventricles into right and left bundle branches. The left bundle branch itself divides into two. Within the mass of the ventricular muscle, conduction spreads somewhat more slowly, through specialized tissue called ´Purkinje fibers`. The word ´rhythm´ is used to refer to the part of the heart which is control-

ling the activation sequence. The normal heart rhythm, with the electrical activation beginning in the SA node, is called ´sinus rhythm´.

The muscle mass of the atria is small compared with that of the ventricles, and the electrical change accompanying the contraction of the atria is therefore small. Contraction of the atria is associated with the ECG called ´P´ wave. The ventricular mass is large, and so there is a large, and so there is a large deflection of the ECG when the ventricles are depolarized. This is called the ´QRS´ complex. The ´T´ wave of the ECG is associated with the return of the ventricular mass to its resting electrical electrical state (repolarization). (**Hampton** 2013) The various normal ECG waves are represented in Figure (1)

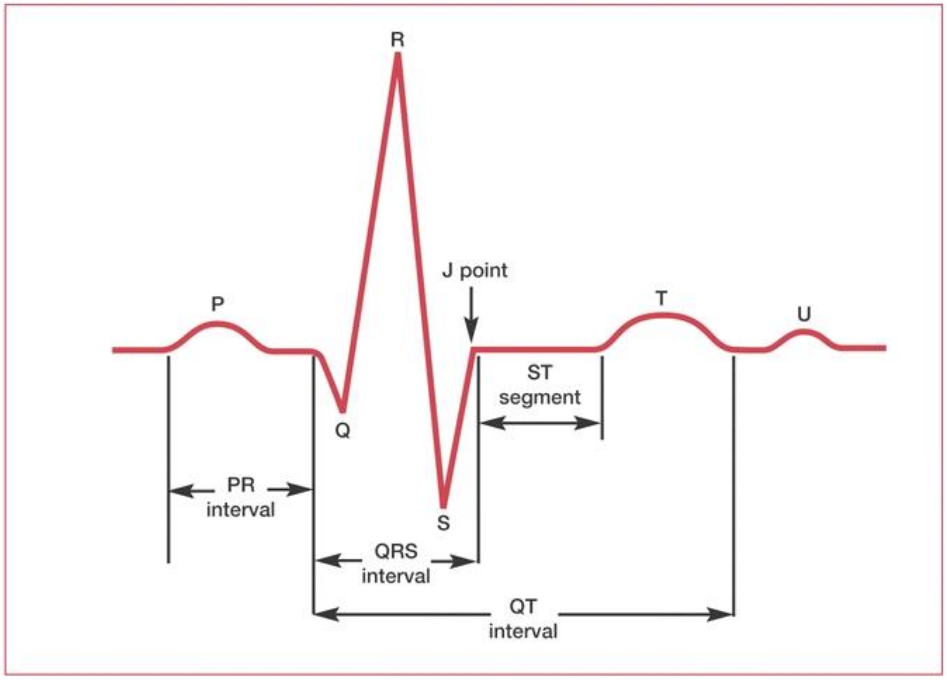

Figure 1: The basic pattern of electrical activity across the heart. (**Ashley und Niebauer** 2004)

The letters P, Q, R, S and T were selected in the early days of the ECG history, and were chosen arbitrary. The P, Q, R, S and T deflections are all called waves; the Q, R and S together make up a complex; and the interval between the S wave and the T wave is called ST ´segment´. If the first deflection is downward, it is called a Q-wave. An upward deflection is called an R wave. Any deflection below the baseline following an R wave is called an S wave whether there has been a preceding Q wave or not. (**Hampton** 2013) The P wave is a small deflection wave that represents atrial depolarization. The PR interval is the time between the first deflection of the P wave and the first deflection of the QRS complex. The three waves of the QRS complex represent ventricular depolarization. For the inexperienced, one of the most confusing aspects of ECG reading is the labeling of these waves. The rule is: if the wave immediately after the P wave is an upward deflection, it is an R wave; if it is a down-

ward deflection, it is a Q wave. Small Q waves correspond to depolarization of the interventricular septum. Q waves can also relate to breathing and are generally small and thin. They can also signal an old myocardial infarction (in which case they are big and wide). The R wave reflects depolarization of the main mass of the ventricles –hence it is the largest wave. The S wave signifies the final depolarization of the ventricles, at the base of the heart. The ST segment, which is also known as the ST interval, is the time between the end of the QRS complex and the start of the T wave. It reflects the period of zero potential between ventricular depolarization and repolarization. T waves represent ventricular repolarization (atrial repolarization is obscured by the large QRS complex). (**Ashley und Niebauer** 2004)

1.5.3 COMPARISON OF HUMAN AND MURINE ECGS

Despite the usefulness for cardiac research, the mouse possesses some electrophysiological characteristics that makes its ECG a little different from that of human and thus challenges the comparison between both ECGs. See figure 2. The action potential in the ventricular myocyte of the mouse lacks a clear plateau phase therefore the depolarization and repolarization are overlapped in ECG. This created much debate on the definition of the T wave and hence the QT interval in the murine ECG. (**Liu** et al. 2004; **Danik** et al. 2002)

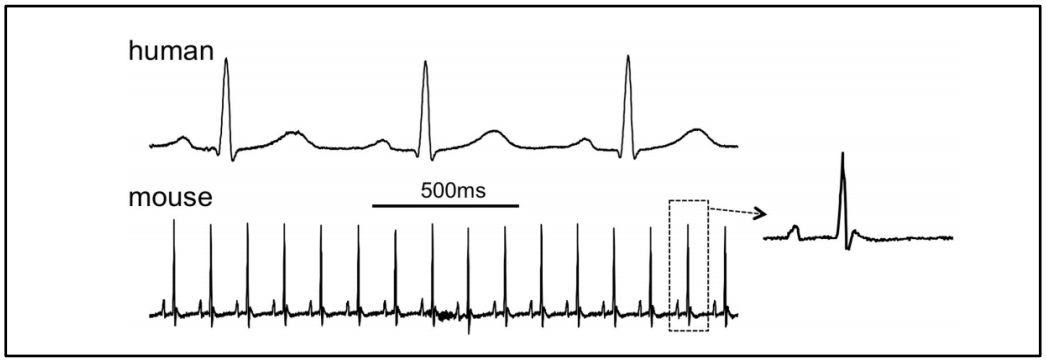

Figure 2: Comparison of the human and murine ECG, 2-s traces showing lead I. Inset shows a single complex from the mouse ECG (human ECG is patient 121 in the PTB database at www.physionet.org, mouse ECG courtesy of Dr. Ricardo Carnicer, Oxford University). (**Kaese and Verheule** 2012)

1.5.4 MORPHOLOGY OF MURINE ELECTROCARDIOGRAM

A representative, unprocessed 6-lead ECG from an anaesthetized mouse is presented in Figure 3. P waves and QRS complexes could be seen in all leads. In addition, short episodes of noise derived from skeletal muscles associated with respiration are visible on the ECG.
Atrial depolarization is clearly seen represented by P wave, which is followed in most leads by a small deviation from the isoelectric line leading up to the onset of the QRS complex (Fig.

3b). This has been speculated as an atrial repolarization. (**Speerschneider and Thomsen** 2013; **Sprague and White** 1925)

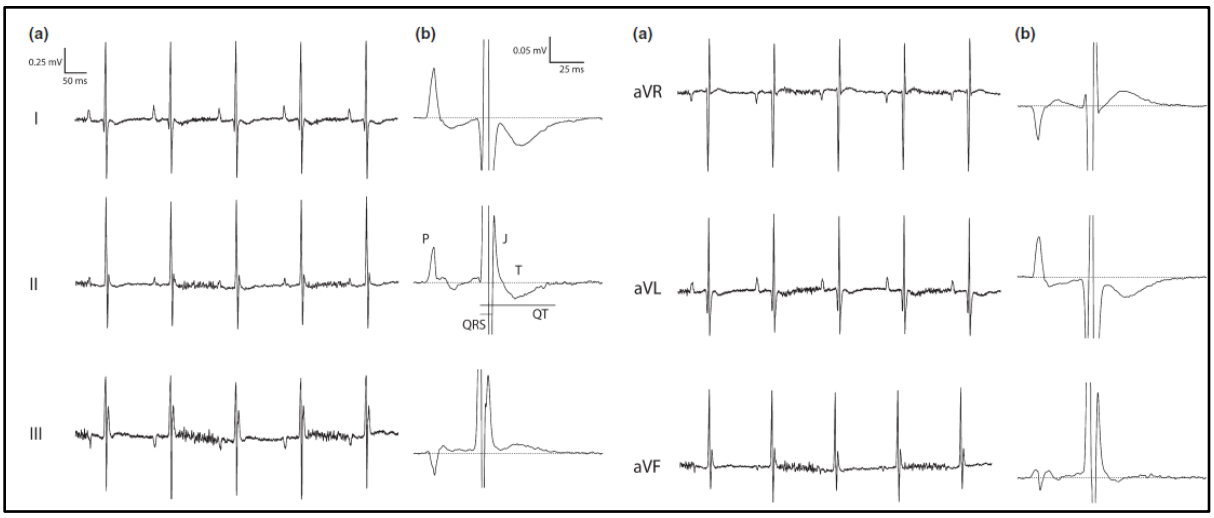

Figure 3: (a) Unprocessed six-lead electrocardiogram (ECG) traces in the mouse recorded by needle electrodes. P waves and QRS complexes are visible in all leads. Activity of skeletal muscles associated with respiration is apparent as isoelectric noise between the second and third, and the fourth and the fifth QRS complex. (b) Averaged ECG complexes obtained from each lead on an enlarged voltage scale. The J wave and the T wave are clearly distinct (indicated in lead II). For clarity, the peak of the QRS complex has been cropped. (**Speerschneider and Thomsen** 2013)

Ventricular depolarization starts with a Q or R wave and ends where the S wave returns to the isoelectric line in lead III and aVF. The PR interval was defined as the time from the start of the P-wave to the first deflection of the QRS complex. The iso-electric line was defined as the line connecting the end of the T-wave and the start of the P-wave of the next beat. The start of the QRS complex was defined as the earliest moment of deviation from baseline in any lead. The end of the QRS complex in each lead was defined as the moment when the S-wave returned to the isoelectric line. The start of the J-wave was defined as the end of the S-wave. The end of the J-wave was defined as the moment where the positive J-wave turned into the negative T-wave. (**Boukens** et al. 2013; **Holm** et al. 2010; **Chambers** et al. 2010) Murine ventricular depolarization and repolarization display a temporal overlap on the ECG producing a conjoined QRS complex and J wave. Hence, the start of the J wave in lead II is determined by the onset of the positive deflection immediately after the QRS complex and represents mixed depolarization and repolarization. The T wave is negative in leads I, II, aVL and aVF and positive in leads III and aVR. The end of ventricular repolarization is indicated by the point where the T wave returns to the isoelectric line. Alternatively, the end of the QT interval can be assessed by the intersection of the isoelectric line and the tangent to the upslope of the T wave. (**Boukens** et al. 2013)

1.5.5 MURINE ECG CHANGES IN MYOCARDIAL INFARCTION

The typical ECG changes noticed in the mouse in case of myocardial infarction are R-wave enlargement and ST-segment elevation which are seen within 5 minutes from LAD occlusion. Q-waves develop after 15 minutes from the start of the LAD ligation and ST-segment elevation becomes even more pronounced. (**Wehrens** et al. 2000) See figure (4).

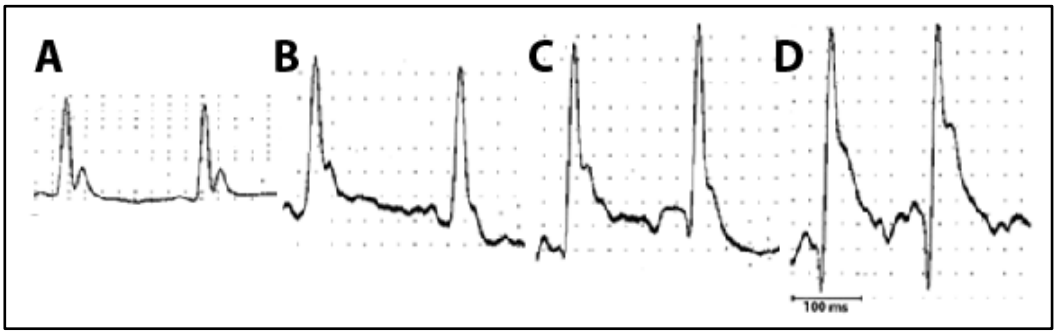

Figure 4: QT-intervals measured in vivo in genetically engineered mice. Bipolar surface electrocardiogram (lead II) obtained from a CD2F1 mouse heart in vivo.
Recording before coronary occlusion (A), after 5 min (B), 15 min (C), and 30 min (D) of coronary artery occlusion. Note the R-wave enlargement (B), ST-segment elevation (B–D), and development of Q-waves (C–D). (**Wehrens** et al. 2000)

The presence of a prominent J wave and the absence of a horizontal ST segment in the murine ECG make it informative to ascertain the electrocardiographic changes to local ischaemia. (**Speerschneider and Thomsen** 2013) This can be seen in figure 5.

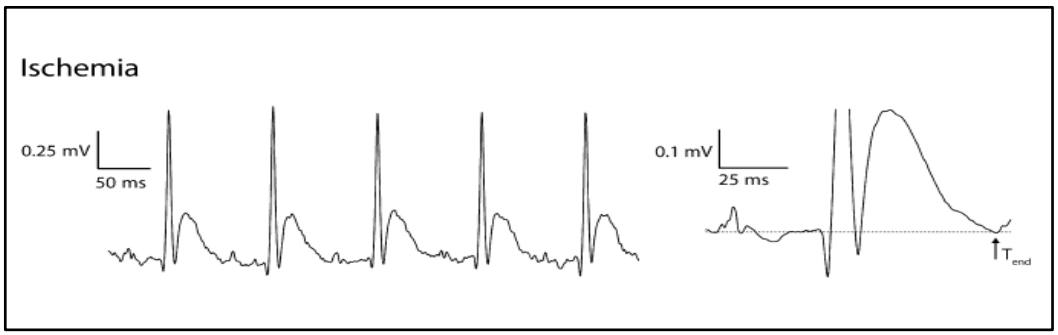

Figure 5: Unprocessed (left) and averaged electrocardiogram (ECG; right) traces from lead II recorded during ischaemia. Ischaemia produced a prolonged QRS interval and a JT segment with a positive, large T wave (n = 6). (**Speerschneider and Thomsen** 2013)

1.5.6 IMPLANTED ECG TELEMETRY SYSTEM

The ECG radiotelemetry units are the gold standard for monitoring the heart rates in conscious mice. A typical mouse ECG telemetry system contains two electrical ECG leads connected to a radio transmitter. The radio transmitter is placed into a subcutaneous pocket on the back of the mouse. And the leads are implanted with one lead toward the right upper chest and the other near the left lower chest. Upon activation of the transmitter by a magnet the electrical signals are transmitted wirelessly to a nearby receiver attached to an amplifier and computer system for data acquisition, storage and analysis. (**Ho** et al. 2011)
With the use of an implanted telemetry device, a continuous conscious recording of the mouse heart rate is possible. This provides a method for long term monitoring of the mice in their natural living environment that is often needed to detect circadian variations, as well as a mean to monitor arrhythmia frequencies and to determine if arrhythmias are the cause of death in transgenic mice. Recently, the telemetry systems that allow simultaneous monitoring of ECG and arterial pressures in mice are in development. The disadvantages include high cost as well as surgically related morbidity and mortality. Since only two electrodes are present, only a single lead of ECG recording is obtainable. (**Ho** et al. 2011) See Figure 6.

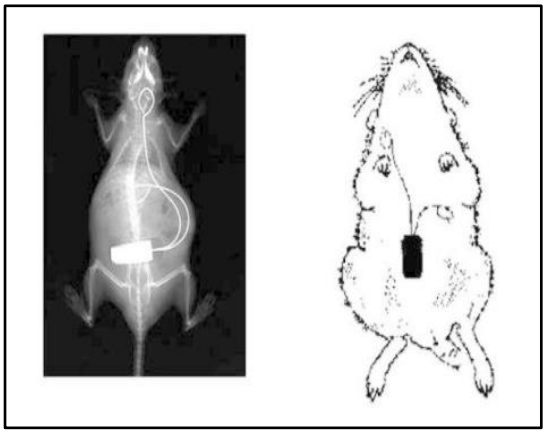

Figure 6: Radiograph/sketch showing location of the implanted telemetry transmitter. The body of the transmitter is positioned in the abdominal cavity. The positive lead is formed into a wire loop and fixed to the xiphoid process with sutures. The negative lead is tunneled subcutaneously from the thorax to the neck and fixed as a wire loop between the muscles directly next to the trachea. (**Späni** et al. 2003)

The advantages of subcutaneous implantation over the abdominal or intraperitoneal implantation are such that it is recommended under certain circumstances for use in rat as well as in the mouse. It is less stressful surgically and is characterized by a faster return to presurgical weight and circadian patterns than abdominal placement. Nonetheless, it is important to

note that telemetry studies have consistently demonstrated that full recovery from anesthesia and surgery does not occur for 5–7 days, as indicated by the return of normal circadian rhythms in activity, blood pressure, and heart rate. (**Lorenz** 2002)

Therefore, the implanted telemetry system is most suited for studies where long term monitoring of mouse heart rate and cardiac rhythm in their natural living environment is needed and has been used as a powerful tool for the evaluation of the occurrence of various cardiac arrhythmias like ventricular tachycardia, sudden cardiac death, Atrioventricular (AV) nodal block and atrial fibrillation. (**Ho** et al. 2011; **Cerrone** et al. 2005; **Chelu** et al. 2009; **Sood** et al. 2008)

1.5.7 HUMAN CARDIAC CONDUCTION SYSTEM

Cardiac arrhythmias are the abnormalities or perturbations in the normal activation or beating of heart myocardium. The sinus node sends a depolarization wave over the atrium and depolarizing atrioventricular (AV) node propagating over His-Purkinje system and depolarizes ventricle in systematic way. (**Fu** 2015) The gross anatomy of the human cardiac conduction system is illustrated in figure 7.

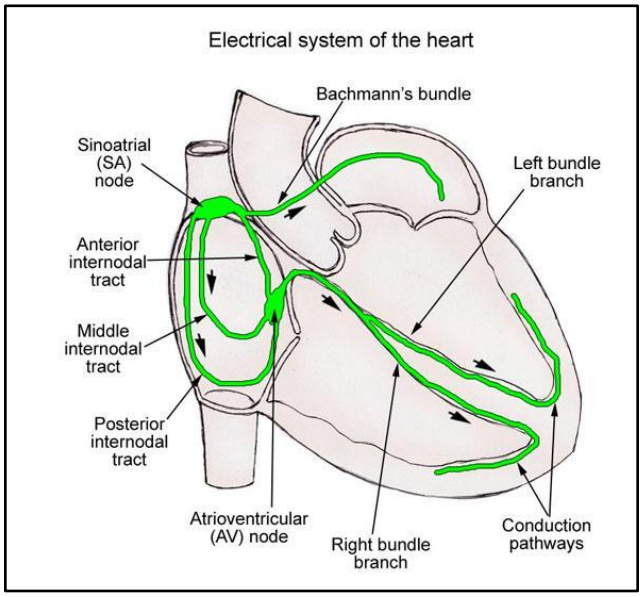

Figure 7: Schematic illustration of the human cardiac conduction system. (**Assadi and Motabar** 2016)

1.5.8 MURINE CARDIAC CONDUCTION SYSTEM

The murine cardiac conduction system has been delineated through the use of a generated stable transgenic line from the MC4 *Engrailed-2/lacZ* fusion construct. After a special tissue preparation and staining and through detection of robust β-galactosidase activity in the neo-

natal right atrium (RA) the atrial conductive system has been delineated. The most discrete expression of robust β-galactosidase has been seen within the sinoatrial (SA) node, atrioventricular (AV) node and ring, and in the left and right venous valves (Figure 8D-F). The SA node could be visualized as a cylinder in the subepicardial region of the right atrium, near the junction of the medial wall of the superior vena cava, with the conspicuous SA nodal artery running through the node, as shown in Figure. 8D. Right and left prolongations of the SA node were also seen as it coursed posteriorly through the right atrium. The AV node was discernible in the inferior portion of the interatrial septum to the right and above the mitral annulus, as seen in Figure 8E. Transgene expression also delineated fibers originating within the right atrium and coursing toward the left atrium (Figure 8A). These fibers presumably are components of Bachmann's bundle, which is responsible for bringing the depolarizing impulse into left atrial tissue. (**Logan** et al. 1993; **Rentschler** et al. 2001; **Virágh und Challice** 1982; **Lev und Thaemert** 1973)

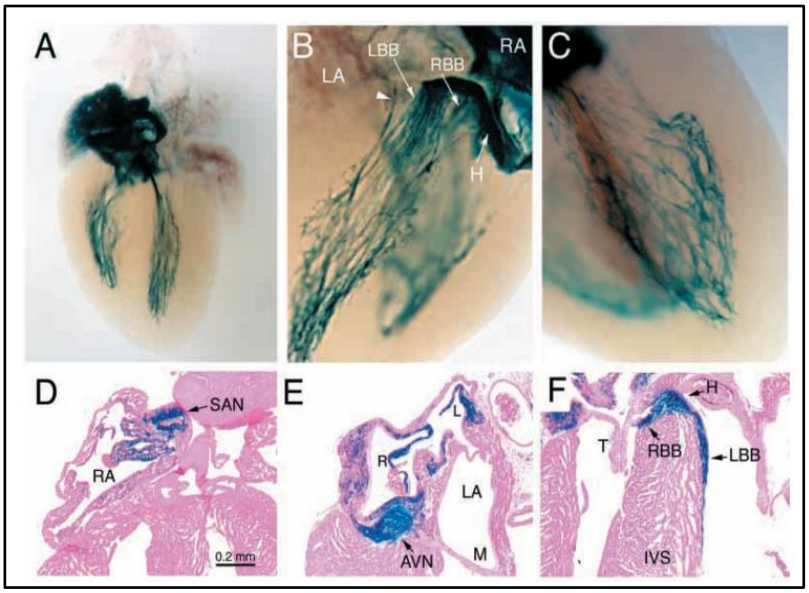

Figure 8: *LacZ* expression in the cardiac conduction system (CCS) of neonatal hearts. (A) Low magnification view of *lacZ* expression within the heart, which delineates components of the entire cardiac conduction system. (B) Higher magnification of the region of the His bundle (H) and bundle branches. Several fibers split off from the His bundle and travel along the right side of the interventricular septum (IVS) giving rise to the right bundle branch (RBB), which is out of the plane of focus. The termination of the His bundle gives rise to the fibers of the left bundle branch (LBB), which has a characteristic fan-shaped appearance. Fibers coursing directly from left atrium (LA) to left ventricle (LV) are indicated (arrowhead). (C) Higher magnification of the extensive Purkinje fiber network within the LV. (D-F) Analysis of Eosin-stained sections demonstrates preferential transgene expression within specific regions of the right atrium (RA), including the SA node (SAN), the right (R) and left (L) venous valves and the AV node (AVN). Ventricular transgene expression delineated the His bundle, located beneath the tricuspid annulus, and the bundle branches. M, mitral valve; T, tricuspid valve. Scale bar for D-F is shown. (**Rentschler** et al. 2001)

1.5.9 MECHANISMS AND PATHOGENESIS OF CARDIAC ARRHYTHMIAS IN HUMAN

In order to understand the mechanisms of cardiac arrhythmias it is crucial to understand the normal action potentials of the conductive system cells. The SA nodal action potential can be divided into three phases; phase 4, phase 0 and phase 3. (**Tse** 2016) See figure 9.

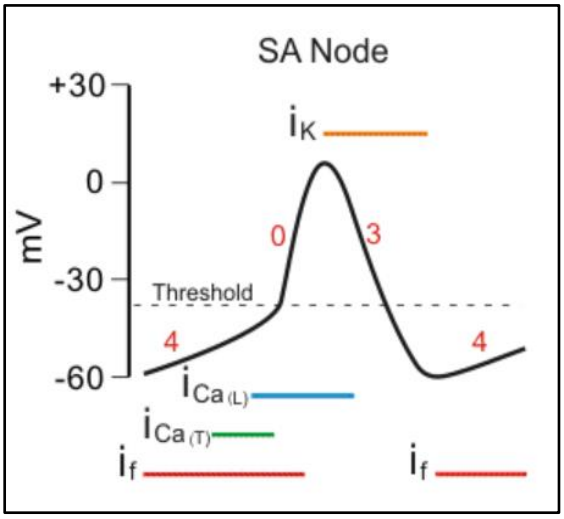

Figure 9: Phases of SA nodal action potential. (**Klabunde** 2008)

Phase 4 starts with the spontaneous depolarization, a special property of the pacemaker cells. The spontaneous depolarization starts at a membrane potential of -60 mV. At which time the slow Na^+ channels (also called “funny” currents and abbreviated as I_f) open and there is an inward movement of the Na+ current which depolarizes the cell membrane. Once the membrane potential reaches -50 mV transient or T-type Ca^{++} channels open and Ca^{++} currents move down its electrochemical gradient which further depolarizes the membrane. When the membrane depolarizes to -40 mV, second type of Ca^{++} channels open. These are called long-lasting or L-type Ca^{++} channels. The channels allow entering more Ca^{++} into the cell which further depolarizes the membrane until the action potential threshold is reached, usually between -40 and -30 mV. During phase 0, depolarization occurs due to inward of the Ca^{++} through the L-type Ca^{++} channels. At this time the funny Na^+ channels and T-type Ca^{++} channels close. Repolarization of the membrane, which occurs at the phase 3, is caused primarily by the outward movement of K^+ ions with the termination of the inward flow of the Ca^{++} currents through the close of L-type Ca^{++} channels. A deep repolarization of -60 mV is required for the next cycle to start. Cellular hypoxia affects the cellular repolarization and slows the start of the next cycle; i.e. bradycardia. (**Tse** 2016)

Different schemes have been utilized to classify the mechanisms of cardiac arrhythmias. The traditional classification describes the mechanisms of arrhythmias as reentrant and non-reentrant activity. (**Antzelevitch and Burashnikov** 2011)

Others have proposed that the basic mechanisms of the cardiac arrhythmias are the enhanced or suppressed automaticity, triggered activity, or re-entry. (**Fu** 2015) A dynamics-based classification, which focused on the trigger-tissue substrate interactions, has divided the mechanisms of cardiac arrhythmias into unstable calcium cycling, reduced repolarization reserve and excess repolarization reserve. (**Weiss** et al. 2015) An overview of the basic mechanisms of cardiac arrhythmias is illustrated in figure 10.

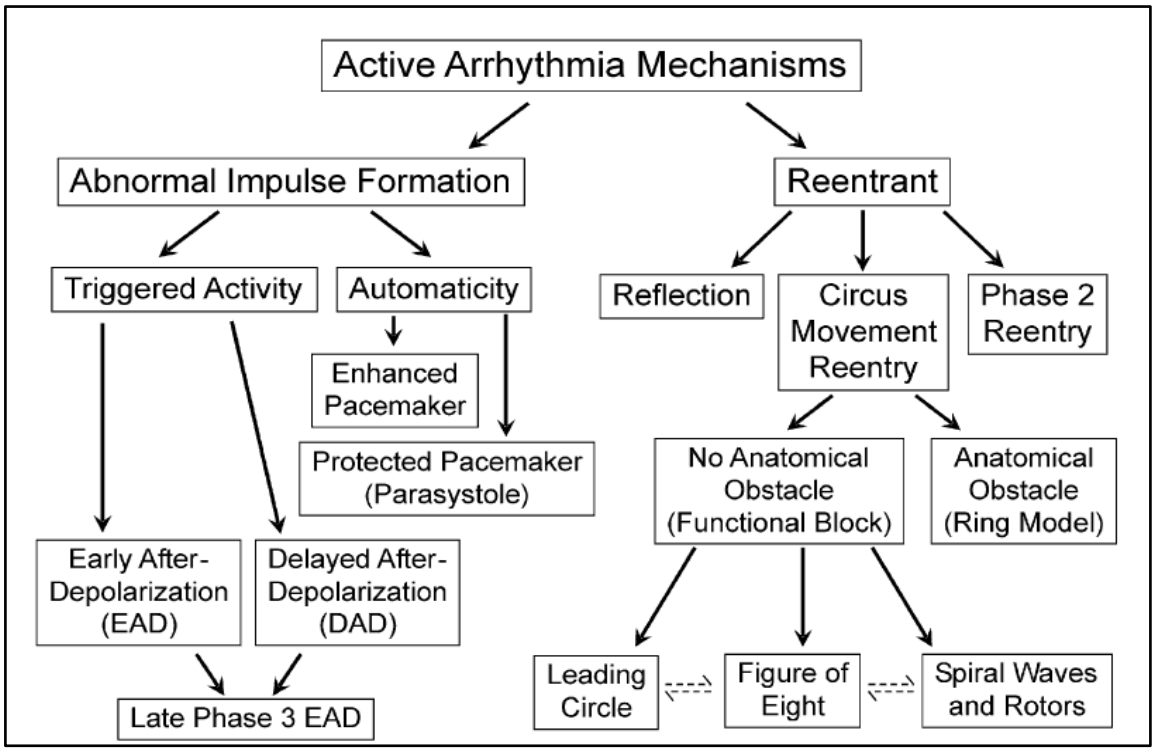

Figure 10: Classification of active cardiac arrhythmias. (**Antzelevitch and Burashnikov** 2011)

Here the mechanisms of arrhythmias would be classified into *focal activity* and *reentry*. The focal activity can arise from enhanced automaticity or triggered activity. In enhanced automaticity of the pacemaker cells results in increase the rate of discharge of action potentials. Pacemaker cells are present in SA node, atria, AV node and the His-Purkinje system. Those of SA nodes are called dominant pacemaker cells and fire, in human, at rate between 60-100 beats per minute (bpm). The other pacemaker cells in other parts of the conduction system are called subsidiary pacemakers and they are usually latent and reset by dominant pacemakers and they fire at a slower rate (40-60 bpm for AV node and 20-40 bpm for Purkinje system). Increase the rate of discharge of action potentials at the pacemaker cells can be due to three mechanisms; (1) a negative shift in the threshold potential (TP), (2) a positive

shift in the maximum diastolic potential (MDP), and (3) an increased rate of phase 4 depolarization. See figure 11. When this happens in the SA node, it leads to a sinus tachycardia, which could be a physiological response to sympathetic overstimulation in case of exercise for example or a pathophysiological reaction to a state of hypovolemia, ischemia or electrolytes disturbance. (**Tse** 2016)

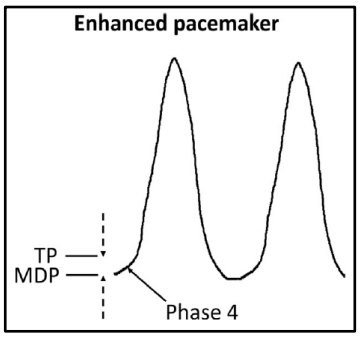

Figure 11: Enhanced pacemaker. TP: threshold potential, MDP; maximum diastolic potential. (**Tse** 2016)

Under conditions of acute myocardial infarction, digitalis toxicity, iso-prenaline administration, and recent cardiac surgery enhanced automaticity could also occur in the AV node. When the discharge rate of the AV node is higher than the sinus rate, it can lead to abnormal rhythms called accelerated junctional rhythms. (**Azevodo** et al. 1973)

The other cause of enhanced automaticity is what is called protected pacemaker which results in production of parasystoles. This occurs when an entrance block blocks a latent pacemaker from the dominant pacemaker (figure 12). This makes from the latent pacemaker to act ectopically and discharge action potentials independently. This block happens when the dominant pacemaker is surrounded by an ischemia, infarction or otherwise compromised tissue which prevents reaching of the action potential to the latent pacemaker. In this case the independently acting latent pacemaker stimulates the rest of the cardiac tissue. (**Gussak** 2003)

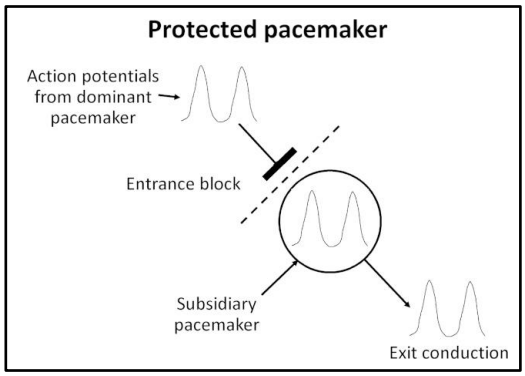

Figure 12: Protected pacemaker. Entrance block of the dominant pacemaker allows exit conduction of the subsidiary pacemaker, which can generate action potentials that excite the rest of the myocardium. (**Tse** 2016)

Other variants of the parasystole are modulated parasystole and automudulation. In modulated parasystole there an incomplete entrance block of the latent pacemaker. This means that the dominant pacemaker or other cardiac tissue has an electrotonic influence on the latent pacemaker and can modulate its firing. If the action potential arrives early at the cycle of the latent pacemaker, it will delay its firing, and if it arrives late at the cycle it will accelerate its firing. The automodulation is a condition where the latent focus exerts an electrotonic influence on the focus itself. Repetition of these influences leads to the development of tachycardia. (**Jalife** et al. 1982; **Satullo** et al. 1992; **Saoudi** et al. 1989)

The other cause of focal activity is the triggered activity, which results from premature activation of cardiac tissues by afterdepolarizations. These are depolarizations triggered by one or more preceding action potentials. These may occur early, i.e. during Phase 2, late, i.e. during phase 3, or delayed, i.e. during phase 4 (figure 13), of action potential. (**January and Riddle** 1989; **Szabo** et al. 1994; **Xie** et al. 2015; **Guinamard** et al. 2004)

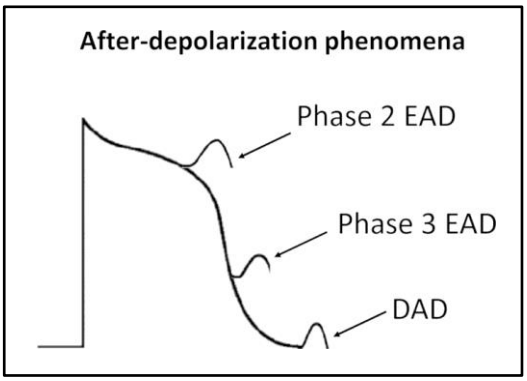

Figure 13: Afterdepolarization phenomena: early afterdepolarization (EAD) occurs early (phase 2) or late (phase 3), and delayed afterdepolarization (DAD) occurs during phase 4 of the action potential. (**Tse** 2016)

The other arm of the mechanism of cardiac arrhythmias is reentry. This occurs when an impulse fails to extinguish itself and reactivates a region of the myocardium that has recovered from refractoriness. This can be divided into reentry that occurs in the presence of an obstacle, whether a structural or functional, or reentry that occurs without the presence of an obstacle, which could be further divided into reflection or phase 2 reentry. (**Janse and Wit** 1989; **Tse** 2016) Figure 14 illustrates this phenomenon.

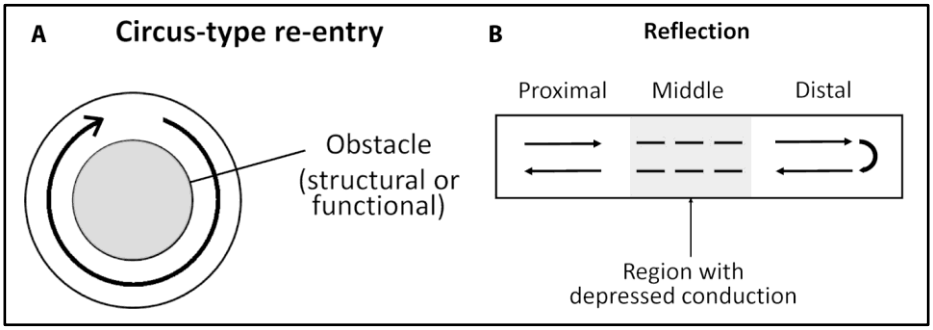

Figure 14: (A) Circus-type reentry requires a structural or functional obstacle (graycenter) around which an action potential can circulate. (B) Reflection. Stimulation of the proximal segment elicits an-action potential. Its conduction across the middle segment cannot take place actively as the extracellular region is ion-free. Instead, it involves electrotonic current spread intracellularly. After a delay, when the membrane potential reaches threshold at the distal segment, another action potential is generated. (**Tse** 2016)

1.5.10 MECHANISM OF ISCHEMIC ARRHYTHMIAS IN ANIMAL MODELS AND THE ROLE OF GAP JUNCTIONS

Mice can be used to validate the genetic basis of human arrhythmias. The reason behind that is that many genes of the mice have a high homology with corresponding human genes. (**Wehrens** et al. 2000) Different mouse models have been used in experimental studies to clerify the various genetic and acquired factors that contribute to classic arrhythmia mechanisms such as abnormal impulse formation caused by triggered activity or enhanced automaticity, or reentry caused by altered conduction or enhanced heterogeneity of conduction and excitability. (**Nattel and Dobrev** 2017; **Dobrev and Wehrens** 2018) Besides the different genetic knockout and knock-in animal models, there is a clear interest of defining the role of gap junctions in cardiac arrhythmias following myocardial ischemia and infarction. (**Wit and Peters** 2012; **Cascio** et al. 2005)

Gap junctions are myocardial protein conduits through which intercellular communication of ions and small signaling molecules occurs. Each gap junction is formed by the union of 2 hemichannels (connexons), each composed of 6 protein subunits known as connexins. (**Söhl and Willecke** 2004) Connexin 43, connexin 40, and connexin 45 are the most prominent connexins in the heart and are associated with electrically active tissue. (Figure 15) The type of connexin expressed, their rates of expression and degradation, distribution, density, and the architecture of the tissue modulate the magnitude of cell-to-cell electrical coupling in heart. These factors are affected by heart disease and therefore contribute to the conditional susceptibility of diseased myocardium to arrhythmia. (**Saffitz** et al. 2000; **Severs** et al. 2004)

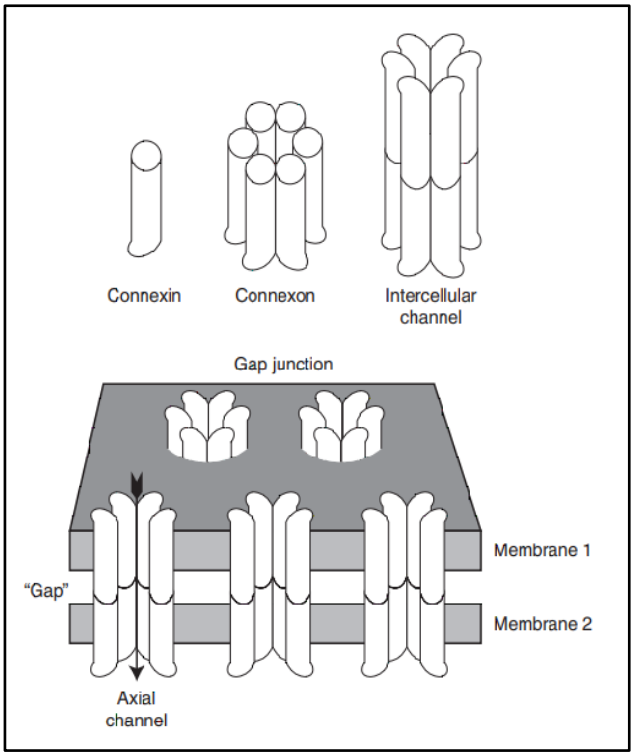

Figure 15: A diagram showing the multiple levels of gap junction structure. Individual connexins assemble intracellularly into hexamers, called connexons, which then traffic to the cell surface. There, they dock with connexons in an adjacent cell, assembling an axial channel spanning two plasma membranes and a narrow extracellular "gap". (**Goodenough and Paul** 2009)

Ventricular arrhythmias caused by myocardial ischemia or infarction can be subdivided into phases based on duration of ischemia. Each phase has a different arrhythmogenic substrate and the nature of the gap junction remodeling and changes differs in each phase. (**Peters and Wit** 1998; **Wit and Peters** 2012; **Wit and Janse** 1993; **Carmeliet** 1999)

These phases are acute phase, which is further divided into phase 1a and phase 1b, delayed phase and subacute and chronic phase.

During phase 1a of the acute phase there is K^+ loss with subsequent Ca^{++} overload. These changes occur within minutes after myocardial ischemia first 10 to 15 minutes. This leads to partial membrane depolarization, decreased action potential amplitude, and velocity of depolarization and postrepolarization refractoriness. During this period of time resistance through intracellular pathways from cell to cell occurring mainly through gap junctions remains unchanged. A reduction in extracellular space occurs as a result of vascular bed collapse and osmotic cell swelling following increased myocardial resistivity. These changes in the membrane potentials and extracellular resistance lead to slowing and heterogeneity of conduction and block resulting in development of polymorphic reentrant arrhythmias. (**Wit and Janse** 1993; **Carmeliet** 1999)

At 15 to 45 minutes of myocardial ischemia, phase 1b, there is a marked decrease in gap junction conductance. This reduction in gap junction conductance is implicated in this phase of arrhythmias. A reduction of oxygen availability leads to K^+ loss from the cells and its accumulation in the extracellular space which leads to intracellular acidosis, a decrease in pH, which closes gap junction channels and renders gap junctions more sensitive to effects of increasing intracellular calcium. Accumulation of other substances, like lysophosphglycerides and arachidonic acid also reduce gap junctional conductance. The presence of catecholamines may also decrease the conductance in the presence of calcium overload. (**Wit and Janse** 1993; **Carmeliet** 1999; **Groot** et al. 2001) These changes are accompanied by focal separation of intercalated disc membranes and reduction in gap junction surface density which is related to reduction of connexin 43 (Cx43) quantity. This is accompanied by appearance of Cx43 on lateral sacrolemmal membranes, a process called lateralization. The lateralized Cx43 represent protein that is not functional junctions and is part of removal of gap junctions from intercalated disks triggered by intracellular acidosis. Gap junction uncoupling is greater intramurally than in border zone regions of ischemic area, where some recovery of the severely depressed transmembrane potentials may occur. As a consequence of these changes, conduction velocity in intramural regions falls steeply and inhomogeneously, creating a suitable environment for reentry. (**Peters and Wit** 1998; **Kieken** et al. 2009; **Macia** et al. 2011)

At 12 to 96 hours of myocardial ischemia, delayed phase, the frequency of ventricular beats increases gradually again. Although it was previously not well known, whether the arrhythmias occurring at this period arise from gap junction remodeling in the endocardial border (Purkinje) zone, it is now well defined that automaticity in surviving Purkinje fibers which give rise to re-entry facilitated by localized unidirectional conduction block, and triggered activity due to delayed after-depolarizations, which are all heavily influenced by sympathetic tone, plays a major role in the mechanism of ischemic arrhythmias. (**Wit and Janse** 1993; **Thomas** et al. 2017)

Over several weeks after myocardial infarction, the subacute and chronic phases, during healing and scar formation, gap junctions disappear from necrotic regions. Survival of myocytes adjacent to scar leads to formation of border zones. Reentry in border zones or myocyte bundles traversing the scar is the principal mechanism of ventricular arrhythmias, but the electrophysiology of reentry is different from acute arrhythmias. Regions of connexin lateralization adjacent to more normal regions of gap junction distribution have poor gap junctional coupling leading to formation of lines of conduction block in reentrant circuits in healing infarcts. (**Peters and Wit** 1998; **Wit and Janse** 1993)

In case of myocardial reperfusion the electrophysiological consequences are variable and depend on the duration of ischemia, with most reperfusion arrhythmias occurring after brief

durations of ischemia (<30 minutes). After the acute intracellular ion changes in acute ischemia, depolarization of the cardiomyocyte transmembrane potential occurs and there will be shortening of the action potential duration. Reperfusion results in a rise in intracellular Ca^{++}, normalization of extracellular K^{+} concentration and recovery of the action potential duration. However, these changes occur in an inhomogeneous manner, reflecting the spatial heterogeneity of regional blood flow restoration within the ischemic zone. This leads to dispersion of refractoriness, which forms the substrate for re-entry. (**Tofler** et al. 1987)

1.5.11 DEFINITIONS OF CARDIAC ARRHYTHMIAS IN EXPERIMENTAL ANIMAL MODELS

Previously, it has been generally accepted that myocardial tissue with an area smaller than 100 mm^2 – 200 mm^2 is not capable of undergoing reentrant and fibrillatory activity. (**Garrey** 1914) It has been found later that the induction of ventricular fibrillation in the mouse heart is possible and reentry and fibrillatory activity has been observed in ventricular tissue with a surface of about 100 mm^2. (**Vaidya** et al. 1999) Later, reentry in the neonatal mouse heart with a surface much smaller than 100 mm^2 was demonstrated. (**Vaidya** et al. 2001) Hence, only a few *in vivo* studies had previously reported the observation of atrial tachycardias in the rat and mouse. A recent experimental study showed induction of the atrial fibrillation (figure 16) after a surgical induction of myocardial infarction through left anterior descending artery ligation without a clear definition of the ECG criteria of atrial fibrillation. (**Ovsepyan** et al. 2011)

The ‘Lambeth Conventions’ is a guidance document, written in 1987 (**Walker** et al. 1988) intended to be of practical value in the investigation of experimental arrhythmias induced by ischaemia, infarction, and reperfusion. (**Curtis** et al. 2013)

1.5.11.1 VENTRICULAR ARRHYTHMIAS

A ventricular premature beat (VPB) is defined as a ventricular electrical complex (complete electrical event: QRS, RS, QRST or RST) that is different in shape (voltage and/or duration, i.e., height and/or width) from the preceding (non-VPB) ventricular complex, and is premature in relation to the preceding ventricular complex (Figure 16). The VPB is usually preceded immediately by a non-VPB ventricular complex but, if it occurs late in the cardiac cycle, the VPB may be preceded by a P wave that is not coupled to it, giving rise to an apparently short PR interval. Atrial premature beats may result in ventricular activation in an aberrant sequence (e.g., bundle branch block) but the arrhythmia should not be classified as a VPB. (**Curtis** et al. 2013)

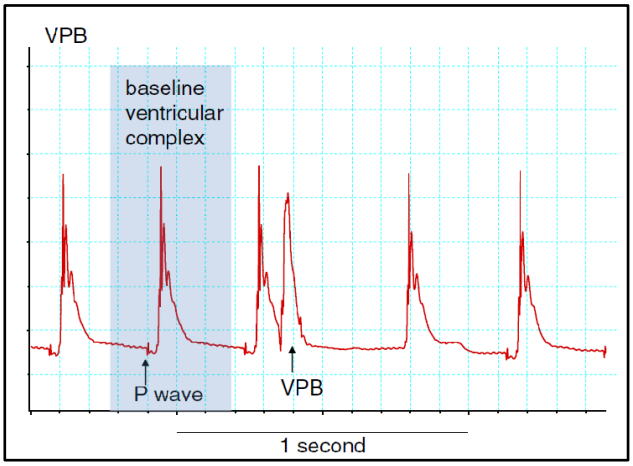

Figure 16: A VPB recorded by unipolar electrocardiogram from a rat heart perfused in the Langendorff mode. The VPB was caused by regional ischaemia. Normal sinus rhythm was present, and an example of a baseline P wave and ventricular complex are shown (set in darker background). (**Curtis** et al. 2013)

Bigeminy has the minimum sequence VPB, normal sinus beat, VPB (which may be repeated) in which the VPBs have the same shape and timing. A run of 2 or 3 consecutive VPBs is defined as a salvo (Figure 17). (**Curtis** et al. 2013)

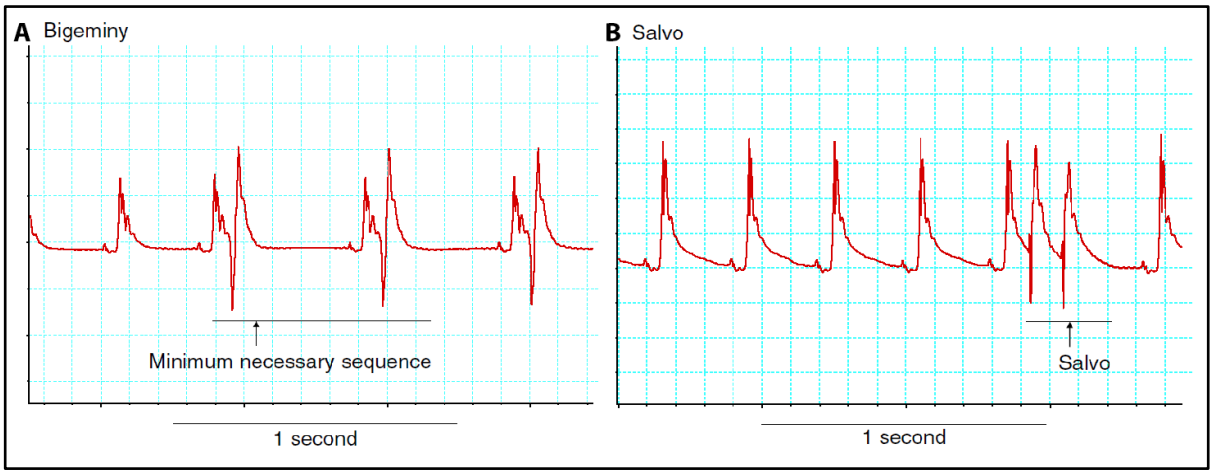

Figure 17: (A) A bigeminy recorded by unipolar electrogram from a rat heart perfused in the Langendorff mode. The bigeminy was caused by regional ischaemia. The bigeminy continued beyond the frame of the figure. The minimum sequence of rhythm sufficient for the diagnosis is labelled. (B) A salvo recorded by unipolar electrogram from a rat heart perfused in the Langendorff mode. The salvo was caused by regional ischaemia. The minimum sequence of rhythm sufficient for the diagnosis is labelled. (**Curtis** et al. 2013)

Ventricular tachycardia VT is defined as a run of four or more consecutive VPBs in the original Lambeth Conventions (**Walker** et al. 1988), but the revised Lambeth Conventions (**Curtis** et al. 2013) propose a change to acknowledge that VT is composed of ventricular complexes that may not necessarily be VPBs. In monomorphic VT, by definition there is a regularity of repetition of ventricular complexes, so it is reasonable to suppose that each complex is an identical VPB (Figure 17A). However this is not necessarily the case when consecutive component complexes vary in peak–peak interval or height. Indeed, a run of VT will comprise of oscillations that may be complete ventricular complexes, or parts of larger complexes (containing multiple oscillations). Thus it is sufficient to define VT as a sequence of ventricular complexes. (**Curtis** et al. 2013)

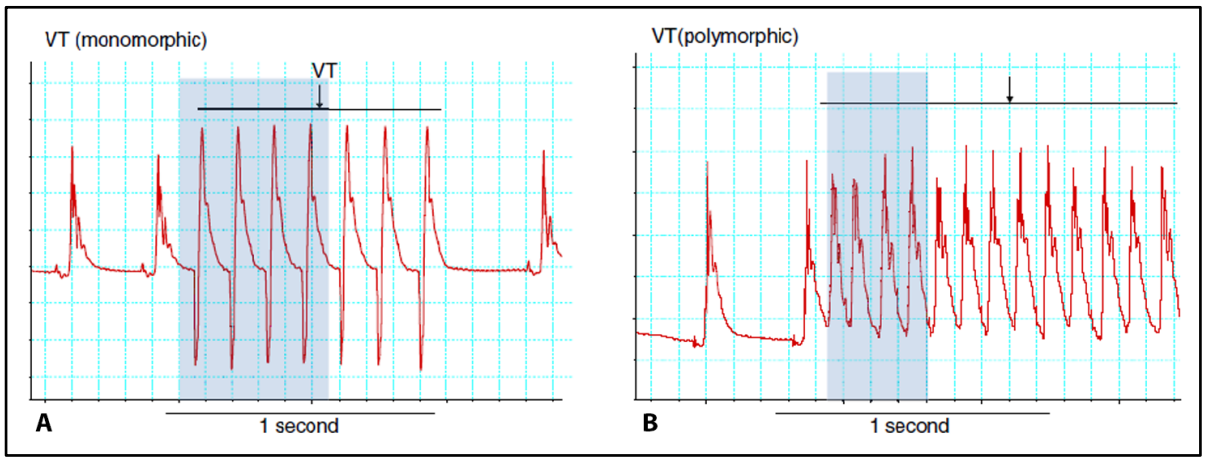

Figure 18: (A) A single episode of VT recorded by unipolar electrocardiogram from a rat heart perfused in the Langendorff mode. The VT was caused by regional ischemia. The minimum sequence of rhythm sufficient for the diagnosis is set in a darker background. The entire run of VT is labeled. In this example the VT is monomorphic. (B) single episode of VT recorded by unipolar electrocardiogram from a rat heart perfused in the Langendorff mode. The VT was caused by regional ischemia. The minimum sequence of rhythm sufficient for the diagnosis is set in a darker background. The entire run of VT is labeled. In this example the VT is polymorphic. (**Curtis** et al. 2013)

Torsade(s) de pointes (TDP) is a type of polymorphic VT defined as a sequence of a minimum of 4 consecutive ventricular complexes for which height varies progressively (with the possible inclusion of a characteristic twisting of the peaks, which constitutes progressive variation in intrinsic shape) and for which peak–peak interval may be constant or may vary (Figure 19). To fit with the definitions of VT, the minimum number of consecutive complexes necessary to define TDP is 4. However, TDP is regarded in the cardiology community as a condition defined by observing twisting of peaks in the ECG. One cannot always readily identify twists from 4 consecutive complexes. (**Curtis** et al. 2013)

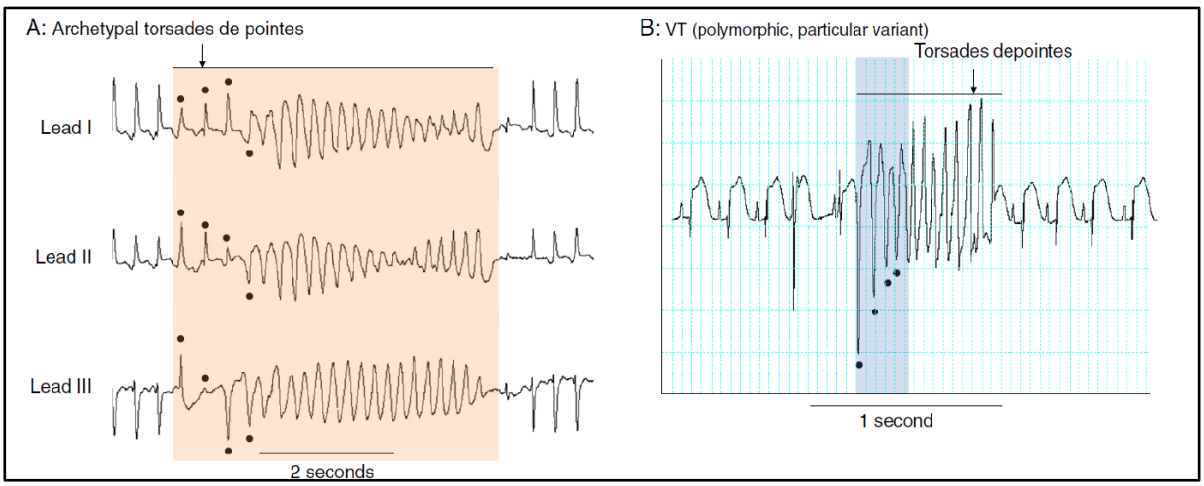

Figure 19: (A) An archetypal example of TDP recorded in an anaesthetized rabbit. Black dots indicate the 'peaks' of the first four ventricular complexes that 'twist' around the isoelectric line. Not all TDP is archetypal, so the minimum sequence for the definition requires elaboration. (B) A single episode of polymorphic VT of the TDP variety, recorded by unipolar electrocardiogram from a normal guinea pig heart perfused in the Langendorff mode. The entire run of polymorphic VT is labeled, and the minimum sequence of rhythm sufficient for the diagnosis of TDP is set in a darker background. Black dots indicate the 'peaks' of the first 4 ventricular complexes. In this example TDP is preceded by a VPB that provides a 'short-long-short' RR interval sequence before TDP onset. (**Curtis** et al. 2013)

Ventricular fibrillation (VF) is defined as a sequence of a minimumof 4 consecutive ventricular complexes without intervening diastolic pauses, in which the intrinsic shape, the peak–peak interval and the height vary, and the variation between each is non-progressive (Figure 20). It is the nonprogressive nature of the variation of all 3 variables that distinguishes VF from polymorphic VT and TDP. (**Curtis** et al. 2013)

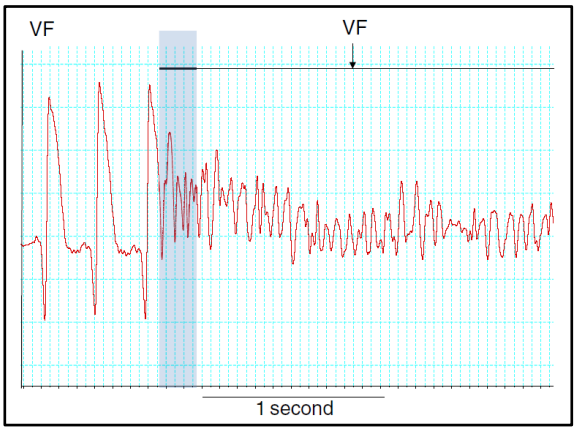

Figure 20: A single episode of VF recorded by unipolar electrogram from a marmoset (Callithrix jacchus) heart perfused in the Langendorff mode. The VF was caused by regional ischaemia. The minimum sequence of rhythm sufficient for the diagnosis is set in a darker background. The start of the run of VF is labelled; it continued beyond the frame of the figure. (**Curtis** et al. 2013)

1.5.11.2 ATRIAL ARRHYTHMIAS

An atrial premature beat (APB) is a P wave premature in relation to the timing of prevailing P waves. It may vary or be identical in morphology to the P waves of the baseline rhythm. P wave timing may change as a consequence of a ventricular arrhythmia, but an APB is not coupled to (i.e., driven by) the ventricular complex of an underlying ventricular arrhythmia, since the locus is atrial. A series of 2 or 3 APBs represents an atrial salvo (consistent with the definition of a ventricular salvo, albeit this is not common parlance yet) and 4 or more APBs corresponds to an atrial tachycardia (AT), which is defined by the presence of discrete P wave activity separated by an isoelectrical line (this differs from VT where no 'diastolic interval' is present). These P waves may appear identical to the sinus rhythm P wave. The rate and morphology of these P waves is constant. (**Curtis** et al. 2013)

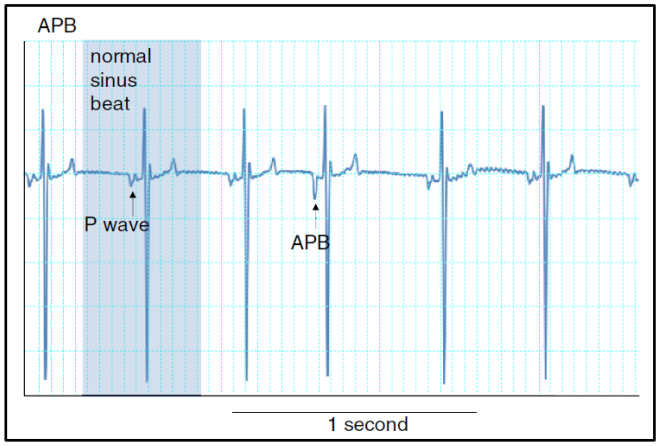

Figure 21: A single Atrial Premature Beat (APB) recorded on a continuous volume conducted ECG in a Langendorff perfused rabbit heart. The 4th beat is an APB with a clear difference in P wave morphology from the other sinus rhythm beats (example set in darker background). Note the 'compensatory pause' following APB. (**Curtis** et al. 2013)

Atrial flutter (AFL) is defined as identifiable consecutive repetitive P waves of identical morphology, but with no clear isoelectrical diastolic interval (Figure 22A). A minimum of 4 such P waves is required for classification of an arrhythmia as AFL. The associated ventricular rhythm may be regular or irregular. (**Curtis** et al. 2013)

Atrial fibrillation (AF) is defined as a sequence of uninterrupted atrial complexes that can no longer be distinguished from one another as P waves, and where consecutive complexes vary in peak–peak interval, height and in intrinsic shape, with the variation being neither progressive nor repetitive (Figure 22B). A minimum of 4 such complexes is required for classification of an arrhythmia as AF. (**Curtis** et al. 2013)

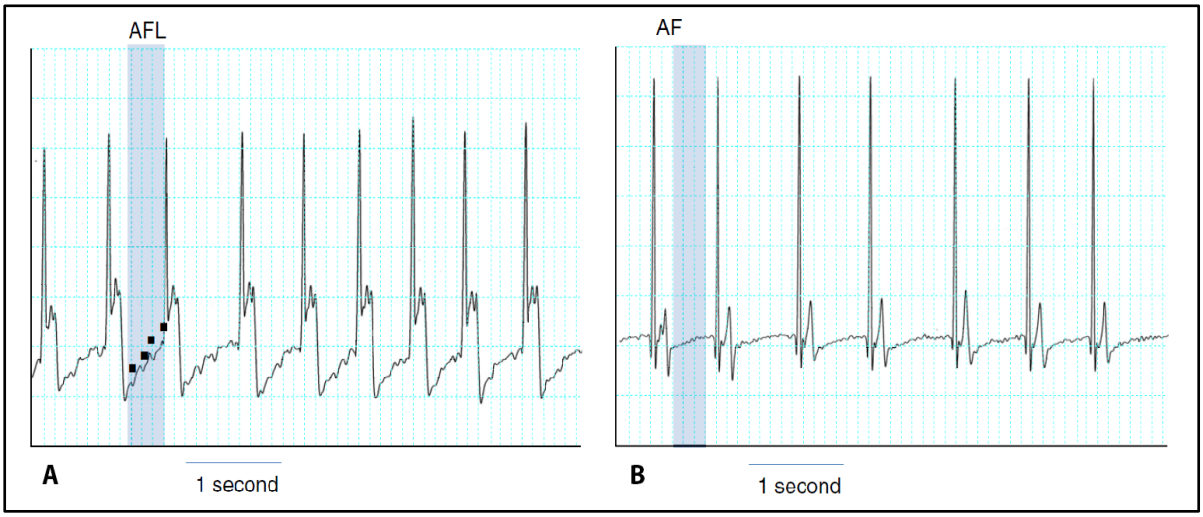

Figure 22: (A) A single episode of atrial flutter (AFL) recorded using body surface ECG lead II in a conscious mixed breed mongrel dog. The minimum sequence of rhythm sufficient for diagnosis is set in the darker background. The AFL occurred following acute myocardial ischemia (2 min occlusion of left circumflex artery) in an animal with a healed anterior wall myocardial infarction. Baseline HR was 114 beats/min. (B) A single episode of atrial fibrillation (AF) recorded using body surface ECG lead II in a conscious mixed breed mongrel dog. The minimum sequence of rhythm sufficient for diagnosis is set in the darker background. The AF occurred following acute myocardial ischemia (2 min occlusion of left circumflex artery) in an animal with a healed anterior wall myocardial infarction. Baseline HR was 98 beats/min. (**Curtis** et al. 2013)

1.6 MESENCHYMAL STEM CELLS (MSCS)

The bone marrow is seen as an organ composed of the hematopoietic tissue proper and the associated supporting stroma. The bone marrow is also the only known organ in which two separate and distinct stem cells not only co-exist but also functionally cooperate. Originally examined because of their critical role in the formation of the hematopoietic microenvironment, marrow stem cells appeared more recently at the center stage with the recognition that mesenchymal stem cells (MCS) may be induced experimentally to undergo unorthodox differentiation like neuronal, myogenic, and liver cells. (**Bonnet** 2003)

Hematopoieisis occurs with bone marrow in association with an heterogeneous population of non-hematopoietic cells, including mesenchymal cells, connective tissue-type cells, and their associated extracellular matrix components and growth factors which constitute collectively the stroma of the bone marrow. (**Lichtman** 1981; **Weiss** 1976)

No unique cell surface marker unequivocally distinguishes mesenchymal stem cells (MSCs) from other hematopoietic stem cells (HSCs), making a uniform definition difficult. (**Williams and Hare** 2011) The International Society for Cell Therapy (ISCT) proposed a criteria that includes: (1) adherence to plastic in standard culture conditions; (2) expression of the surface

molecules CD73, CD90, CD105 in the absence of CD34, CD45, HLA-DR, CD14 or CD11b, CD79a or CD19 surface molecules as assessed by fluorescence-activated cell sorting (FACS) analysis; (3) capacity for differentiation to osteoblasts, adipocytes, and chondroblasts in vitro. (**Dominici** et al. 2006)

A subset of MSCs expressing the marker neurotrophic growth factor (CD271) has been shown to have similar differentiation capacity as traditional MSCs, but secrete higher levels of cytokines and have greater immunosuppressive properties. (**Kuçi** et al. 2010)

1.7 REGENERATIVE MEDICINE AND ITS ROLE IN CARDIAC ARRHYTHMIAS

New innovative therapeutic approaches has been emerged to overcome the various shortcomings of the currently utilized gold-standard therapies of the arrhythmias, such as drugs, electronic pacemakers, implantable cardioverter defibrillators, heart transplantation. (**Monteiro** et al. 2017) These innovative approaches focus on the improvement of cardiac function in pathological situatons involving loss of working cardiomyocytes, as is the case of acute myocardial infarction (**Hirt** et al. 2014) or are intended to decrease the occurrence of arrhythmias and/or to restore the disrupted cardiac conduction or action potential (**Motloch and Akar** 2015)

A close interaction between specialized excitatory and conductive components and the working cardiomyocytes (contractile component) is essential for the successive and rhythmic contractions and relaxations of the myocardium. This functionally proficient cardiac electrical coupling is highly dependent on molecular components (e.g., ion channels, gap junctions) thus, gene-related therapies with their targeted delivery, may potentially repair cardiac electrophysiology. Additionally, the potential of cell therapies to modulate cardiac electrical integrity has also been under recent study. (**Monteiro** et al. 2017)

1.7.1 GENE THERAPIES TO TREAT ARRHYTHMIAS

Gene therapy approaches for treating or reducing cardiac arrhythmias involve: (1) direct repair of intercellular conduction mainly through overexpressing connexins (**Greener** et al. 2012; **Igarashi** et al. 2012); (2) modulation of action potential characteristics (**Protas** et al. 2009; **Lau** et al. 2009; **Coronel** et al. 2010); and (3) restoration of calcium cycling primarily by upregulating SERCA2a. (**Lyon** et al. 2011; **Cutler** et al. 2012) SERCA2a is a key regulator of cardiac contractile force. (**Györke and Györke** 1998; **Bode** et al. 2011).

In most studies, the effects of gene therapies have been demonstrated in animal models of MI and atrial fibrillation. In general, these strategies resulted in a reduced rate of occurrence of ventricular arrhythmias; reduced ventricular arrhythmia inducibility, assessed by pro-

grammed electrical stimulation of the myocardium and ECGs; and increased conduction velocities, observed through *ex vivo* optical mapping and *in vivo* invasive electrograms. Of note, restoration of Ca2+ cycling through SERCA2a overexpression has been applied not only in animal models, but also in humans, particularly in the calcium-upregulation by percutaneous administration of gene therapy in cardiac disease (CUPID) phase 1/2 clinical trial. (**Jaski** et al. 2009; **Zsebo** et al. 2014)

1.7.2 ROLE OF CELL THERAPIES ON CARDIAC ELECTRICAL INTEGRITY

Cell therapies are one of the most extensively explored approaches, which involve different cell types (e.g., mesenchymal stem/stromal cells (MSC), skeletal myoblasts, embryonic stem cell-derived cardiomyocytes, cardiac progenitor cells). (**Sanganalmath and Bolli** 2013)

1.7.2.1 MESENCHYMAL STEM/STROMAL CELLS (MSC) AND CARDIAC ARRHYTHMIAS

Studies involving mesenchymal stem cells or bone marrow-derived cells have shown promising results, in both animal models and clinical trials, in terms of neovascularization, reduced infarct size and improved LV function. (**Mathiasen** et al. 2015; **He** et al. 2013; **Santos Nascimento** et al. 2014) However these cells raised controversy concerning their arrhythmogenicity. (**Wang** et al. 2011; **Wei** et al. 2012; **Mureli** et al. 2013; **Askar** et al. 2013)

Some authors showed that MSC or bone marrow-derived cells have a pro-arrhythmic potential in vivo hypothesizing that such effect could be a consequence of the electrical unexcitability of these cells, paracrine factors or the accumulation of inflammatory mediators. (**Pak** et al. 2003; **Price** et al. 2006; **Kim** et al. 2010) Although MSC are electrically unexcitable cells, *in vitro* studies showed that they are capable of repairing conduction block, in neonatal cardiomyocyte cultures, through connexin-mediated coupling. (**Beeres** et al. 2005; **Pijnappels** et al. 2006) Other authors consider MSCs to have antiarrhythmic effect stating that heterocellular electrical coupling may cause reduced action potential propagation velocities and gradients of duration of repolarization, which could promote the occurrence of reentry circuits and consequently arrhythmias. (**Chang** et al. 2006; **Askar** et al. 2013)

Additionally, disruption of the myocardial electrical integrity caused by paracrine factors released from MSCs can also be promoted not only by altering action potential characteristics, ion channel expression and increase re-entry inducibility of cardiomyocytes (**Askar** et al. 2013); but also by promoting cardiac nerve sprouting and sympathetic hyperinnervation. (**Pak** et al. 2003; **Kim** et al. 2010)

Oppositely, other studies indicate that MSCs can reduce the electrical disruption in a myocardial infarction scenario or even exert an anti-arrhythmic effect. (**Mills** et al. 2007; **Wang** et

al. 2011; **Wei** et al. 2012) These studies showed that MSC decreased ventricular arrhythmia inducibility, reduced the disruption of gap junction organization in cardiomyocytes and improved the electrical activity of the infarct border zone. Although the mechanism of this positive effect is unclear, it has been assumed that MSC-cardiomyocytes gap junction-mediated coupling support action potential propagation into the infarcted area, reducing the length of the anatomical conduction path and reducing the incidence of reentry arrhythmias. Additionally, it was suggested that the lack of electrical excitability in combination with the intercellular coupling could not have a significant pro-arrhythmic effect because the number of surviving MSCs in the myocardium decreases in few days, being the proportion of MSC to cardiomyocyte much lower than in *in vitro* experiments where arrhythmogenicity was shown.
Thus, although MSCs are electrically unexcitable and incapable of electromechanical coupling with the host myocardium, evidences point to beneficial effects in cardiac function in the absence of side effects. (**Monteiro** et al. 2017)

1.7.2.2 SKELETAL MYOBLASTS AND CARDIAC ARRHYTHMIAS

Skeletal myoblasts were among the first cell types applied in animal and clinical studies as cell therapies targeting cardiovascular diseases. This interest mainly arose from their proliferation capacity, increased resistance to ischemia, electrical excitability and the possibility for autologous use. (**Durrani** et al. 2010) However, skeletal muscle cells do not express connexins upon the formation of myotubes thus exhibiting minimal intercellular coupling. This feature makes efficient integration of skeletal myoblasts within the myocardium impossible which leads to an increased frequency of arrhythmic events, despite reported positive effects regarding other aspects. (**Fernandes** et al. 2006; **Mills** et al. 2007; **Menasché** et al. 2008)
Lacking intercellular coupling, these cells form clusters which are electrically isolated from the myocardium, blocking action potential propagation in that region, thus rendering the electrical activity of the cells almost irrelevant. To overcome this limitation, some authors overexpressed Cx43 on cultured skeletal myoblasts which improved electrical coupling with cardiomyocytes. (**Suzuki** et al. 2001; **Tolmachov** et al. 2006) Intramyocardial injection of these cells in a cryoinjury induced myocardial infarction in murine model improved electrical coupling between skeletal myoblasts and host cardiomyocytes, with lower incidence of sustained arrhythmias and the ventricular arrhythmia inducibility decreased when compared to regular skeletal myoblast injection. (**Roell** et al. 2007)
As the clinical relevance of skeletal myoblast relies on Cx43 overexpression, alternative non-viral methods of gene expression should be further explored. (**Kolanowski** et al. 2014)
As a conclusion one can say that for cells that are able to survive and proliferate after transplantation into the myocardium, intercellular coupling and electrical and mechanical proper-

ties that closely mimic native cardiomyocytes, are necessary to significantly improve electro-mechanical function. (**Monteiro** et al. 2017)

1.7.2.3 EMBRYONIC STEM CELLS AND INDUCED PLEURIPOTENT STEM CELLS AND CARDIAC ARRHYTHMIAS

Pluripotent stem cells, which include embryonic stem cells (ESCs) and induced pluripotent stem cells (iPSCs), possess highly *in vitro* proliferative capacity and are capable to differentiate into a variety of cell lineages, including cardiomyocytes. These features allow generation of a great number of cells representing immature cardiomyocytes' phenotype and function. ESC-derived cardiomyocytes display immature contractile components and are capable of spontaneous action potential generation. This inherent automaticity increases the possibility of induced arrhythmias after their intra-myocardial transplantation. (**Fernandes** et al. 2006; **Fernandes** et al. 2009; **Chong** et al. 2014; **Shiba** et al. 2014)

2 MATERIALS AND METHODS

2.1 BONE MARROW ASPIRATION

Written consents were given to the informed donors for the aspiration of their bone marrow according to the Declaration of Helsinki. This study was approved by the ethical committee of the University of Rostock (registered as no. A 2010 23) as of April 29th, 2010. Bone marrow samples were obtained through sternal aspiration from patients who underwent coronary artery bypass graft (CABG) surgery at Rostock University Medical Center, Germany. After skin incision and dissection until the sternum 100 ml of bone marrow were aspirated prior to performing a median sternotomy. The aspirated bone marrow has been instilled in 2 tubes with 50 ml capacity. Anticoagulation was done by heparinization with 250 I.U./ml sodium heparine (B. Braun Melsungen GmbH, Melsungen, Germany). The aspiration procedure did not lead to any complication. The heparinized samples were delivered to the research laboratory in a protected manner with the standard transport of the Rostock University Hospital.

2.2 CD271+ CELL ISOLATION

Mononuclear cells fraction was isolated by density gradient centrifugation using Lymphocyte Separation Medium (LSM;1.077 g/l, PAA, Pasching, Austria). Mononuclear cells have been indirectly labeled with CD271-APC/anti-APC-microbeads (Miltenyi Biotec, Bergisch Gladbach, Germany) and enrichment of $CD271^+$ cells has been performed by positive magnetic selection using the magnet activated cell sorting (MACS) system (Miltenyi Biotec).

2.2.1 MATERIALS

During the isolation of the CD271+ stem cells from the human bone marrow samples the following materials has been utilized:

- Leukosep tubes 50 ml, 15 ml and 1 ml (Greiner)
- Sterlie 3 ml serum pipet (Greiner)
- Counting chamber, Neubauer improved (Marienfeld)
- RPMI 1640 Medium
- Collagenase B
- DNAse (I)

- Lymphocyte separations medium (LSM 1077) (PAA)
- 3% Acetic acid / Methylene Blue (Stem Cell Technologies)
- MACS 25 MS columns (Miltenyi Biotec)
- MACS 25 LS columns (Miltenyi Biotec)
- Pre-separation filter (Miltenyi Biotec)
- CD271 Micro Bead Kit, (APC) human (Miltenyi Biotec), contains:
- 1x2 ml FCR Blocking Reagent
- 1x2 ml Anti-APC-Microbeads
- 1x1 ml CD 271 (LNGFR)-APC
- Buffer
    - PBS/EDTA, 2 mM; buffer (sigma) from:
    - PBS (1x)
    - EDTA (Powder)
- MACS buffer (sigma) from:
    - PBS / EDTA, 2mM Buffer
    - plus Albumin, from bovine serum (BSA)

2.2.2 THE PROCEDURE OF CD271+ CELL ISOLATION FROM HUMAN BONE MARROW

After receiving the bone marrow aspiration samples from the clinic of cardiac surgery, as described above, with an average amount of about 50 ml, the clot were collected with 10 ml pipet.

RPMI medium was prepared with 1 aliquot each of collagenase and DNAse per 20 ml of received bone marrow.

Portions of 10 ml of bone marrow were pipetted in 50 ml tubes and 6 ml of PBS/EDTA were added to each tube. Then 20 ml of prewarmed RPMI were added, 175 µl collagenase B stock solution and 175 µl of DNAse (I) stock solution (10 mg/ml) to each tube. The final concentration of collagenase B was 0,02%, and that of DNAse (I) was 100 U/ml. This was then incubated for 30 minutes at room temperature with gentle shaking. Then 15 ml of LSM were applied into a 50 ml Leukosep tube and then spin down.

35 ml of diluted bone marrow locating on the top were then carefully layered and centrifuged with 445xg for 35 minutes at room temperature. The tubes were then carefully removed without shaking. The fatty layer and the grease drops was carefully taken off from the surface of the liquid. The white/clear layer of monocytes with a 1000 µl pipet was then collected (usually about 15 ml). These monocytes were the transferred into new 50 ml tube and filled it up with PBS/EDTA until 50 ml marker of the tube.

A sample of 10 µl mononuclear cells was taken and transferred into 1,5 ml Eppendorf tube for counting (mononuclear cells/total-nuclear cells) and was mixed with 10 µl 3% acetic acid / methylene blue and applied 10 µl into a counting chamber and the cells were counted while centrifuging cell in the tube at 300xg at room temperature for 10 minutes and the supernatant was discarded.

A slow re-suspension of cells in cold MACS buffer (4°C), 800 µl total volume per $1*10^8$ total cells, was performed. Then 100 µl FCR blocking reagent per $1*10^8$ total cells were added, and finally 100 µl anti-CD271-APC per $1*10^8$ total cells were added.

This was then mixed well and incubated for 10 minutes at 4 °C and during the incubation this was manually and softly shaken 2-3 times.

The cells were then washed with MACS buffer at 4°C, (1-2 ml per $1* 10^8$ total cells**)** and then centrifuged with 300xg at 4°C for 10 minutes. The supernatant was after centrifugation discarded.

The cell pellet was then re-suspended in cold MACS buffer (4°C), 700 µl total volume per $1*10^8$ total cells. Then 100 µl FCR blocking reagent per $1*10^8$ total cells were added and re-suspend and finally 200 µl anti- APC-MicroBeads per $1*10^8$ total cells were added.

This was mixed well and incubated for 15 minute at 4°C and during the incubation this was manually and softly shaken 2-3 times.

The cells were then washed with 10 ml cold MACS buffer (4°C) per $1*10^8$ total cells and centrifuged with 300xg at 4°C for 10 minutes and the supernatant were then discarded.

The cell pellet was re-suspended in cold MACS buffer (4°C), 500µl per $1*10^8$ total cells (minimum amount).

MACS column were chosen according the cell count. For less than $1,2*10^8$ cells, MS columns were used and for more than $1,2*10^8$ cell, use LS columns were used. Columns and pre-separation filter were previously stored at 4°C.

The MACS MS / LS column with pre-separation filter were equilibrated with 0,5 ml (MS) / 3 ml (LS) MACS buffer (4°C). The supernatant were then discarded.

The cell pellet was re-suspended in cold MACS buffer (4°C), 500µl per $1*10^8$ total cells (minimum amount) and then applied to MACS MS/LS column. See figure 23.

This was washed 3 times with 0,5 ml (MS) / 3 ml (LS) cold MACS buffer (4°C).

During 3rd washing step, a second (new) MACS MS / LS column was equilibrated with 0,5 ml (MS) / 3 ml (LS) cold MACS buffer (4°C). The cell fraction was then eluted with 1 ml (MS) / 5 ml (LS) MACS buffer (4°C), using the supplied plunger, directly into the second equilibrated column while keeping column and plunger sterile. This was washed also 3 times with 0,5 ml (MS) / 3 ml (LS) cold MACS buffer (4°C). and then the cell fraction was eluted from the second column with 1 ml (MS) / 5 ml (LS) cold MACS buffer (4°C) into an 1,5 ml Eppendorf

tube / 15 ml tube, using the supplied plunger. The cells were then spin down at 300xg at 4°C for 10 minutes and the supernatant were carefully removed.

The cells were re-suspended in 100 µl cold MACS buffer (4°C), and a sample of 10 µl CD271+ was taken and mixed with 10 µl 0,025% Trypan Blue. 10 µl of the mixture were applied into a counting chamber and a cell count was performed. The 1,5 ml Eppendorf tube of CD271+ were at 4°C stored for further use in the experiment.

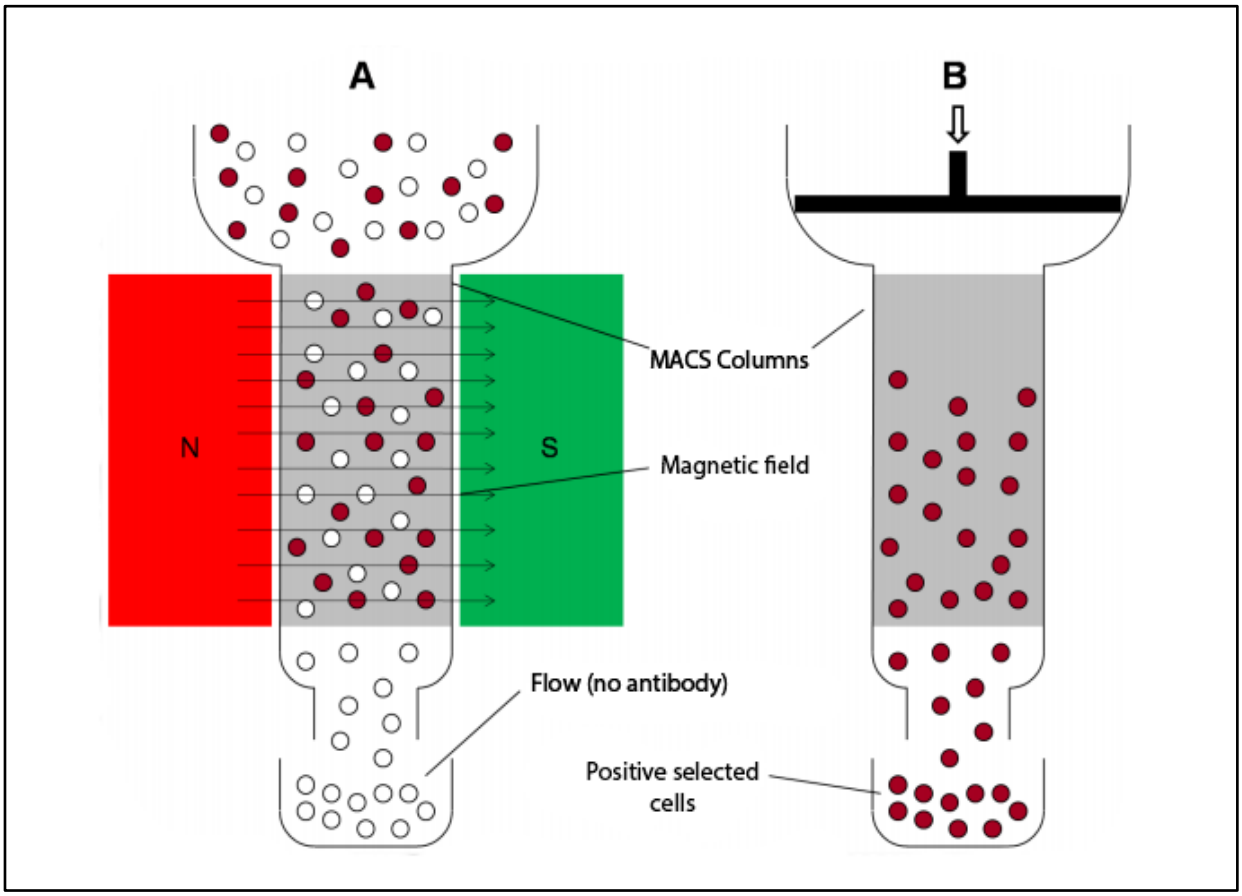

Figure 23: The principle of magnetic separation. (A) A cell suspension passes through a strong magnetic field. The MicroBeads-markerd cells would be retained (red colored cells) and the cells without MicroBeads would pass through. (B) The retained cells would be washed out of the column. (**Johannes Frank** 2013)

2.3 FLOW CYTOMETRIC ANALYSIS

This part of the laboratory work has been done by Ms. Sarah Sasse in our research laboratory as part of her medical doctorate and the data has been provided friendly by her. The materials and methods are briefly described below.

The Purity and the viability of all isolated human bone marrow derived CD271+ cells were verified by flow cytometry. All the Antibodies were mouse-anti-human and for the control of gating strategy appropriate mouse-isotype antibodies have been considered.

For optimal multicolor setting and correction of the spectral overlap single stained controls were utilized and gating strategy was performed with matched isotype/fluorescence minus one control. $CD271^{+}$ cells with a low granularity (SSC^{low}) were included for further flow cytometric analysis and positivity for mesenchymal markers such as CD29, CD44, CD73, CD105 and CD271 was evaluated based on viable $CD45^{-}$ cells in an established 6 fold staining as previously described. (Lemcke et al. 2017b) After performing antibody staining as described above, 15µM DAPI was added, cells were incubated for 2 minutes at room temperature and then immediately acquired.

2.3.1 MATERIALS

- BD LSRII flow cytometer (BD Biosciences)
- BD Falcon 5 ml Tubes (BD Biosceinces)
- Anti-CD271-allophycocyanine (Miltenyi Biotec)
- Anti-CD45-allophycocyanin-H7 (BD Biosciences)
- Anti-CD45-Horizon V500 (BD Biosciences)
- Anti-CD29-allophycocyanin (BD Biosciences)
- Anti-CD44-Peridinin chlorophyll protein-Cyanine 5.5 tandem dye (BD Biosciences)
- Anti-CD73-phycoerythrin (BD Biosciences)
- Anti-CD73-7-aminoactinomycin (BD Biosciences)
- Anti-CD105-Alexa Fluor 488 (AbD Serotec)
- Near-IR live dead stain and 4',6-Diamidino-2-phenylindole (DAPI) (Thermo Fisher)
- MACS-buffer (PBS, 2mM EDTA, 0.5% bovine serum albumin)
- FcR blocking reagent (Miltenyi Biotec)
- RBC lysis buffer (Red Blood Cell, eBioscience
- FACSDiva™ software, version 6.1.2 (BD Biosciences)
-

2.4 ANIMALS

The study protocol was approved by the federal animal care committee of LALLF Mecklenburg-Vorpommern/Germany (approval number LALLF M-V/TSD/7221.3-1-020/14). $Rag2^{-/-}\gamma c^{-/-}$-mice (strain C;129S4-*Rag2*$^{tm1.1Flv}$*Il2rg*$^{tm1.1Flv}$/J) have been purchased from the Jackson Laboratory (Bar Harbor, USA).

The animals were kept in the institute of Experimental Surgery of the faculty of medicine of the Rostock University during both pre- and postoperative periods. The animals were placed

in a special cage with a free access to water and clean standard feed. The bedding of the cage has been made with special wood fibers (Alton) and cellulose with regular changes. The animals were placed in a room with obtained 12 hour-day-night cycle.

2.5 EXPERIMENTAL PROCEDURE

2.5.1 EXPERIMENT DESIGN

Twelve to fourteen-week-old female Rag2$^{-/-}$γc$^{-/-}$-mice (n=22) were randomly assigned to undergo the experiment and they were divided into three groups:

- Untreated re-infarction group (URI, n=9), implantation of telemetry device with induction of myocardial infarction-reperfusion using temporary LAD ligation with a permanent re-ligation after 1 week.
- Stem cell treated re-infarction group (SRI, n=6), implantation of telemetry device with induction of myocardial infarction-reperfusion using temporary LAD ligation with concomitant intra-myocardial injection of isolated fresh CD271+ human bone marrow stem cells (MSC) with a permanent re-ligation after 1 week.
- Myocardial infarction control group (MIC, n=6), implantation of telemetry device with induction of myocardial infarction-reperfusion using temporary LAD ligation with a re-thoracotomy after 1 week (without performing a second myocardial infarction).
- One mouse died early after the induction of the second infarction and has been excluded from the experiment.

2.5.2 MATERIALS

- Rag2$^{-/-}$γc$^{-/-}$-mice, 12-14 weeks old, female (Jackson Laboratory, Bar Harbor, USA)
- Telemetric transmitter, TA11ETA-F10 Implant (Data Sciences International “DSI”, New Brighton, USA)
- Ponemah Physiology Platform (DSI)
- ecgAUTO 1.5.11.26 software (EMKA Technologies, Paris, France).
- Operation plate, with warming ability, (Leica)
- Stereo microscope (Carl Zeiss)
- Harvard Apparatus Mouse ventilator, MiniVent (Hugo Sachs Elektronik GmbH, Germany)
- Scissors, Vannas, 8 mm straight (Aesculap)
- Micro scissors, 120 mm curved (Aesculap)

- Cuticle Scissors, curved, extra fine, 90 mm (Aesculap)
- Micro pins, 110 mm (Aesculap)
- Surgical pins, (Aesculap)
- Anatomical pins, 115 mm, very fine, (Aesculap)
- Micro needle holder, 160 mm, curved (Aesculap)
- Wound retractor, 50 mm (Aesculap)
- Microliter syringe, RN, (Hamilton)
- Prolene 8/0, non-absorbable suture material (Ethicon)
- VasoFix I.V. Cannula, Blue, 22 Gauge, 25 mm, (B. Braun)
- Safil violet, DS 19, absorbable suture material (B. Braun)
- Phenobarbital ampoule, 200 mg/ml (DESITIN)
- 0,9% NaCl Slution
- 20 µl BD Matrigel^{TM} Matrix (BD Biosciences)
- MACS-buffer

2.5.3 AMBULATORY ECG MONITORING AND LIGATION OF THE LEFT ANTERIOR DESCENDING ARTERY

For the purpose of ambulatory electrocardiogram (ECG) monitoring, Rag2$^{-/-}$γc$^{-/-}$-mice (n=22) were implanted with a telemetric device. The mice have been anesthetized with intraperitoneal injection of pentobarbital (200 mg/ml ampoule with 1:25 dilution with 0,9% NaCl solution, 50 mg/kg). A surgical incision was made on the left side of thorax parallel to the rips in order to implant a telemetric transmitter into a subcutaneous pocket with two wire electrodes placed over the thorax. The leads were inserted after tunneling them to the right upper and left lower thorax (figure 24). The acquired ECG signals were recorded using Ponemah Physiology Platform until 48 hours following LAD ligation and the start of myocardial infarction. Telemetric ECG signals were manually analyzed for the developed ventricular arrhythmias which were then classified and counted using ecgAUTO 1.5.11.26 software.

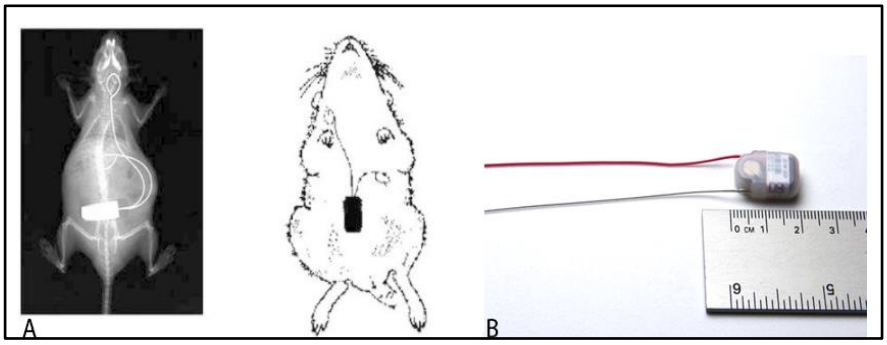

Figure 24: (A) Radiograph/sketch showing location of the implanted telemetry transmitter. (**Späni** et al. 2003) (B) DSI PhysioTel® ETA-F10 for mice. (**DSI**, a division of Harvard Biosceince, Inc.)

For the induction of myocardial infarction, mice were randomly divided into three groups: (untreated re-infarction, URI; stem cell treated re-infarction, SRI; MI control, MIC). All the three groups underwent 1st thoracotomy in addition to the ligation of the left anterior descending artery (LAD). After 45 minutes from the LAD ligation each mouse received an intramyocardial application of 20 µl BD Matrigel™ Matrix (BD Biosciences USA)/MACS-buffer in a ratio of 1:2. In animals with stem cell treatment (SRI group) the solution contained 100,000 CD271+MSC. 4×5 µl were injected along the border of the blanched myocardium and then the node was re-opened allowing a reperfusion of the myocardium (here: ischemia/reperfusion) leaving the suture, as described in figure 25, in a flexible atraumatic tube under the skin. The ECG signals were recorded for 48 hours. Seven days after this ischemia/reperfuison, mice underwent a 2nd thoracotomy at which animals of URI as well as SRI group underwent permanent LAD ligation at the same position of the vessel using the already placed suture from the 1st ligation (here: re-infarction). The flexible tube was useful to easily find the suture material which then simply exempted from the surrounding tissue. The mice of the MIC group underwent a similar 2nd surgical procedure, thoracotomy, without performing LAD ligation.

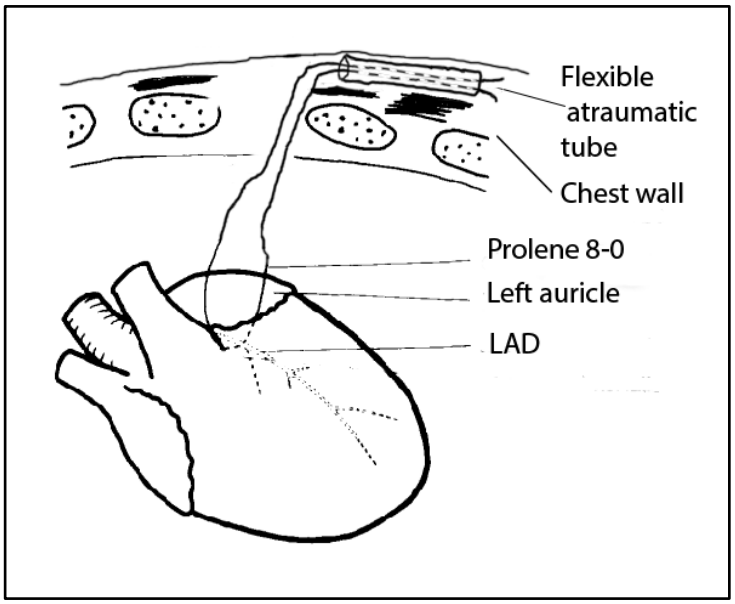

Figure 25: Schematic drawing of the LAD ligature positioning. After 1st LAD ligation, the node was re-opened leaving the ligature in the heart looped around the LAD with their ends kept inserted in a soft flexible tube placed subcutaneously.

2.6 ORGAN HARVESTING

After 9 days from the start of the experiment, 48 hours after 2nd operation, the mice underwent euthanization. This was performed after anesthetizing the mice with phenobarbital by giving 5% potassium chloride (KCL) solution. Each heart was removed, embedded in

O.C.T.™ Compound (Tissue-Tek®; Zoeterwoude, Netherlands) and snap-frozen in liquid nitrogen which then stored in -80 °C freezer (Heraeus). For the purpose of later histological examination of the heart tissue, the explanted hearts were sectioned into four horizontal levels from the apex to the base and cut into 5 µm thick, figure 26, using cryomicrotome (CM1850, Leica)

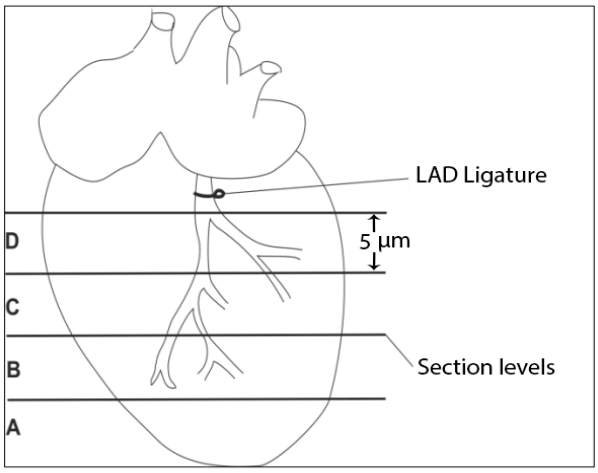

Figure 26: Illustration of the section levels of the frozen mouse heart.

2.7 HUMAN CELLS DETECTION

To prove the retention of the intramyocardially injected human bone marrow derived CD271+ stem cells in the mouse heart cryosections, a special histological test with staining of the human nuclei has been performed. For this purpose the instructions of Vector® M.O.M.™ Immunodetection Kit (Linaris; Wertheim-Bettingen, Germany) has been followed.

2.7.1 MATERIALS

- Monoclonal anti-human-nuclei (CHEMICON; Billerica, MA, USA)
- Vector® M.O.M.™ Immunodetection Kit (Linaris).
    - M.O.M.™ Mouse Ig Blocking Reagent
    - M.O.M.™ Protein Concentrate
- Donkey anti-mouse Alexa-Fluor® 594 (Molecular Probes™, Thermo Fisher).
- DAPI (4′,6-Diamidin-2-phenylindol) (Molecular Probes™, Thermo Fisher).
- 2 % Paraformaldehyde (PFA)
- PBS (Phosphate Buffer Saline), 1x, pH 7,4 (PAA)
- Magnetic stirrer
- DakoCytomation Pen
- Plate shaker, 3015 (GFL)

- Table shaker, Vortex-Genie 2, G-560E (Scientific Industries)
- Micropipet (different sizes), micropipet plus (Eppendorf)
- Cellstar® tubes; 15 ml, 50 ml (Greiner Bio-One)
- Cellstar® 6- and 24-Well plates (Greiner Bio-One)
- Microscopy slides (Marienfeld)
- Cover glasses (Marienfeld)

2.7.2 STAINING PROCEDURE

Firstly, the tissue sections were fixed by covering the slides with 2 % Paraformaldehyde (PFA) for 10 min at room temperature. Then the samples were washed two times by covering with PBS and one time by immersing the slides in PBS for 5 min at room temperature using a magnetic stirrer. The samples were then left to air dry and boundaries of sections were carefully drawn using DakoCytomation Pen and let it dry for 2 minutes.

M.O.M.™ Mouse Ig Blocking Reagent was then prepared using PBS (60 µl) and M.O.M.™ Mouse Ig Block (15 µl). Then endogenous mouse immunoglobulins were then blocked by covering the slides with M.O.M.™ Mouse Ig Blocking Reagent and shaken constantly for 1 hour at 37 °C. The samples were then washed two times by covering with PBS and one time by immersing the slides in PBS for 5 min at room temperature using a magnetic stirrer.

M.O.M.™ Diluent was prepared using PBS (225 µl) and M.O.M.™ Protein Concentrate (18 µl). The slides were then covered with M.O.M.™ Diluent for 10 minutes at room temperature.

Mouse anti-human nuclei dilution was then prepared using M.O.M.™ Diluent (38 µl) and-mouse anti-human nuclei (2 µl). The liquid was then removed from the tissue and stain samples by covering sections with mouse anti human nuclei dilution. The negative control section was covered with M.O.M.™ diluent alone and shaken it constantly for 2 hours at 37 °C. The samples were then washed three times by covering with PBS and two times by immersing the slides in PBS for 5 minutes at room temperature using a magnetic stirrer.

Alexa Flour 568 anti-mouse dilution was then prepared using PBS (700 µl) and Alexa 568 donkey anti-mouse (2 µl). During all the next coming steps, light exposure of the slides has been avoided.

The samples were then stained by covering the slides with Alexa Flour 568 anti-mouse dilution for 2 hour at 37 °C. The samples were then washed three times by covering with PBS and two times by immersing the slides in PBS for 5 minutes at room temperature using a magnetic stirrer.

Lastly, the slides were mounted by dropping 10 µl Fluoroshield-with-DAPI per section and closing with a cover glass. The edges of the cover glasses were sealed with clear nail polish and left to dry for permanent protection at 4 °C.

2.8 INFARCTION SIZE AREA ANALYSIS AND LEUKOCYTES INFILTRATION

Histological heart sections of 4 horizontal infarct levels described above were randomly chosen and stained with Fast Green FCF (Sigma-Aldrich) and Sirius Red (Division Chroma, Münster, Germany) assessing tissue localization and distribution of connective fibers. Two neighbor levels of the heart (n=6 for each mouse group) which showed the major infarction ratio were estimated using computer aided image analysis (Axio Vision LE Rel. 4.5 software; Zeiss, Jena, Germany). To assess leukocytes infiltration area 48 hours after 2nd ligation, the two neighbor levels of the heart were stained with Hematoxylin (Merck) and Eosin (Shandon), and images were taken using computerized planimetry (AxioVision, Zeiss).

2.8.1 FIRST INFARCTION SIZE AREA ANALYSIS

2.8.1.1 MATERIALS

- Sirius red F3BA (Division Chroma)
- Fast green FCF (Sigma-Aldrich)
- Distilled water, Aqua dest (Baxter S.A)
- Formalin (Formafix 37%) (Grimm MED logistic)
- 1 % colour stock solution (100 ml picric acid and 1 gram colour powder)
- 0,1 % colour working solution (90 ml picric acid, 10 ml of 1 % colour stock solution, 50 µl of 100 % acetic acid) (UKR)
- Microscopy slides (Marienfeld)
- Cover glasses (Marienfeld)
- Xylol (J.T. Baker)
- Ethanol 100% (UKR)
- Mounting media, Pertex® (Medite)

2.8.1.2 STAINING PROCEDURE

The tissue sections were firstly fixed by immersing the slides in 10 % formalin, after its dilution (50 ml Formalin 37% with 135 ml distilled water), at room temperature for 10 minutes. The slides were washed then two times by immersing them in distilled water for 5 minutes at room temperature. At this time, both 1 % colour stock solutions (100 ml of picric acid and 1 gram of colour powder) and 0,1 % colour working solutions (90 ml picric acid, 10 ml of 1 % colour stock solution, 50 µl of 100 % acetic acid) have been prepared.

The samples were then stained by immersing the slides in 0,1 % Siriusred working solution for 3 minutes at room temperature and then washed by immersing the slides in distilled water as often as the water becomes clear. After that the samples were stained by immersing the slides in 0,1 % Fastgreen working solution for 10 minutes at room temperature, which were then washed by immersing the slides in distilled water as often as the water becomes clear.
The samples were then transferred to 70 % ethanol, prepared by diluting 70 ml of ethanol 100% with 26 ml distilled water, for 1 minute at room temperature. This was followed by a second transfer of the samples to 80 % ethanol, prepared by diluting 80 ml of Ethanol 100% with 16 ml distilled water, for another 1 minute at room temperature. A third transfer of the samples to 90 % ethanol, prepared by diluting 90 ml of Ethanol 100% with 6 ml distilled water, was performed for 2 minutes at room temperature. Then the samples were then transferred to 100 % ethanol for 6 minutes at room temperature.
The samples were then transferred to the first and second xylol. Each one performed for 5 minutes at room temperature.
The slides were then mounted by dropping 10 µl of mounting media, Pertex®, per section and closed with cover glasses.

2.8.2 ANALYSIS OF LEUKOCYTES INFILTRATION AREA AFTER SECOND INFARCTION

2.8.2.1 MATERIALS

- 1 % Eosin Y stock solution (20,8 ml distilled water, 79,2 ml ethanol 96 %, 1 gram Eosin powder) (UKR)
- 0,25 % Eosin Y working solution (12,5 ml distilled water, 62,5 ml ethanol 96 %, 25 ml of 1 % Eosin Y stock, 0,5 ml acetic acid 100 %) (UKR)
- Distilled water, Aqua dest (Baxter S.A)
- Formalin (Formafix 37%) (Grimm MED logistic)
- Microscopy slides (Marienfeld)
- Cover glasses (Marienfeld)
- Xylol (J.T. Baker)
- Ethanol 96% (UKR)
- Mounting media, Pertex® (Medite)

2.8.2.2 STAINING PROCEDURE

The tissue sections have been fixed by immersing the slides in 10 % formalin (50 ml Formalin 37% with 135 ml distilled water), at room temperature for 10 minutes. This was followed by washing the slides two times by immersing them in distilled water for 5 minutes at room

temperature. The slides were then stained by immersing them in Mayer Hematoxylin solution for 8 minutes at room temperature, which were then washed by immersing the slides in warm running tap water for up to 10 minutes. The samples were then rewashed by immersing the slides in distilled water as often as the water becomes clear. The samples were then washed by immersing (10 dips) the slides in 80 % Ethanol, which is prepared from dilution of 80 ml ethanol 96% with 16 ml of distilled water.

At this time, both 1 % Eosin Y stock solution (20,8 ml distilled water, 79,2 ml ethanol 96 %, 1 gram Eosin powder) and 0,25 % Eosin Y working solution (12,5 ml distilled water, 62,5 ml ethanol 96 %, 25 ml of 1 % Eosin Y stock, 0,5 ml acetic acid 100 %) were prepared.

The samples were then stained by immersing the slides in Eosin Y working solution for 30 seconds at room temperature and then dehydrated in 95 % ethanol (1 ml distilled water and 95 ml ethanol 96%) for 5 minutes at room temperature. The slides were then transferred 2 times to Ethanol 96%. Each time performed for 5 minutes at room temperature. This was followed by 2-times transfer of the slides to xylol. Each one lasted 5 minutes at room temperature. The slides were then mounted by dropping 10 µl of mounting media, Pertex®, per section and closed with cover glasses.

2.9 DEFINITIONS OF VARIOUS VENTRICULAR ARRHYTHMIAS

We have analyzed, named and defined the observed ventricular arrhythmias in this mouse model in accordance with a standard that fits the previously established guidelines for labeling and describing each type of ventricular arrhythmia. (**Curtis** et al. 2013) The single lead ECG signal acquired through the implanted telemetry device was manually analyzed and the detected ventricular arrhythmias were qualitatively and quantitatively analyzed with ecgAUTO 1.5.11.26 software. To simplify the study of the mechanisms underlying the developed ventricular arrhythmias, the ECG analyses were subdivided into acute phase until 15 minutes and 15-45 minutes post intervention as well as delayed phase after 12 hours as previously classified. (**Wit and Peters** 2012)

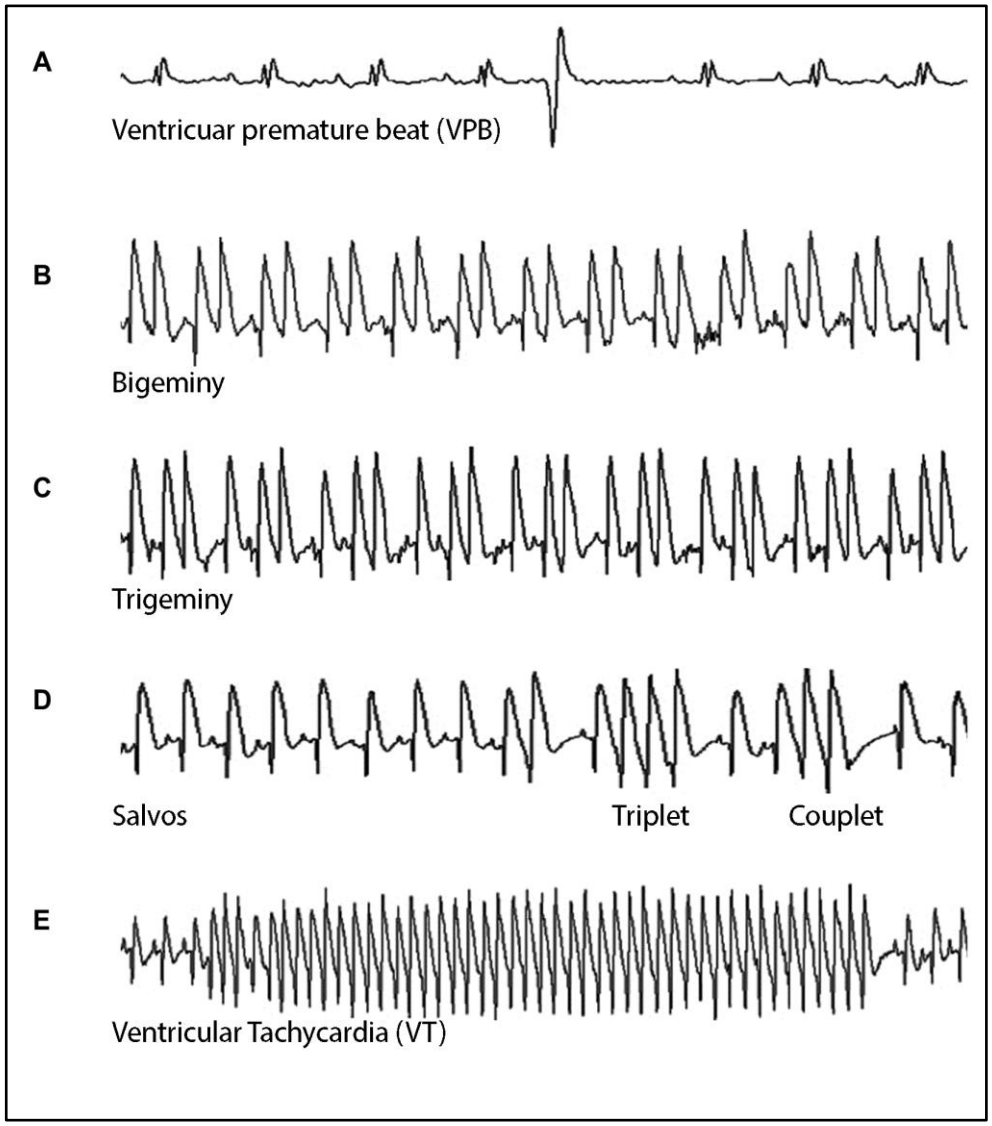

Figure 27: Various ventricular arrhythmias detected after induced myocardial infarction via LAD ligation. (A) A single ventricular premature beat (VPB) is shown. Note that the QRS-complex is not preceded by P-wave and varies with the other QRS complexes in width and height. (B) Ventricular bigeminy rhythm showing alternating “normal” QRS-complex with a VPB. (C) Ventricular trigeminy rhythm; “normal” QRS-complexes are separated with 2 consecutive VPBs. (D) The ECG strip shows 2 salvos. Note the 3 consecutive VPBs (trigeminy) and 2 consecutive VPBs (bigeminy) (E) Non-sustained self-terminating ventricular tachycardia; more than 4 consecutive VPBs.

2.9.1 VENTRICULAR PREMATURE BEATS (VPB)

We have defined VPB, as a ventricular electrical complex which varies in voltage (i.e. height) and/or duration (i.e. width) from the preceding non-VPB ventricular complex and occurs prematurely in relation to it. This means that VPB are not preceded by a P-wave if they ap-

pear during the early cardiac cycle or they have shorter PR-intervals than those of non-VPB if they appear later in the cardiac cycle. See figure 27, A.

2.9.2 VENTRICULAR BIGEMINY (BG) AND TRIGEMINY (TG)

A minimum sequence of VPB, normal sinus beat and VPB repeated at least three times has been defined as bigeminy. The number of repetitions has been defined as three in our model. Additionally, we have defined a sequence of VPB, two sinus beats (non-VPB) and a consecutive VPB with a repetition of three times as trigeminy. See figure 27, B and 27, C.

2.9.3 SALVOS

The observation of two or three consecutive VPB has been defined as salvo. See figure 27, D.

2.9.4 VENTRICULAR TACHYCARDIA (VT)

VT is defined as a sequence of four or more consecutive VPB (**Walker** et al. 1988; **Curtis** et al. 2013) This varies between three or more consecutive VPB (**Zipes** et al. 2006) to ten or more consecutive VPB (**Fiedler** 1983). In this experiment a sequence of four or more consecutive VPB has been defined as ventricular tachycardia, but a detailed description of the morphological and durational subtypes and classifications of VT has not been performed in this experiment. See figure 27, E.

2.10 STATISTICAL ANALYSIS

The data analysis and statistics has been done using SigmaStat 3.5 (Chicago, USA) and IBM SPSS Statistics for Windows (Version 22.0. Armonk, New York: IBM Corp.). Comparisons of two experimental groups were performed using Mann-Whitney *U* test. P values ≤0.05 has been considered to be statistically significant.

3 RESULTS

3.1 INDUCED VENTRICULAR ARRHYTHMIAS

With the induction of ischemia-reperfusion and once the LAD of the mouse heart has been ligated a rapid onset of hyperacute T-waves along with ST-segment elevation was observed in the ECG record. Return of the ST-segment to the isoelectric line has been shortly after releasing the LAD-ligature after 45 minutes from its closure noticed. This indicated the reperfusion of the myocardium. Figure 28 shows the recorded ECG before LAD occlusion and at different times after LAD ligation.

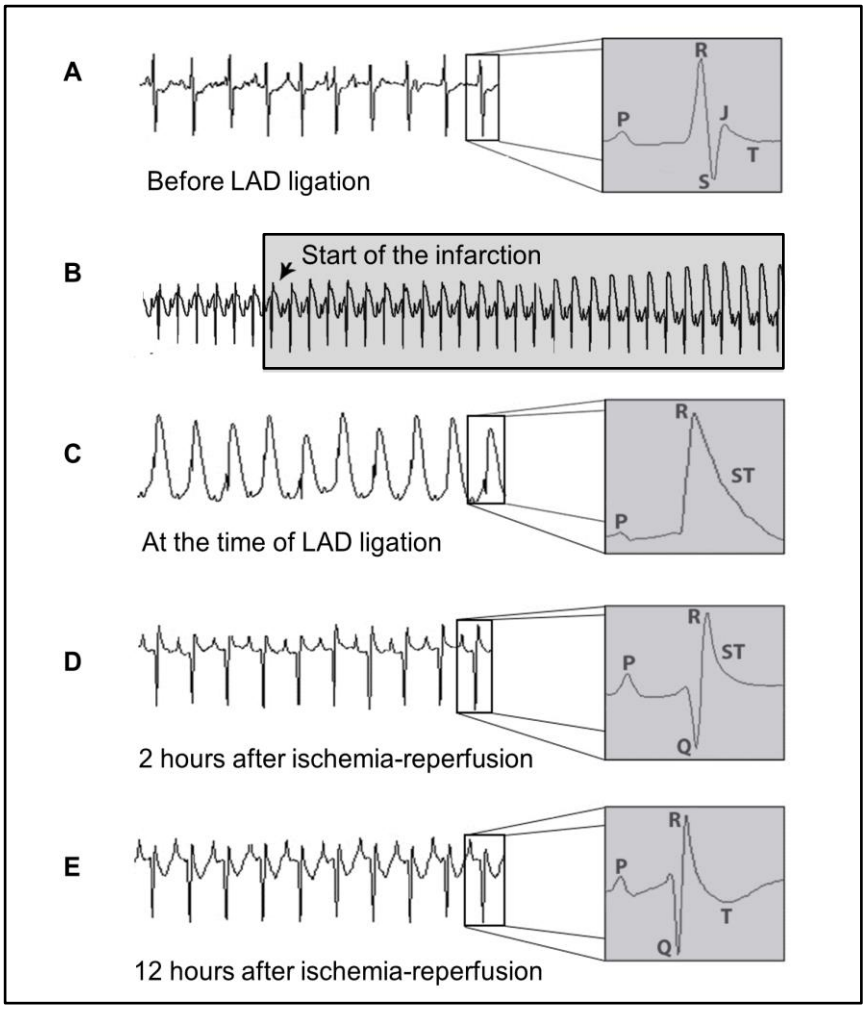

Figure 28: Mouse ECG changes at different times of the 1st LAD ligation during ischemia-reperfusion infarction. ECG signal prior to LAD ligation (A). Mouse ECG signal showing the initiation of infarction through the 1st LAD ligation (B). ECG changes during LAD ligation represented by a clear ST-segment elevation (C). ECG recorded 2 hours after ischemia reperfusion which illustrates development of Q-waves with disappearance of ST-segment elevation (D). ECG signal 12 hours after ischemia-reperfusion with clear Q-waves and recognizable T-waves (E).

In case of the second operation, the permanent closure of the LAD led to an immediate ST-segment elevation with subsequent development of Q-wave. Figure 29 shows the start of the 2nd infarction after permanent ligation of the already placed suture during the first ischemia one week earlier.

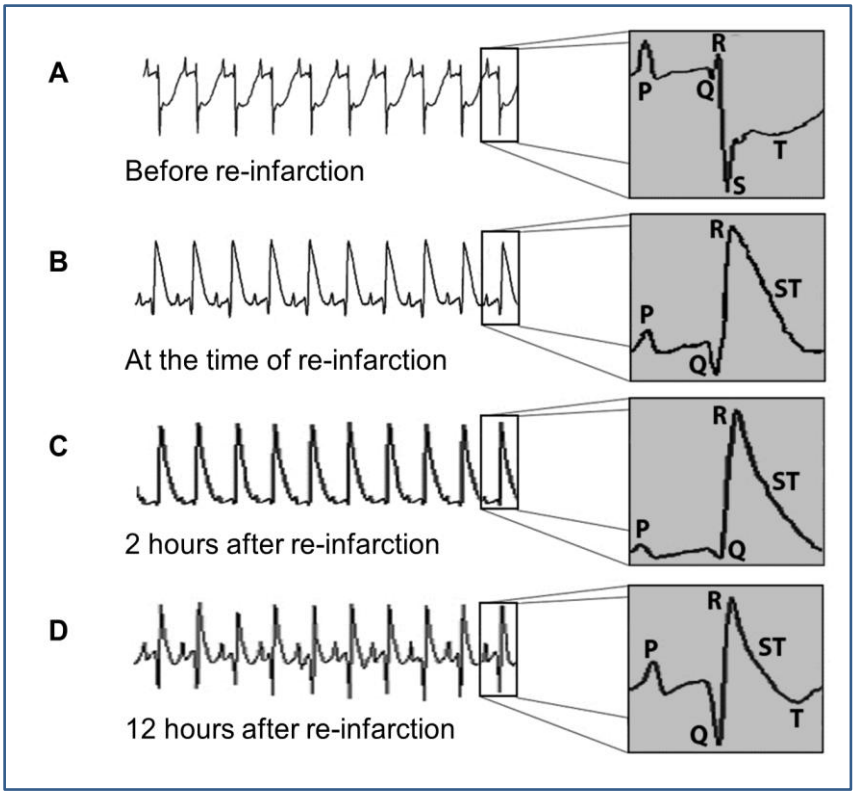

Figure 29: Mouse ECG changes at different times of the permanent 2nd LAD ligation (re-infarction; URI group). ECG just before performing re-infarction through 2nd LAD ligation i.e. 7 days after the 1st operation (ischemia-reperfusion) which shows deep S-waves with deeply depressed ST-segment (A). ECG at the time of re-infarction represented with an obvious ST-segment elevation (B). ECG signal 2 hours after re-infarction which shows a still elevated ST-segment reflecting the permanent LAD ligation (C). ECG with the development of Q-waves with still elevated ST-segment with reappearance of T-waves (D).

Out of 22 operated mice one mouse is died after performing the second operation after development of bradycardia and third degree heart block. Consequently this specimen has been excluded from the statistical analysis. No other complications has been seen after subcutaneous implantation of the telemeter and also after the 1st the second 2nd LAD ligations. The 1st and 2nd infarctions resulted in the development of various types of ventricular arrhythmias. These were ventricular premature beats (VPB), ventricular salvos, ventricular bigeminy and trigeminy and ventricular tachycardia (VT) (Figure 27, A-E).

No significant difference in the developed arrhythmias could be seen between the groups after the 1st infarction. Similarly the quantitative analysis of the different ventricular arrhythmias didn't show any significant difference in the frequency of the development of VPB, ventricular salvos, ventricular bigeminies and trigeminies 12 hours after the 1st myocardial infarction (Figure 30).

The quantitative measurement of the number of VPB within 12 hours after the 2nd LAD ligation (URI) showed a significant difference in comparison with the control group MIC (1105.0±1146.72 vs. 7.5±8.98, respectively; figure 30). This significant difference could also been observed during the time interval between 45 minutes and 12 hours after performing the permanent infarction (URI: 1082.2±1127.77 vs. MIC: 3.3±2.42; Fig. 34). There was no significant difference between URI group and MIC group in the total number of the developed VPB after the 1st LAD ligation (URI: 60.1±42.19 vs. MIC: 259.0±457.69) for the first 12 hours and at the time point between 45 minutes and 12 hours (URI: 54.5±39.85 vs. MIC: 246.8±440.84).

Regarding ventricular arrhythmia (VT) a significant development of VT after the 2nd LAD ligation has been observed in URI group (32.6±52.5), whereas none of that was observed in the MIC group. This happened during the first 12 hours after the 2nd infarction and also during the time interval between 45 minutes and 12 hours after the 2nd infarction (Figure 31). There was no significant difference in terms of the development of VT after the 1st infarction (URI: 1±2.6 vs. MIC: 1.6±1.8).

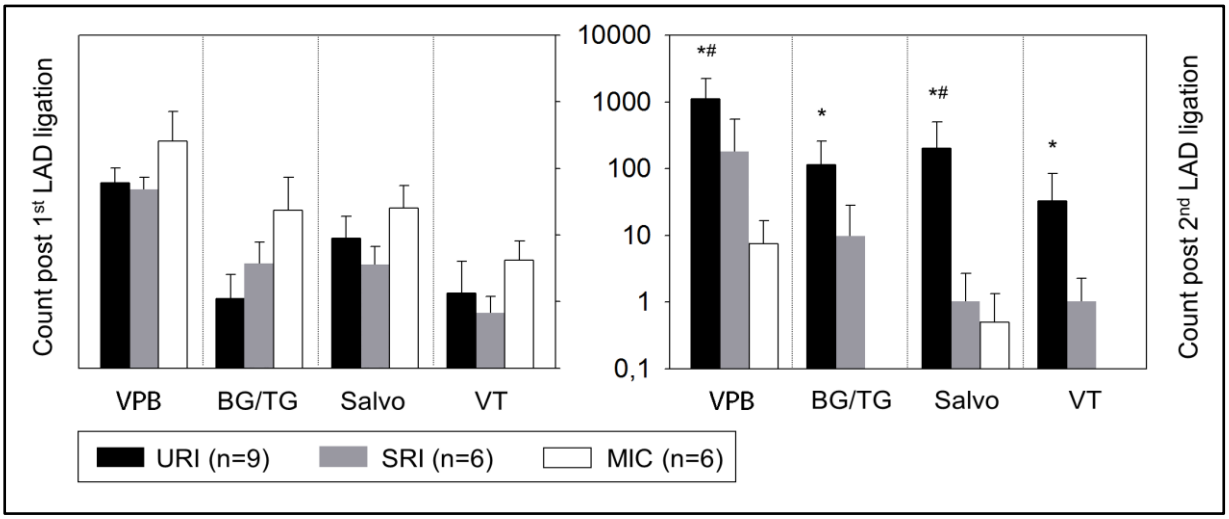

Figure 30: Developed ventricular arrhythmias in mouse groups until 12 hours post LAD ligation. Mean±SD; * P≤0.02 compared to MIC; # P≤0.02 compared to SRI (Mann-Whitney *U* Test). URI – untreated re-infarction, SRI – stem cell treated re-infarction, MIC – re-perfused myocardial infarction control, VPB – ventricular premature beat, BG/TG – bigeminy/trigeminy, VT – ventricular tachycardia.

A similar significant difference in the number of the developed ventricular bigeminy and trigeminy and salvos could be observed between URI and MIC group counted during the first 12 hours after the second operation and also during the time interval between 45 minutes and 12 hours after the second LAD ligation.

3.2 ANTIARRHYTHMIC EFFECTS OF CD271$^+$MSC ENGRAFTMENT

The intramyocardial implantation of human CD271$^+$ MSC did not lead to a significant difference in the number of ventricular arrhythmias early after the 1st MI (Fig. 30), but showed antiarrhythmic effects by significantly reducing the quantitatively measured VPB which occurred after a re-infarction during the time frame between LAD-ligation until 12 hours thereafter (URI: 1105.0±1146.72 vs. CD271$^+$ treatment group, SRI: 178.16±370.12 (Fig. 30). Such significant antiarrhythmic behavior was also reflected in a reduction of the number of VT 45 minutes after the 2nd LAD ligation until 12 hours post re-infarction (URI: 32.6±52.51 vs. SRI: 0±0, Fig. 31). Moreover, there was no significant difference in bigeminy/trigeminy and salvos occurrence between the two groups.

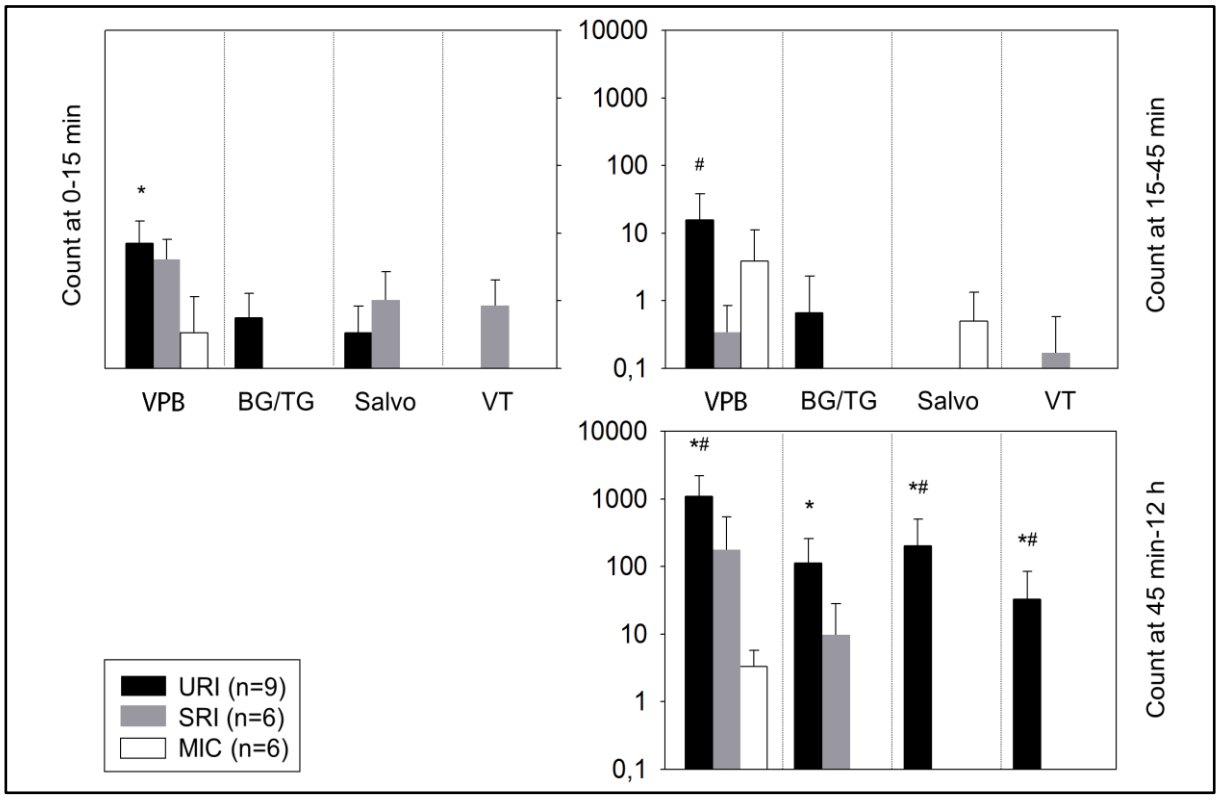

Figure 31: Developed ventricular arrhythmias in mouse grups at different time periods following 2nd LAD ligation. Mean±SD; * P≤0.02 compared to MIC; $^{\#}$ P≤0.02 compared to SRI (Mann-Whitney *U* Test). URI – untreated re-infarction, SRI – stem cell treated re-infarction, MIC – re-perfused myocardial infarction control, VPB – ventricular premature beat, BG/TG – bigeminy/trigeminy, VT – ventricular tachycardia.

3.3 RETENTION OF HUMAN CELLS

After 9 days the engrafted human cells were successfully detected in heart cryosections of SRI predominantly in the peri-infarct area by immunofluorescent staining (Figure 32).

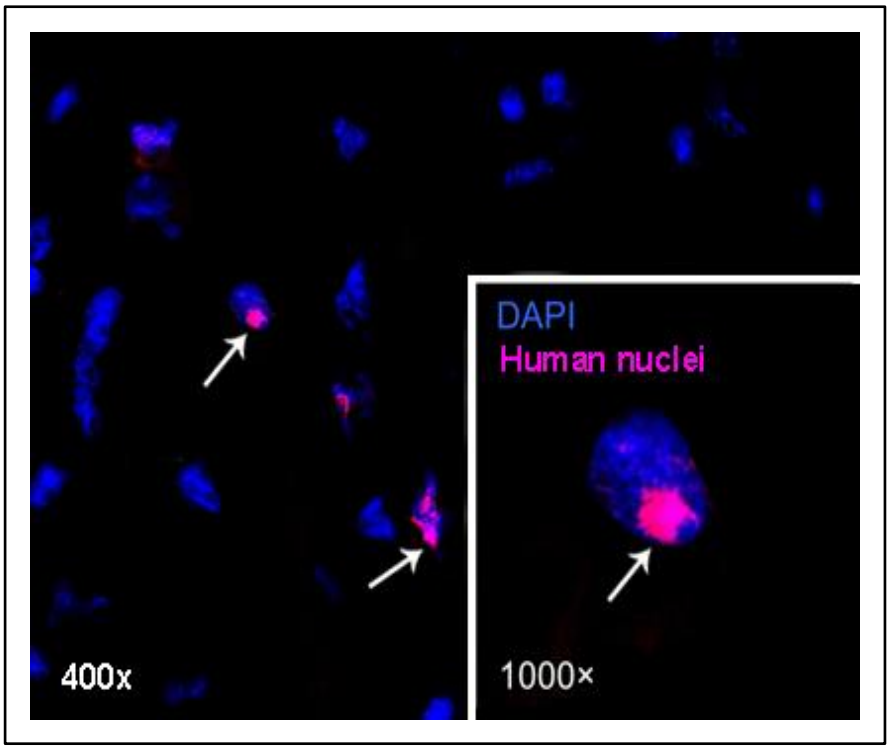

Figure 32: Retention of human cells. DAPI staining with 400x and 1000x magnifications of mouse heart section show the detected human nuclei (arrows) 9 days after their intramyocardial delivery.

3.4 ALTERATIONS OF THE INFARCT SCAR

A thinning of the left ventricular free wall (Fast green) and extensive collagen deposition (Sirius red) 9 days post intervention has been observed after performing an ischemia-reperfusion infarction. i.e. after the first LAD ligation. (Figure 33). After stem cell injection there was no significant reduction in infarct scar formation (SRI: 14.78±5.85 %) in comparison with untreated infarction (URI: 17.28±5.10 % URI) as well as to control group (MIC: 19.42±3.66 %; figure 35).

The permanent 2nd LAD ligation resulted in leukocyte infiltration into the infarction area as showed in the images of Hematoxylin and Eosin stained slices from explanted hearts 48 hours following myocardial infarction (Figure 34). The cellular infiltration led to a significant enlargement of the myocardial scar area in URI (38.54±14.28 %, P=0.029) as well as SRI (29.36±8.63 %, P=0.039) in comparison to MIC (20.1±4.04 %; figure 35).

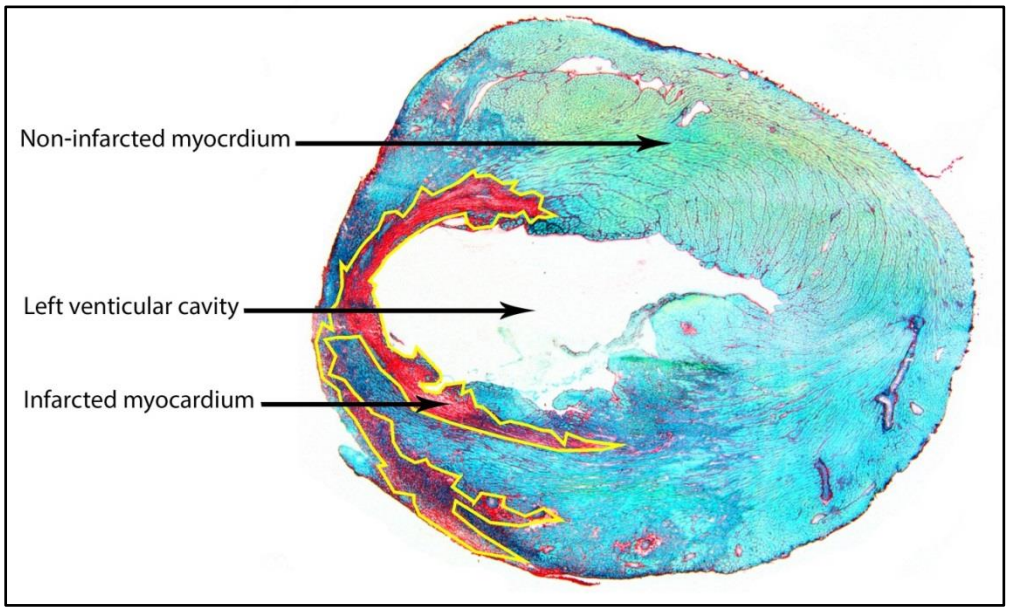

Figure 33: Cross section of mouse heart stained with sirius red and fast green showing the demarcated infarcted area, stained red, which outlined with a yellow line to distinct it form the light green area, non-infarcted myocardium.

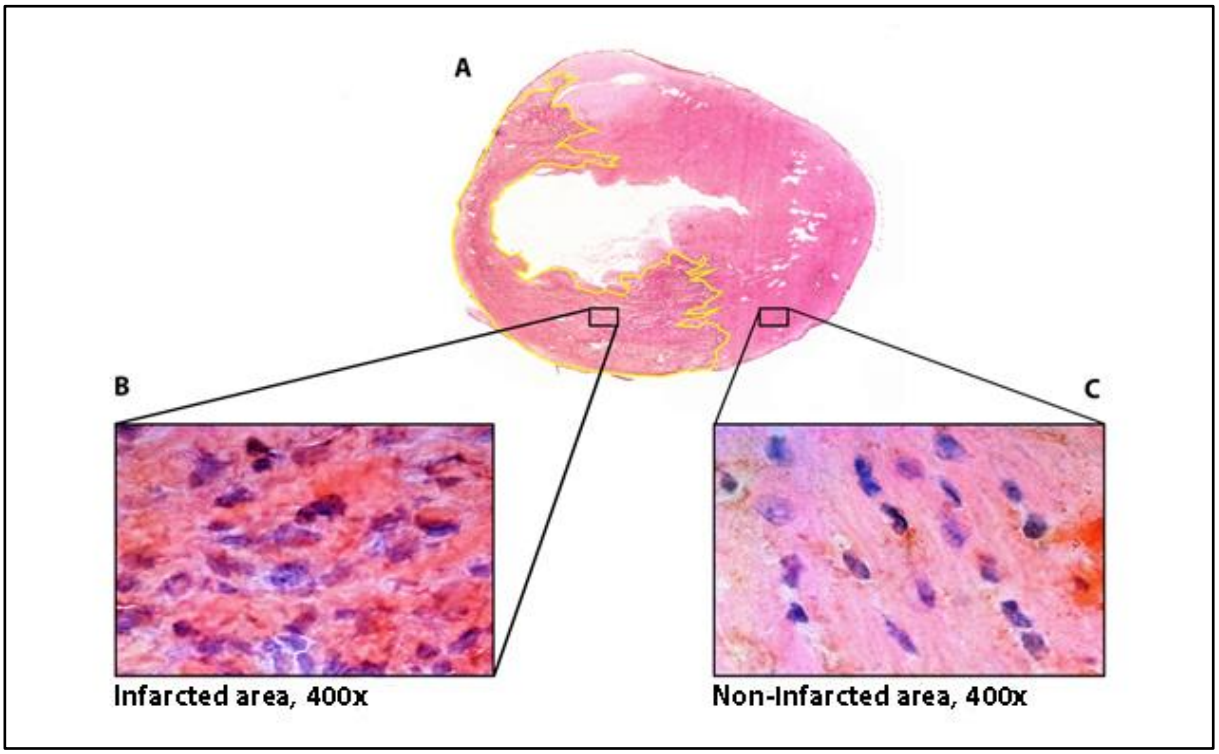

Figure 34: (A) Cross section of mouse heart stained with eosin and hematoxylin for leukocyte infiltration shows the fresh infarcted area, outlined with yellow line, with distinct non-infarcted area. (B) 400x magnification of the infarcted area showing the leukocyte infiltration. (C) 400x magnification of the non-infarcted area.

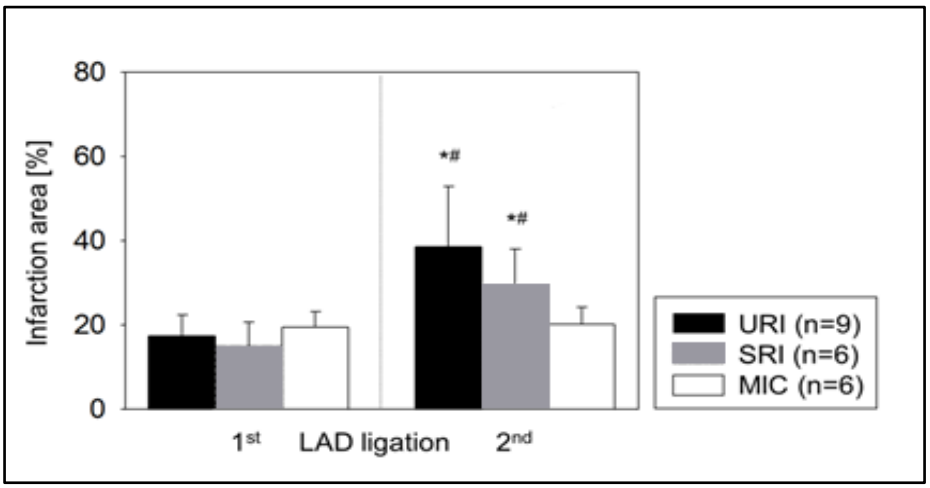

Figure 35: Alterations in myocardial infarction size. Significant increase of the infarction size after 2nd LAD ligation; Mean±SD; * P≤0.009 compared to 1st LAD ligation; # P≤0.041 in contrast to MIC. (Mann-Whitney *U* test).

4 DISCUSSION

4.1 DEVELOPMENT OF A NEW MOUSE MODEL FOR *IN VIVO* RHYTHMOLOGICAL STUDY OF STEM CELLS

This mouse model has been developed to reproduce ventricular arrhythmias several days after myocardial infarction. In order to study the engraftment and the rhythmological behavior of human cells it is essential to use immune deficient mouse strain. At the time of development of this mouse model it has been found that the ventricular arrhythmias following induction of myocardial infarction were primarily seen during the first day following the myocardial infarction. Since the human stem cells have been at the time of performing myocardial infarction, the stem cells didn't exert antiarrhythmic effects, a hypothesis has been previously shown (**Roell** et al. 2007). This indicates that the intramyocardially transplanted human cells require some time to engraft themselves and exert a detectable effect.

A transjuglar venous catheter mediated burst stimulation for *in vivo* induction of ventricular arrhythmias after myocardial infarction in murine model has been done by Roell and coworkers (**Roell** et al. 2007). However, this method could not be utilized in the immune defivi=cient mouse strain used in this experiment (data not shown). This was due to the fact that all mice, $Rag2^{-/-}\gamma c^{-/-}$-mice, have developed ventricular tachycardia even the healthy ones without a previous myocardial infarction. With this fact creating a control group for comparison purposes was not possible. As a consequence there was a need to develop an animal model *to in vivo* test the human stem cells for their potential antiarrhythmic effects.

In this context a new mouse model has been developed to reproduce ventricular arrhythmias by performing a second permanent LAD ligation one week after performing the first reperfused myocardial infarction through a temporary LAD ligation. The 2^{nd} ligation one week after the 1^{st} infarction in $Rag2^{-/-}\gamma c^{-/-}$-mice has indeed reproduced different cardiac arrhythmias. In regard the stressfulness of this experiment it has been found that performing 2 operations in anesthetized mice was tolerable and yield only one death out of 22 mice. The previously described small animal models in this field have used immune competent mice or rats subjected them to a higher stress by performing recurrent transient ischemia following an operatively instrumented mice with the possibility to induce recurrent transient closure of the LAD (**Lujan and DiCarlo** 2014; **Leprán** et al. 1983).

4.2 THE CLINICAL RELEVANCE OF THE MOUSE MODEL

For *in vivo* testing of antiarrhythmic behavior of human stem cells and the feasibility of its future implication in the clinical practice, development of a mouse model mimicking clinical scenarios were the primary goal of this experiment. The developed mouse model, in which a re-perfused myocardial infarction was followed by induction of a permanent infarction, mimics the clinical scenario when the affected coronary vessel which caused a myocardial insult and infarction and has been re-canalized to re-establish myocardial perfusion tends to reclose after successful initial recanalization. This could be seen in the case of thrombolytic therapy. After a successful thrombolysis and re-establishment of the myocardial perfusion using various systemic thrombolytic agents, the vessel tends to reclose with a rate of about 5-10 % during the first 2 weeks (**Verheugt** et al. 1996). A similar scenario can also be observed in case of percutaneous coronary intervention after stenting of the culprit vessel responsible for the acute myocardial infarction. The stented re-canalized vessel may face an early stent thrombosis of with a rate of 0.5-2% (**Holmes** et al. 2010) which may cause a re-infarction. Furthermore this animal model can even mimic the situation occurring after a surgical revascularization (coronary artery bypass graft) of the myocardiaum after myocardial infarction, with following early graft failure rate of about 1-3% (**Thielmann** et al. 2006) causing a re-infarction.

4.3 HUMAN CD271+ MSC REDUCE THE OCCURRENCE OF VENTRICULAR ARRHYTHMIAS AFTER MYOCARDIAL INFARCTION

The observed significant reduction of ventricular tachycardia during the time period between 45 minutes and 12 hours following the 2nd LAD ligation could be possibly explained through the coupling of MSC with cardiomyocytes via building connexin43 gap junctions as shown previously in our research group (Lemcke et al. 2017a). This is especially possible as it has been previously described that the changes in connexin43 gap junction are the main causative of the developed ventricular tachycardia after myocardial infarction at this time period (**Wit and Peters** 2012).

In this test a new novel mouse model for testing arrhythmias in the Rag2$^{-/-}$γc$^{-/-}$-mouse has been introduced. Interestingly, CD271^{+} MSC transplanted into the infarcted area were retained as it has been later in histological sections detected and did not show any arrhythmogenic properties. Knowing that brings us to the conclusion that CD271+ MSC are rhythmologically safe. The transplanted CD271^{+} stem cells showed their safety and efficacy after their intramyocardial transplantation. With these findings one can conclude, that human bone marrow derived MSCs, i.e. CD271^{+}, are suitable cell type preventing arrhythmias after myo-

cardial infarction. These results supports the previous descriptions and observations on the safety of intra-myocardial transplantation of bone marrow derived stem cells (**Beeres** et al. 2007) so that a further evaluation for the future clinical implementation of these cells could be done.

4.4 INTRA-MYOCARDIAL IMPLANTATION OF HUMAN CD271+ MSC AFTER MYOCARDIAL INFARCTION DOES NOT REDUCE INFARCT SIZE

The significant increase in the infarct area size after performing the second myocardial infarction in this mouse model together with corresponding ECG changes after the second LAD ligation proves the effectiveness of the model in induction of a second myocardial infarction.

This animal experiment has shown that intramyocardial transplantation of human CD271+ MSCs in $Rag2^{-/-}\gamma c^{-/-}$-mouse after myocardial infarction does not reduce the infarct area size. Hence one can say that the significant reduction of the ventricular arrhythmias following myocardial infarction in the stem cell treated group could not be due the smaller infarct size as it is well known that there is a direct relation between the infarct size and the incidence of ventricular arrhythmias. (**Bhar-Amato** et al. 2017)

5 CONCLUSION

Since ventricular arrhythmias are seen as common cause of sudden death after myocardial infarction, developing new safe therapeutic methods for prevention and treatment of cardiac arrhythmias is of paramount importance. This experiment has tested the potential anti-arrhythmic effects of human bone marrow derived mesenchymal stem cells transplanted intra-myocardially directly after induction of myocardial infarction in immune deficient mice and with electrocardiogram monitoring using ECG telemetry. Apart from ventricular fibrillation, different types of ventricular arrhythmias have been developed. These were however only seen during the first day of induction of myocardial infarction. Therefore a new mouse model has been developed, inducing ventricular arrhythmias by performing a 2^{nd} permanent MI one week after a re-perfused 1^{st} MI. This is to test the possible antiarrhythmic effects of human stem cells.

The developed animal model warranted the time required for stem cell engraftment and allowed *in vivo* analysis and verification of significant antiarrhythmic effects of human $CD271^+$ mesenchymal stem cells using immune deficient $Rag2^{-/-}\gamma c^{-/-}$-mice with high relevance for transference to a realistic clinical situation as reperfused myocardium may suffer a second new ischemia anytime during the first 30 days after successful initial recanalization of the affected vessel or myocardial revascularization leading to fatal arrhythmias thereafter.

With this mouse model the intramyocardial transplantation of human bone marrow-derived $CD271^+$ MSC are rhythmologically safe and bear antiarrhythmic effects developed early after myocardial infarction. This provides a base for further preclinical studies establishing new cell-mediated prevention and therapeutic strategies of ventricular arrhythmias following myocardial infarction.

6 LITERATURVERZEICHNIS

Ahn, Dongchoon; Cheng, Linda; Moon, Chanil; Spurgeon, Harold; Lakatta, Edward G.; Talan, Mark I. (2004): Induction of myocardial infarcts of a predictable size and location by branch pattern probability-assisted coronary ligation in C57BL/6 mice. In: *American journal of physiology. Heart and circulatory physiology* 286 (3), H1201-7. DOI: 10.1152/ajpheart.00862.2003.

Antzelevitch, Charles; Burashnikov, Alexander (2011): Overview of Basic Mechanisms of Cardiac Arrhythmia. In: *Cardiac electrophysiology clinics* 3 (1), S. 23–45. DOI: 10.1016/j.ccep.2010.10.012.

Ashley, Euan A.; Niebauer, Josef (2004): Cardiology Explained. London.

Askar, Saïd F. A.; Ramkisoensing, Arti A.; Atsma, Douwe E.; Schalij, Martin J.; Vries, Antoine A. F. de; Pijnappels, Daniël A. (2013): Engraftment patterns of human adult mesenchymal stem cells expose electrotonic and paracrine proarrhythmic mechanisms in myocardial cell cultures. In: *Circulation. Arrhythmia and electrophysiology* 6 (2), S. 380–391. DOI: 10.1161/CIRCEP.111.000215.

Assadi, Ramin; Motabar, Ali (2016): Conduction System of the Heart. Hg. v. Richard A. Lange. Online verfügbar unter https://emedicine.medscape.com/article/1922987-overview.

Azevodo, I. M. de; Watanabe, Y.; Dreifus, L. S. (1973): Atrioventricular junctional rhythm: classification and clinical significance. In: *Chest* 64 (6), S. 732–740.

Beeres, Saskia L. M. A.; Zeppenfeld, Katja; Bax, Jeroen J.; Dibbets-Schneider, Petra; Stokkel, Marcel P. M.; Fibbe, Willem E. et al. (2007): Electrophysiological and arrhythmogenic effects of intramyocardial bone marrow cell injection in patients with chronic ischemic heart disease. In: *Heart rhythm* 4 (3), S. 257–265. DOI: 10.1016/j.hrthm.2006.10.033.

Bhar-Amato, Justine; Davies, William; Agarwal, Sharad (2017): Ventricular Arrhythmia after Acute Myocardial Infarction: 'The Perfect Storm'. In: *Arrhythmia & electrophysiology review* 6 (3), S. 134–139. DOI: 10.15420/aer.2017.24.1.

Bode, E. F.; Briston, S. J.; Overend, C. L.; O'Neill, S. C.; Trafford, A. W.; Eisner, D. A. (2011): Changes of SERCA activity have only modest effects on sarcoplasmic reticulum Ca2+ content in rat ventricular myocytes. In: *The Journal of physiology* 589 (Pt 19), S. 4723–4729. DOI: 10.1113/jphysiol.2011.211052.

Bonnet, D. (2003): Biology of human bone marrow stem cells. In: *Clinical and experimental medicine* 3 (3), S. 140–149. DOI: 10.1007/s10238-003-0017-9.

Boukens, Bas J.; Hoogendijk, Mark G.; Verkerk, Arie O.; Linnenbank, Andre; van Dam, Peter; Remme, Carol-Ann et al. (2013): Early repolarization in mice causes overestimation of ventricular activation time by the QRS duration. In: *Cardiovascular research* 97 (1), S. 182–191. DOI: 10.1093/cvr/cvs299.

Brede, Marc; Roell, Wilhelm; Ritter, Oliver; Wiesmann, Frank; Jahns, Roland; Haase, Axel et al. (2003): Cardiac hypertrophy is associated with decreased eNOS expression in angiotensin AT2 receptor-deficient mice. In: *Hypertension (Dallas, Tex. : 1979)* 42 (6), S. 1177–1182. DOI: 10.1161/01.HYP.0000100445.80029.8E.

Carmeliet, E. (1999): Cardiac ionic currents and acute ischemia: from channels to arrhythmias. In: *Physiological reviews* 79 (3), S. 917–1017. DOI: 10.1152/physrev.1999.79.3.917.

Cascio, Wayne E.; Yang, Hua; Muller-Borer, Barbara J.; Johnson, Timothy A. (2005): Ischemia-induced arrhythmia: the role of connexins, gap junctions, and attendant changes in impulse propagation. In: *Journal of electrocardiology* 38 (4 Suppl), S. 55–59. DOI: 10.1016/j.jelectrocard.2005.06.019.

Cerrone, Marina; Colombi, Barbara; Santoro, Massimo; Di Barletta, Marina Raffaele; Scelsi, Mario; Villani, Laura et al. (2005): Bidirectional ventricular tachycardia and fibrillation elicited in a knock-in mouse model carrier of a mutation in the cardiac ryanodine receptor. In: *Circulation research* 96 (10), e77-82. DOI: 10.1161/01.RES.0000169067.51055.72.

Chambers, John C.; Zhao, Jing; Terracciano, Cesare M. N.; Bezzina, Connie R.; Zhang, Weihua; Kaba, Riyaz et al. (2010): Genetic variation in SCN10A influences cardiac conduction. In: *Nature genetics* 42 (2), S. 149–152. DOI: 10.1038/ng.516.

Chelu, Mihail G.; Sarma, Satyam; Sood, Subeena; Wang, Sufen; van Oort, Ralph J.; Skapura, Darlene G. et al. (2009): Calmodulin kinase II-mediated sarcoplasmic reticulum Ca2+ leak promotes atrial fibrillation in mice. In: *The Journal of clinical investigation* 119 (7), S. 1940–1951.

Chong, James J. H.; Yang, Xiulan; Don, Creighton W.; Minami, Elina; Liu, Yen-Wen; Weyers, Jill J. et al. (2014): Human embryonic-stem-cell-derived cardiomyocytes regenerate non-human primate hearts. In: *Nature* 510 (7504), S. 273–277. DOI: 10.1038/nature13233.

Colledge, Nicki R.; Walker, Brian R.; Ralston, Stuart; Davidson, Stanley (2010): Davidson's principles and practice of medicine. 21st ed. / the editors, Nicki R. Colledge, Brian R. Walker, Stuart H. Ralston illustrated by Robert Britton. Edinburgh: Churchill Livingstone (18:524,595-596.).

Conci E; Pachinger O; Metzler B (2006): Mouse Models for Myocardial Ischaemia/Reperfusion. In: *Austrian Journal of Cardiology* (13), S. 239–244.

Coronel, Ruben; Lau, David H.; Sosunov, Eugene A.; Janse, Michiel J.; Danilo, Peter; Anyukhovsky, Evgeny P. et al. (2010): Cardiac expression of skeletal muscle sodium channels increases longitudinal conduction velocity in the canine 1-week myocardial infarction. In: *Heart rhythm* 7 (8), S. 1104–1110. DOI: 10.1016/j.hrthm.2010.04.009.

Curtis, Michael J.; Hancox, Jules C.; Farkas, András; Wainwright, Cherry L.; Stables, Catherine L.; Saint, David A. et al. (2013): The Lambeth Conventions (II): guidelines for the study of animal and human ventricular and supraventricular arrhythmias. In: *Pharmacology & therapeutics* 139 (2), S. 213–248. DOI: 10.1016/j.pharmthera.2013.04.008.

Cutler, Michael J.; Wan, Xiaoping; Plummer, Bradley N.; Liu, Haiyan; Deschenes, Isabelle; Laurita, Kenneth R. et al. (2012): Targeted sarcoplasmic reticulum Ca2+ ATPase 2a gene delivery to restore electrical stability in the failing heart. In: *Circulation* 126 (17), S. 2095–2104. DOI: 10.1161/CIRCULATIONAHA.111.071480.

Danik, Stephan; Cabo, Candido; Chiello, Christine; Kang, Sacha; Wit, Andrew L.; Coromilas, James (2002): Correlation of repolarization of ventricular monophasic action potential with ECG in the murine heart. In: *American journal of physiology. Heart and circulatory physiology* 283 (1), H372-81. DOI: 10.1152/ajpheart.01091.2001.

Degabriele, Naomi M.; Griesenbach, Uta; Sato, Kaori; Post, Mark J.; Zhu, Jie; Williams, John et al. (2004): Critical appraisal of the mouse model of myocardial infarction. In: *Experimental physiology* 89 (4), S. 497–505. DOI: 10.1113/expphysiol.2004.027276.

Dobrev, Dobromir; Wehrens, Xander H. T. (2018): Mouse Models of Cardiac Arrhythmias. In: *Circulation research* 123 (3), S. 332–334. DOI: 10.1161/CIRCRESAHA.118.313406.

Dominici, M.; Le Blanc, K.; Mueller, I.; Slaper-Cortenbach, I.; Marini, Fc; Krause, Ds et al. (2006): Minimal criteria for defining multipotent mesenchymal stromal cells. The International Society for Cellular Therapy position statement. In: *Cytotherapy* 8 (4), S. 315–317. DOI: 10.1080/14653240600855905.

DSI, a division of Harvard Biosceince, Inc. DSI PhysioTel® ETA-F10 for Mice. Online verfügbar unter https://www.datasci.com/products/implantable-telemetry/mouse-(miniature)/eta-f10.

Duerr, Georg D.; Elhafi, Naziha; Bostani, Toktam; Ellinger, Joerg; Swieny, Louay; Kolobara, Elvis et al. (2011): Comparison of myocardial remodeling between cryoinfarction and reperfused infarction in mice. In: *Journal of biomedicine & biotechnology* 2011, S. 961298. DOI: 10.1155/2011/961298.

Durrani, Shazia; Konoplyannikov, Mikhail; Ashraf, Muhammad; Haider, Khawaja Husnain (2010): Skeletal myoblasts for cardiac repair. In: *Regenerative medicine* 5 (6), S. 919–932. DOI: 10.2217/rme.10.65.

Fauci, Anthony S.; Harrison, Tinsley Randolph (2008): Harrison's principles of internal medicine. 17th ed. / editors, Anthony S. Fauci … [et al.]. New York, London: McGraw-Hill Medical (II:4:32).

Fernandes, Sarah; Amirault, Jean-Christophe; Lande, Gilles; Nguyen, Jean-Michel; Forest, Virginie; Bignolais, Olivier et al. (2006): Autologous myoblast transplantation after myocardial infarction increases the inducibility of ventricular arrhythmias. In: *Cardiovascular research* 69 (2), S. 348–358. DOI: 10.1016/j.cardiores.2005.10.003.

Fernandes, Sarah; van Rijen, Harold V. M.; Forest, Virginie; Evain, Stéphane; Leblond, Anne-Laure; Mérot, Jean et al. (2009): Cardiac cell therapy: overexpression of connexin43 in skeletal myoblasts and prevention of ventricular arrhythmias. In: *Journal of cellular and molecular medicine* 13 (9B), S. 3703–3712. DOI: 10.1111/j.1582-4934.2009.00740.x.

Fiedler, V. B. (1983): Reduction of myocardial infarction and dysrhythmic activity by nafazatrom in the conscious rat. In: *European journal of pharmacology* 88 (2-3), S. 263–267.

Fu, Du-Guan (2015): Cardiac Arrhythmias: Diagnosis, Symptoms, and Treatments. In: *Cell biochemistry and biophysics* 73 (2), S. 291–296. DOI: 10.1007/s12013-015-0626-4.

Garrey, Walter E. (1914): THE NATURE OF FIBRILLARY CONTRACTION OF THE HEART.—ITS RELATION TO TISSUE MASS AND FORM. In: *The American journal of physiology* 33 (3), S. 397–414. DOI: 10.1152/ajplegacy.1914.33.3.397.

Goodenough, Daniel A.; Paul, David L. (2009): Gap junctions. In: *Cold Spring Harbor perspectives in biology* 1 (1), a002576. DOI: 10.1101/cshperspect.a002576.

Greener, Ian D.; Sasano, Tetsuo; Wan, Xiaoping; Igarashi, Tomonori; Strom, Maria; Rosenbaum, David S.; Donahue, J. Kevin (2012): Connexin43 gene transfer reduces ventricular tachycardia susceptibility after myocardial infarction. In: *Journal of the American College of Cardiology* 60 (12), S. 1103–1110. DOI: 10.1016/j.jacc.2012.04.042.

Groot, J. R. de; Wilms-Schopman, F. J.; Opthof, T.; Remme, C. A.; Coronel, R. (2001): Late ventricular arrhythmias during acute regional ischemia in the isolated blood perfused pig heart. Role of electrical cellular coupling. In: *Cardiovascular research* 50 (2), S. 362–372.

Guinamard, Romain; Chatelier, Aurélien; Demion, Marie; Potreau, Daniel; Patri, Sylvie; Rahmati, Mohammad; Bois, Patrick (2004): Functional characterization of a Ca(2+)-activated non-selective cation channel in human atrial cardiomyocytes. In: *The Journal of physiology* 558 (Pt 1), S. 75–83. DOI: 10.1113/jphysiol.2004.063974.

Gussak, Ihor (2003): Cardiac repolarization. Bridging basic and clinical science / edited by Ihor Gussak … [et al.] ; foreword by Douglas P. Zipes. Totowa, N.J., Great Britain: Humana Press (Contemporary cardiology).

Györke, I.; Györke, S. (1998): Regulation of the cardiac ryanodine receptor channel by luminal Ca2+ involves luminal Ca2+ sensing sites. In: *Biophysical journal* 75 (6), S. 2801–2810. DOI: 10.1016/S0006-3495(98)77723-9.

Hampton, John R. (2013): The ECG made easy. 8th ed. Edinburgh, New York: Churchill Livingstone/Elsevier.

He, Jigang; Teng, Xiaomei; Yu, Yunsheng; Huang, Haoyue; Ye, Wenxue; Ding, Yinglong; Shen, Zhenya (2013): Injection of Sca-1+/CD45+/CD31+ mouse bone mesenchymal stromal-like cells improves cardiac function in a mouse myocardial infarct model. In: *Differentiation; research in biological diversity* 86 (1-2), S. 57–64. DOI: 10.1016/j.diff.2013.07.002.

Hirt, Marc N.; Hansen, Arne; Eschenhagen, Thomas (2014): Cardiac tissue engineering: state of the art. In: *Circulation research* 114 (2), S. 354–367. DOI: 10.1161/CIRCRESAHA.114.300522.

Ho, David; Zhao, Xin; Gao, Shumin; Hong, Chull; Vatner, Dorothy E.; Vatner, Stephen F. (2011): Heart Rate and Electrocardiography Monitoring in Mice. In: *Current protocols in mouse biology* 1, S. 123–139. DOI: 10.1002/9780470942390.mo100159.

Holm, Hilma; Gudbjartsson, Daniel F.; Arnar, David O.; Thorleifsson, Gudmar; Thorgeirsson, Gudmundur; Stefansdottir, Hrafnhildur et al. (2010): Several common variants modulate heart rate, PR interval and QRS duration. In: *Nature genetics* 42 (2), S. 117–122. DOI: 10.1038/ng.511.

Holmes, David R.; Kereiakes, Dean J.; Garg, Scot; Serruys, Patrick W.; Dehmer, Gregory J.; Ellis, Stephen G. et al. (2010): Stent thrombosis. In: *Journal of the American College of Cardiology* 56 (17), S. 1357–1365. DOI: 10.1016/j.jacc.2010.07.016.

Hood WB Jr, McCarthy B, Lown B (1967): Myocardial infarction following coronary ligation in dogs. Hemodynamic effects of isoproterenol and acetylstrophanthidin. (2), 191-9.

Igarashi, Tomonori; Finet, J. Emanuel; Takeuchi, Ayano; Fujino, Yoshihisa; Strom, Maria; Greener, Ian D. et al. (2012): Connexin gene transfer preserves conduction velocity and prevents atrial fibrillation. In: *Circulation* 125 (2), S. 216–225. DOI: 10.1161/CIRCULATIONAHA.111.053272.

Jalife, Jose; Antzelevitch, Charles; Moe, Gordon K. (1982): The Case for Modulated Parasystole. In: *Pacing and Clinical Electrophysiology* 5 (6), S. 911–926. DOI: 10.1111/j.1540-8159.1982.tb00030.x.

Janse, M. J.; Wit, A. L. (1989): Electrophysiological mechanisms of ventricular arrhythmias resulting from myocardial ischemia and infarction. In: *Physiological reviews* 69 (4), S. 1049–1169. DOI: 10.1152/physrev.1989.69.4.1049.

January, C. T.; Riddle, J. M. (1989): Early afterdepolarizations: mechanism of induction and block. A role for L-type Ca2+ current. In: *Circulation research* 64 (5), S. 977–990.

Jaski, Brian E.; Jessup, Mariell L.; Mancini, Donna M.; Cappola, Thomas P.; Pauly, Daniel F.; Greenberg, Barry et al. (2009): Calcium upregulation by percutaneous administration of gene therapy in cardiac disease (CUPID Trial), a first-in-human phase 1/2 clinical trial. In: *Journal of cardiac failure* 15 (3), S. 171–181. DOI: 10.1016/j.cardfail.2009.01.013.

Johannes Frank (2013): Der Einfluss von CD105 auf das Regenerationspotential humaner multipotenter mesenchymaler Stromazellen in einem Myokardinfarktmodell der Maus. Medical Doctorate Thesis. Department of Cardiac Surgery. Rostock University. Online verfügbar unter http://rosdok.uni-rostock.de/file/rosdok_disshab_0000001255/rosdok_derivate_0000019028/Dissertation_Frank_2014.pdf.

Johansson, B. W. (2001): Elektrokardiografins utveckling. In: *Dansk medicinhistorisk arbog*, S. 163–176.

Kaese, Sven; Verheule, Sander (2012): Cardiac electrophysiology in mice: a matter of size. In: *Frontiers in physiology* 3, S. 345. DOI: 10.3389/fphys.2012.00345.

Kieken, Fabien; Mutsaers, Nancy; Dolmatova, Elena; Virgil, Kelly; Wit, Andrew L.; Kellezi, Admir et al. (2009): Structural and molecular mechanisms of gap junction remodeling in epicardial border zone myocytes following myocardial infarction. In: *Circulation research* 104 (9), S. 1103–1112. DOI: 10.1161/CIRCRESAHA.108.190454.

Kim, Sook Kyoung; Pak, Hui-Nam; Park, Jae Hyung; Fang, Yong Fu; Kim, Gwang Il; Park, Yong Doo et al. (2010): Cardiac cell therapy with mesenchymal stem cell induces cardiac nerve sprouting, angiogenesis, and reduced connexin43-positive gap junctions, but concomitant electrical pacing increases connexin43-positive gap junctions in canine heart. In: *Cardiology in the young* 20 (3), S. 308–317. DOI: 10.1017/S1047951110000132.

Klabunde, Richard E. (2008): Cardiovascular Physiology Concepts, Arrhythmias, Sinoatrial action potentials. Online verfügbar unter www.cvphysiology.com.

Kolanowski, T. J.; Rozwadowska, N.; Malcher, A.; Szymczyk, E.; Kasprzak, J. D.; Mietkiewski, T.; Kurpisz, M. (2014): In vitro and in vivo characteristics of connexin 43-modified human skeletal myoblasts as candidates for prospective stem cell therapy for the

failing heart. In: *International journal of cardiology* 173 (1), S. 55–64. DOI: 10.1016/j.ijcard.2014.02.009.

Kuçi, Selim; Kuçi, Zyrafete; Kreyenberg, Hermann; Deak, Erika; Pütsch, Kathrin; Huenecke, Sabine et al. (2010): CD271 antigen defines a subset of multipotent stromal cells with immunosuppressive and lymphohematopoietic engraftment-promoting properties. In: *Haematologica* 95 (4), S. 651–659. DOI: 10.3324/haematol.2009.015065.

Kumar, Dinender; Hacker, Timothy A.; Buck, Jennifer; Whitesell, Larry F.; Kaji, Eugene H.; Douglas, Pamela S.; Kamp, Timothy J. (2005): Distinct mouse coronary anatomy and myocardial infarction consequent to ligation. In: *Coronary artery disease* 16 (1), S. 41–44.

Lau, David H.; Clausen, Chris; Sosunov, Eugene A.; Shlapakova, Iryna N.; Anyukhovsky, Evgeny P.; Danilo, Peter et al. (2009): Epicardial border zone overexpression of skeletal muscle sodium channel SkM1 normalizes activation, preserves conduction, and suppresses ventricular arrhythmia: an in silico, in vivo, in vitro study. In: *Circulation* 119 (1), S. 19–27. DOI: 10.1161/CIRCULATIONAHA.108.809301.

Lemcke, Heiko; Gaebel, Ralf; Skorska, Anna; Voronina, Natalia; Lux, Cornelia Aquilina; Petters, Janine et al. (2017a): Mechanisms of stem cell based cardiac repair-gap junctional signaling promotes the cardiac lineage specification of mesenchymal stem cells. In: *Scientific reports* 7 (1), S. 9755. DOI: 10.1038/s41598-017-10122-6.

Lemcke, Heiko; Gaebel, Ralf; Skorska, Anna; Voronina, Natalia; Lux, Cornelia Aquilina; Petters, Janine et al. (2017b): Mechanisms of stem cell based cardiac repair-gap junctional signaling promotes the cardiac lineage specification of mesenchymal stem cells. In: *Scientific reports* 7 (1), S. 9755. DOI: 10.1038/s41598-017-10122-6.

Leprán, István; Koltai, Mátyás; siegmund, Werner; Szekeres, László (1983): Coronary artery ligation, early arrhythmias, and determination of the ischemic area in conscious rats. In: *Journal of Pharmacological Methods* 9 (3), S. 219–230. DOI: 10.1016/0160-5402(83)90041-4.

Lev, M.; Thaemert, J. C. (1973): The conduction system of the mouse heart. In: *Acta anatomica* 85 (3), S. 342–352.

Lichtman, M. A. (1981): The ultrastructure of the hemopoietic environment of the marrow: a review. In: *Experimental hematology* 9 (4), S. 391–410.

Liu, Gang; Iden, Jason B.; Kovithavongs, Kay; Gulamhusein, Rashida; Duff, Henry J.; Kavanagh, Katherine M. (2004): In vivo temporal and spatial distribution of depolarization and repolarization and the illusive murine T wave. In: *The Journal of physiology* 555 (Pt 1), S. 267–279. DOI: 10.1113/jphysiol.2003.054064.

Logan, C.; Khoo, W. K.; Cado, D.; Joyner, A. L. (1993): Two enhancer regions in the mouse En-2 locus direct expression to the mid/hindbrain region and mandibular myoblasts. In: *Development (Cambridge, England)* 117 (3), S. 905–916.

Lopez, Alan D. (2006): Global burden of disease and risk factors. New York, N.Y.: Oxford University Press; Washington. Online verfügbar unter http://www.loc.gov/catdir/enhancements/fy0638/2006040094-d.html.

Lorenz, John N. (2002): A practical guide to evaluating cardiovascular, renal, and pulmonary function in mice. In: *American journal of physiology. Regulatory, integrative and comparative physiology* 282 (6), R1565-82. DOI: 10.1152/ajpregu.00759.2001.

Lujan, Heidi L.; DiCarlo, Stephen E. (2014): Reperfusion-induced sustained ventricular tachycardia, leading to ventricular fibrillation, in chronically instrumented, intact, conscious mice. In: *Physiological reports* 2 (6). DOI: 10.14814/phy2.12057.

Lyon, Alexander R.; Bannister, Mark L.; Collins, Tom; Pearce, Emma; Sepehripour, Amir H.; Dubb, Sukhpreet S. et al. (2011): SERCA2a gene transfer decreases sarcoplasmic reticulum calcium leak and reduces ventricular arrhythmias in a model of chronic heart failure. In: *Circulation. Arrhythmia and electrophysiology* 4 (3), S. 362–372. DOI: 10.1161/CIRCEP.110.961615.

Macia, Ester; Dolmatova, Elena; Cabo, Candido; Sosinsky, Alexandra Z.; Dun, Wen; Coromilas, James et al. (2011): Characterization of gap junction remodeling in epicardial border zone of healing canine infarcts and electrophysiological effects of partial reversal by rotigaptide. In: *Circulation. Arrhythmia and electrophysiology* 4 (3), S. 344–351. DOI: 10.1161/CIRCEP.110.959312.

Mathers, Colin; Fat, Doris Ma; Boerma, J. T. (2008): The global burden of disease. 2004 update. Geneva Switzerland: World Health Organization.

Mathiasen, Anders Bruun; Qayyum, Abbas Ali; Jørgensen, Erik; Helqvist, Steffen; Fischer-Nielsen, Anne; Kofoed, Klaus F. et al. (2015): Bone marrow-derived mesenchymal stromal cell treatment in patients with severe ischaemic heart failure: a randomized placebo-controlled trial (MSC-HF trial). In: *European heart journal* 36 (27), S. 1744–1753. DOI: 10.1093/eurheartj/ehv136.

Menasché, Philippe; Alfieri, Ottavio; Janssens, Stefan; McKenna, William; Reichenspurner, Hermann; Trinquart, Ludovic et al. (2008): The Myoblast Autologous Grafting in Ischemic Cardiomyopathy (MAGIC) trial: first randomized placebo-controlled study of myoblast transplantation. In: *Circulation* 117 (9), S. 1189–1200. DOI: 10.1161/CIRCULATIONAHA.107.734103.

Michael, L. H.; Entman, M. L.; Hartley, C. J.; Youker, K. A.; Zhu, J.; Hall, S. R. et al. (1995): Myocardial ischemia and reperfusion: a murine model. In: *The American journal of physiology* 269 (6 Pt 2), H2147-54. DOI: 10.1152/ajpheart.1995.269.6.H2147.

Mills, William R.; Mal, Niladri; Kiedrowski, Matthew J.; Unger, Ryan; Forudi, Farhad; Popovic, Zoran B. et al. (2007): Stem cell therapy enhances electrical viability in myocardial infarction. In: *Journal of molecular and cellular cardiology* 42 (2), S. 304–314. DOI: 10.1016/j.yjmcc.2006.09.011.

Monteiro, Luís Miguel; Vasques-Nóvoa, Francisco; Ferreira, Lino; Pinto-do-Ó, Perpétua; Nascimento, Diana Santos (2017): Restoring heart function and electrical integrity: closing the circuit. In: *NPJ Regenerative medicine* 2, S. 9. DOI: 10.1038/s41536-017-0015-2.

Motloch, Lukas J.; Akar, Fadi G. (2015): Gene therapy to restore electrophysiological function in heart failure. In: *Expert opinion on biological therapy* 15 (6), S. 803–817. DOI: 10.1517/14712598.2015.1036734.

Mureli, Shwetha; Gans, Christopher P.; Bare, Dan J.; Geenen, David L.; Kumar, Nalin M.; Banach, Kathrin (2013): Mesenchymal stem cells improve cardiac conduction by upregulation of connexin 43 through paracrine signaling. In: *American journal of physiology. Heart and circulatory physiology* 304 (4), H600-9. DOI: 10.1152/ajpheart.00533.2012.

Nattel, Stanley; Dobrev, Dobromir (2017): Controversies About Atrial Fibrillation Mechanisms: Aiming for Order in Chaos and Whether it Matters. In: *Circulation research* 120 (9), S. 1396–1398. DOI: 10.1161/CIRCRESAHA.116.310489.

Ovsepyan, A. A.; Panchenkov, D. N.; Prokhortchouk, E. B.; Telegin, G. B.; Zhigalova, N. A.; Golubev, E. P. et al. (2011): Modeling myocardial infarction in mice: methodology, monitoring, pathomorphology. In: *Acta naturae* 3 (1), S. 107–115.

Pak, Hui-Nam; Qayyum, Mohammed; Kim, Dave T.; Hamabe, Akira; Miyauchi, Yasushi; Lill, Michael C. et al. (2003): Mesenchymal stem cell injection induces cardiac nerve sprouting and increased tenascin expression in a Swine model of myocardial infarction. In: *Journal of cardiovascular electrophysiology* 14 (8), S. 841–848.

Peters, N. S.; Wit, A. L. (1998): Myocardial architecture and ventricular arrhythmogenesis. In: *Circulation* 97 (17), S. 1746–1754.

Protas, Lev; Dun, Wen; Jia, Zhiheng; Lu, Jia; Bucchi, Annalisa; Kumari, Sindhu et al. (2009): Expression of skeletal but not cardiac Na+ channel isoform preserves normal conduction in a depolarized cardiac syncytium. In: *Cardiovascular research* 81 (3), S. 528–535. DOI: 10.1093/cvr/cvn290.

Rentschler, S.; Vaidya, D. M.; Tamaddon, H.; Degenhardt, K.; Sassoon, D.; Morley, G. E. et al. (2001): Visualization and functional characterization of the developing murine cardiac conduction system. In: *Development (Cambridge, England)* 128 (10), S. 1785–1792.

Roell, Wilhelm; Fan, Yun; Xia, Ying; Stoecker, Eva; Sasse, Philipp; Kolossov, Eugen et al. (2002a): Cellular cardiomyoplasty in a transgenic mouse model. In: *Transplantation* 73 (3), S. 462–465.

Roell, Wilhelm; Lewalter, Thorsten; Sasse, Philipp; Tallini, Yvonne N.; Choi, Bum-Rak; Breitbach, Martin et al. (2007): Engraftment of connexin 43-expressing cells prevents post-infarct arrhythmia. In: *Nature* 450 (7171), S. 819–824. DOI: 10.1038/nature06321.

Roell, Wilhelm; Lu, Zhong J.; Bloch, Wilhelm; Siedner, Sharon; Tiemann, Klaus; Xia, Ying et al. (2002b): Cellular cardiomyoplasty improves survival after myocardial injury. In: *Circulation* 105 (20), S. 2435–2441.

Saffitz, J. E.; Laing, J. G.; Yamada, K. A. (2000): Connexin expression and turnover : implications for cardiac excitability. In: *Circulation research* 86 (7), S. 723–728.

Sagmeister, Veronika (2013;21:55): BASICS Kardiologie. Third edition. Munich: Elsevier; Urban & Fischer.

Sanganalmath, Santosh K.; Bolli, Roberto (2013): Cell therapy for heart failure: a comprehensive overview of experimental and clinical studies, current challenges, and future directions. In: *Circulation research* 113 (6), S. 810–834. DOI: 10.1161/CIRCRESAHA.113.300219.

Santos Nascimento, Diana; Mosqueira, Diogo; Sousa, Luís Moura; Teixeira, Mariana; Filipe, Mariana; Resende, Tatiana Pinho et al. (2014): Human umbilical cord tissue-derived mesenchymal stromal cells attenuate remodeling after myocardial infarction by proangiogenic, antiapoptotic, and endogenous cell-activation mechanisms. In: *Stem cell research & therapy* 5 (1), S. 5. DOI: 10.1186/scrt394.

Saoudi, N.; Castellanos, A.; Touboul, P. (1989): Automodulation des parasystolies ventriculaires. La courbe de phase réponse triphasique. In: *Archives des maladies du coeur et des vaisseaux* 82 (2), S. 201–206.

Satullo, G.; Donato, A.; Luzza, F.; Saporito, F.; Oreto, G. (1992): Atrial parasystole and tachycardia. Modulation and automodulation of a parasystolic focus. In: *Chest* 102 (2), S. 622–625.

Severs, Nicholas J.; Coppen, Steven R.; Dupont, Emmanuel; Yeh, Hung-I; Ko, Yu-Shien; Matsushita, Tsutomu (2004): Gap junction alterations in human cardiac disease. In: *Cardiovascular research* 62 (2), S. 368–377. DOI: 10.1016/j.cardiores.2003.12.007.

Shiba, Yuji; Filice, Dominic; Fernandes, Sarah; Minami, Elina; Dupras, Sarah K.; van Biber, Benjamin et al. (2014): Electrical Integration of Human Embryonic Stem Cell-Derived Cardiomyocytes in a Guinea Pig Chronic Infarct Model. In: *Journal of cardiovascular pharmacology and therapeutics* 19 (4), S. 368–381. DOI: 10.1177/1074248413520344.

Söhl, Goran; Willecke, Klaus (2004): Gap junctions and the connexin protein family. In: *Cardiovascular research* 62 (2), S. 228–232. DOI: 10.1016/j.cardiores.2003.11.013.

Sood, Subeena; Chelu, Mihail G.; van Oort, Ralph J.; Skapura, Darlene; Santonastasi, Marco; Dobrev, Dobromir; Wehrens, Xander H. T. (2008): Intracellular calcium leak due to FKBP12.6 deficiency in mice facilitates the inducibility of atrial fibrillation. In: *Heart rhythm* 5 (7), S. 1047–1054. DOI: 10.1016/j.hrthm.2008.03.030.

Späni, D.; Arras, M.; König, B.; Rülicke, T. (2003): Higher heart rate of laboratory mice housed individually vs in pairs. In: *Laboratory animals* 37 (1), S. 54–62. DOI: 10.1258/002367703762226692.

Speerschneider, T.; Thomsen, M. B. (2013): Physiology and analysis of the electrocardiographic T wave in mice. In: *Acta physiologica (Oxford, England)* 209 (4), S. 262–271. DOI: 10.1111/apha.12172.

Sprague, H. B.; White, P. D. (1925): CLINICAL OBSERVATIONS ON THE T WAVE OF THE AURICLE APPEARING IN THE HUMAN ELECTROCARDIOGRAM. In: *The Journal of clinical investigation* 1 (4), S. 389–402. DOI: 10.1172/JCI100020.

Suzuki, K.; Brand, N. J.; Allen, S.; Khan, M. A.; Farrell, A. O.; Murtuza, B. et al. (2001): Overexpression of connexin 43 in skeletal myoblasts: Relevance to cell transplantation to the heart. In: *The Journal of thoracic and cardiovascular surgery* 122 (4), S. 759–766. DOI: 10.1067/mtc.2001.116210.

Szabo, B.; Sweidan, R.; Rajagopalan, C. V.; Lazzara, R. (1994): Role of Na+:Ca2+ exchange current in Cs(+)-induced early afterdepolarizations in Purkinje fibers. In: *Journal of cardiovascular electrophysiology* 5 (11), S. 933–944.

Thielmann, Matthias; Massoudy, Parwis; Jaeger, Beate R.; Neuhäuser, Markus; Marggraf, Günter; Sack, Stephan et al. (2006): Emergency re-revascularization with percutaneous coronary intervention, reoperation, or conservative treatment in patients with acute perioperative graft failure following coronary artery bypass surgery. In: *European journal of cardio-thoracic surgery : official journal of the European Association for Cardio-thoracic Surgery* 30 (1), S. 117–125. DOI: 10.1016/j.ejcts.2006.03.062.

Thomas, D. E.; Jex, N.; Thornley, A. R. (2017): Ventricular arrhythmias in acute coronary syndromes-mechanisms and management. In: *Cont Cardiol Educ* 3 (1), S. 22–29. DOI: 10.1002/cce2.51.

Tofler, G. H.; Stone, P. H.; Muller, J. E.; Rutherford, J. D.; Willich, S. N.; Gustafson, N. F. et al. (1987): Prognosis after cardiac arrest due to ventricular tachycardia or ventricular fibrillation associated with acute myocardial infarction (the MILIS Study). Multicenter Investigation of the Limitation of Infarct Size. In: *The American journal of cardiology* 60 (10), S. 755–761.

Tolmachov, Oleg; Ma, Yu-Ling; Themis, Michael; Patel, Pravina; Spohr, Hilmar; Macleod, Kenneth T. et al. (2006): Overexpression of connexin 43 using a retroviral vector improves electrical coupling of skeletal myoblasts with cardiac myocytes in vitro. In: *BMC cardiovascular disorders* 6, S. 25. DOI: 10.1186/1471-2261-6-25.

Tse, Gary (2016): Mechanisms of cardiac arrhythmias. In: *Journal of arrhythmia* 32 (2), S. 75–81. DOI: 10.1016/j.joa.2015.11.003.

Vaidya, D.; Morley, G. E.; Samie, F. H.; Jalife, J. (1999): Reentry and fibrillation in the mouse heart. A challenge to the critical mass hypothesis. In: *Circulation research* 85 (2), S. 174–181.

Vaidya, D.; Tamaddon, H. S.; Lo, C. W.; Taffet, S. M.; Delmar, M.; Morley, G. E.; Jalife, J. (2001): Null mutation of connexin43 causes slow propagation of ventricular activation in the late stages of mouse embryonic development. In: *Circulation research* 88 (11), S. 1196–1202.

van den Bos, Ewout J.; Mees, Barend M. E.; Waard, Monique C. de; Crom, Rini de; Duncker, Dirk J. (2005): A novel model of cryoinjury-induced myocardial infarction in the mouse: a comparison with coronary artery ligation. In: *American journal of physiology. Heart and circulatory physiology* 289 (3), H1291-300. DOI: 10.1152/ajpheart.00111.2005.

Verheugt, F. W.; Meijer, A.; Lagrand, W. K.; van Eenige, M. J. (1996): Reocclusion: the flip side of coronary thrombolysis. In: *Journal of the American College of Cardiology* 27 (4), S. 766–773.

Virágh, S.; Challice, C. E. (1982): The development of the conduction system in the mouse embryo heart. In: *Developmental biology* 89 (1), S. 25–40.

Walker, M. J.; Curtis, M. J.; Hearse, D. J.; Campbell, R. W.; Janse, M. J.; Yellon, D. M. et al. (1988): The Lambeth Conventions: guidelines for the study of arrhythmias in ischaemia infarction, and reperfusion. In: *Cardiovascular research* 22 (7), S. 447–455.

Wang, Deguo; Zhang, Fengxiang; Shen, Wenzhi; Chen, Minglong; Yang, Bing; Zhang, Yuzhen; Cao, Kejiang (2011): Mesenchymal stem cell injection ameliorates the inducibility of

ventricular arrhythmias after myocardial infarction in rats. In: *International journal of cardiology* 152 (3), S. 314–320. DOI: 10.1016/j.ijcard.2010.07.025.

Wehrens, X. H.; Kirchhoff, S.; Doevendans, P. A. (2000): Mouse electrocardiography: an interval of thirty years. In: *Cardiovascular research* 45 (1), S. 231–237.

Wei, Feng; Wang, Ting-Zhong; Zhang, Jing; Yuan, Zu-Yi; Tian, Hong-Yan; Ni, Ya-Juan et al. (2012): Mesenchymal stem cells neither fully acquire the electrophysiological properties of mature cardiomyocytes nor promote ventricular arrhythmias in infarcted rats. In: *Basic research in cardiology* 107 (4), S. 274. DOI: 10.1007/s00395-012-0274-4.

Weiss, James N.; Garfinkel, Alan; Karagueuzian, Hrayr S.; Nguyen, Thao P.; Olcese, Riccardo; Chen, Peng-Sheng; Qu, Zhilin (2015): Perspective: a dynamics-based classification of ventricular arrhythmias. In: *Journal of molecular and cellular cardiology* 82, S. 136–152. DOI: 10.1016/j.yjmcc.2015.02.017.

Weiss, L. (1976): The hematopoietic microenvironment of the bone marrow: an ultrastructural study of the stroma in rats. In: *The Anatomical record* 186 (2), S. 161–184. DOI: 10.1002/ar.1091860204.

Williams, Adam R.; Hare, Joshua M. (2011): Mesenchymal stem cells: biology, pathophysiology, translational findings, and therapeutic implications for cardiac disease. In: *Circulation research* 109 (8), S. 923–940. DOI: 10.1161/CIRCRESAHA.111.243147.

Wit, A. L.; Janse, M. J. (1993): The Ventricular Arrhythmias of Ischemia and Infarction. Electrophysiological Mechanisms. In: *Futura*.

Wit, Andrew L.; Peters, Nicholas S. (2012): The role of gap junctions in the arrhythmias of ischemia and infarction. In: *Heart rhythm* 9 (2), S. 308–311. DOI: 10.1016/j.hrthm.2011.09.056.

Xie, Yuanfang; Liao, Zhandi; Grandi, Eleonora; Shiferaw, Yohannes; Bers, Donald M. (2015): Slow Nai Changes and Positive Feedback Between Membrane Potential and Cai Underlie Intermittent Early Afterdepolarizations and Arrhythmias. In: *Circulation. Arrhythmia and electrophysiology* 8 (6), S. 1472–1480. DOI: 10.1161/CIRCEP.115.003085.

Xu, Zhaobin; Alloush, Jenna; Beck, Eric; Weisleder, Noah (2014): A murine model of myocardial ischemia-reperfusion injury through ligation of the left anterior descending artery. In: *Journal of visualized experiments : JoVE* (86). DOI: 10.3791/51329.

Zipes, Douglas P.; Camm, A. John; Borggrefe, Martin; Buxton, Alfred E.; Chaitman, Bernard; Fromer, Martin et al. (2006): ACC/AHA/ESC 2006 guidelines for management of patients with ventricular arrhythmias and the prevention of sudden cardiac death: a report of the American College of Cardiology/American Heart Association Task Force and the European

Society of Cardiology Committee for Practice Guidelines (Writing Committee to Develop Guidelines for Management of Patients With Ventricular Arrhythmias and the Prevention of Sudden Cardiac Death). In: *Journal of the American College of Cardiology* 48 (5), e247-346. DOI: 10.1016/j.jacc.2006.07.010.

Zolotareva, A. G.; Kogan, M. E. (1978): Production of experimental occlusive myocardial infarction in mice. In: *Cor et vasa* 20 (4), S. 308–314.

Zsebo, Krisztina; Yaroshinsky, Alex; Rudy, Jeffrey J.; Wagner, Kim; Greenberg, Barry; Jessup, Mariell; Hajjar, Roger J. (2014): Long-term effects of AAV1/SERCA2a gene transfer in patients with severe heart failure: analysis of recurrent cardiovascular events and mortality. In: *Circulation research* 114 (1), S. 101–108. DOI: 10.1161/CIRCRESAHA.113.302421.

AFFIDAVIT

I hereby confirm that my thesis entitled "*Antiarrhythmic effects of human bone marrow derived CD271+ mesenchymal stem cells tested in vivo using a new infarction-re-infarction mouse model*" is the result of my own work. I did not receive any help or support from commercial consultants. All references and / or materials applied are listed and specified in the thesis.

Furthermore, I confirm that this thesis has not yet been submitted as part of another examination process neither in identical nor in similar form.

Rostock _____ _____

(Date of submission) (Signature)

ABBREVIATIONS

°C	degree Celsius
µl	Microliter
AF	Atrial fibrillation
AFL	Atrial flutter
AP	Action potential
APB	Atrial premature beat
AV node	Atrioventricular node
BG	Bigeminy
bpm	Beats per minute
BSA	Bovine serum albumin
Ca^{++}	Calcium
CABG	Coronary artery bypass graft
CCS	Cardiac Conduction System
CD	Cluster of differentiation
CHD	Coronary Heart Disease
CM	Cardiomyocyte
CVD	Cardiovascular Disease
Cx	Connexin
Cx43	Connexin 43
DAD	Delayed after repolarization
DALYs	Disability-Adjusted Life Years
DAPI	4′,6-diamidino-2-phenylindole

DNAse	Deoxyribonuclease
EAD	Early after repolarization
ECG	Electrocardiogram
EDTA	Ethylenediaminetetraacetic acid
EMC	Embryonic stem cell
ex vivo	Latin: "out of the living"
FACS	fluorescence-activated cell sorting
HF	Heart Failure
HF	Heart failure
HLA-DR	Human Leukocyte Antigen – DR isotype
HSC	Hematopoietic stem cells
I.U.	International Unit
in vivo	Latin for "within the living"
iPSC	Induced pleuripotent stem cell
ISCT	International Society for Cell Therapie
IVS	Interventricular septum
K^+	Potassium
LA	Left atrium
LAD	Left Anterior Descending artery
LBB	Left bundle branch
LDL	Low Density Lipoprotein
LSM	Lymphocyte Separation Medium
LV	Left Ventricle

MACS	Magnetic activated cell sorting
MDP	Maximum diastolic potential
MI	Myocardial Infarction
MIC	Myocardial infarction control group
ml	Milliliter
MSC	Mesenchymal stem/stromal cells
mV	Millivolt
Na^+	Sodium
PBS	Phosphate-buffered saline
PTB	Physikalisch-Technische Bundesanstalt; the National Metrology Institute of Germany
PVB	Premature ventricular beat
RA	Right atrium
RBB	Right bundle branch
RPMI	Roswell Park Memorial Institute; RPMI Medium
SA node	Sinoatrial node
SERCA2a	Sarcoplasmic endoplasmic reticulum calcium (Ca2+) ATPase
SRI	Stem cell treated re-infarction group
TDP	Torsades de pointes
TG	Trigeminy
TP	Threshold potential
URI	Untreated re-infarction group
VF	Ventricular fibrillation
VT	Ventricular tachycardia

CURRICULUM VITAE

Haval Sadraddin

Hogenweg 12, D-47137 Duisburg

Mobile: +49 152 22038602 | E-mail: havalandonlyhaval@gmail.com

Personal Data

Full name:	Haval Lutfalla Sadraddin
Date of birth :	19th June, 1985
Place of birth:	Erbil, Kurdistan Region of Iraq
Citizenship:	Iraqi
Marital status:	married

Education

2003	High school, Ainkawa secondary school, Erbil, Kurdistan Region of Iraq. (Average score: 97.85%)
2003-2009	Studied medicine in Hawler Medical University/College of Medicine in Erbil, Kurdistan Region of Iraq. Average score: 80.57% Grade: Bachelor in Medizin und Chirurgie (M.B.Ch.B) Rank: 4th best scored student in a class of 153 Students

Practical Experience

10/2009 – 10/2011 (24 Months)	Resident doctor, rotation in different medical and surgical departments in different hospitals in Erbil, Kurdistan Region of Iraq.
10/2011 – 10/2012 (12 Monthes)	Doctor of rural areas, primary health care, in Mala Omer primary health care center in Erbil, Kurdistan Region of Iraq.
10/2012 – 07/2013 (9	Resident of thoracic and cardiovascular surgery, Surgical Special-

Months)	ty Hospital – Cardiac Center, Erbil, Kurdistan Region of Iraq.
04/2012 - 07/2013 (16 Months)	Resident doctor in cardiac surgery, Jordanian International Hospital – For Heart & Special Surgery, Erbil, Kurdistan Region of Iraq. (part time work)
07/2013	Travel to Germany to pursue career in cardiac surgery
07/2013-12/2013	Intensive German language course, A1-B2 CEFR, Steinke-Institut, Bonn, Germany
10/2013-11/2013 (2 Months)	Training in Bonn University Hospital, Department of Cardiology, Echocardiography, Bonn, Germany
02/2014 – 07/2019	Resident of cardiac surgery, Rostock University Hospital, Department of Cardiac Surgery / *Prof. Dr. med. habil. Gustav Steinhoff*, Rostock, Germany
07/2019 – till now	Resident of cardiac surgery, Duisburg Heart Center, Department of Cardiac Surgery / *Prof. Dr. med. Jochen Börgermann*, Duisburg, Germany
03/2015 - 01/2016	Rotation in surgical intensive care unit of Rostock University Hospital, Department of Anesthesiology and Intensive Therapy, Rostock, Germany
23.02.2015	Granting the medical approbation for practicing medicine in Germany
19.03. – 21.03.2015	Basic course of radiation protection, Chamber of doctors, Mecklenburg-Vorpommern, Rostock, Germany
16.05. – 23.05.2015	Emergency doctor course (Compact course, Emergency medicine), Notfallakademie GmbH, München, Germany
04.06. – 06.06.2015	Special course of radiation protection, Chamber of doctors, Mecklenburg-Vorpommern, Rostock, Germany
13.04. – 14.04.2018	Course of endoscopic harvesting of vessels, University of Eberhard Karls Tübingen, Department of Clinical Anatomy Tübingen in cooperation with GETINGE company
23.08.-26.08.2018	Echo- and Dopplerechocardiography, basic course, „Deutsches Herzzentrum Berlin“, Berlin, Germany.
13.09.-16.09.2018	Echo- und Dopplerechokardiography, advanced course, „Deutsches Herzzentrum Berlin“, Berlin, Germany.